Universidad Autónoma de Madrid
Programa de Doctorado en Biociencias Moleculares

P53 and PUMA in Pluripotent Cell Competition

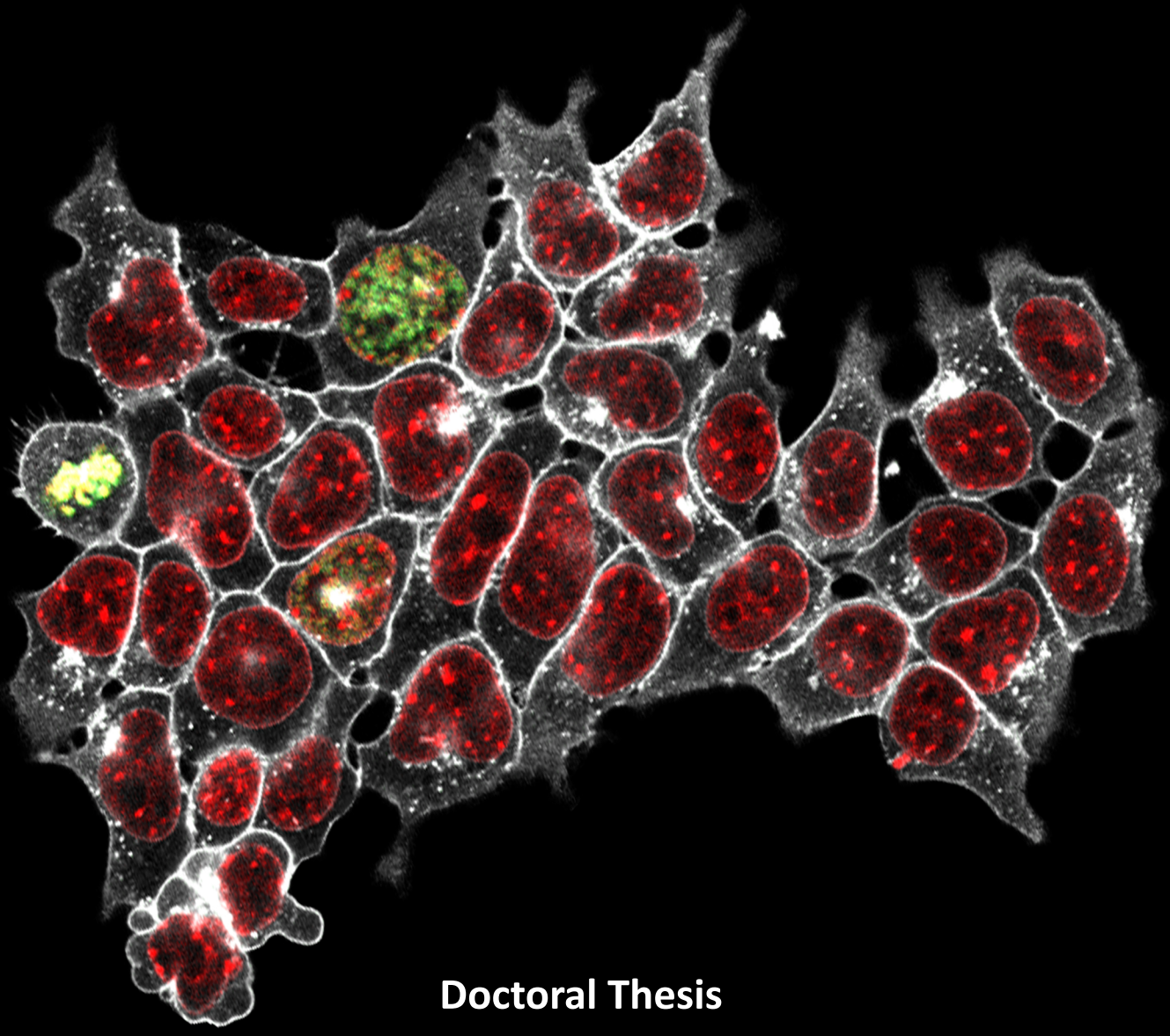

Doctoral Thesis

José Antonio Valverde López

Madrid, 2021

DEPARTAMENTO DE BIOQUÍMICA

FACULTAD DE MEDICINA

P53 and PUMA in Pluripotent Cell Competition

Doctoral thesis

José Antonio Valverde López

Graduado en Biotecnología

Madrid, January 2021

Director: Miguel Torres Sánchez

Centro Nacional de Investigaciones Cardiovasculares (CNIC)

This work was performed in Miguel Torres' laboratory in the Cell and Developmental Biology Area at the Centro Nacional de Investigaciones Cardiovasculares Carlos III (CNIC) in Madrid.

The CNIC is supported by the Ministerio de Ciencia, Innovación y Universidades (MCNU) and the Pro CNIC Foundation.

This study was funded by grants RD12/0019/0005 and RD16/0011/0019 (TerCel, RETICS); S2010-BMD-2315 (Comunidad de Madrid); BFU2012-31086 (MINECO); BFU2015-71519 (MEIC) and ref. 17CVD04 (Leudcq Foundation Transatlantic Networks).

José Antonio Valverde López was recipient of a "Caixa-Severo Ochoa 2015" fellowship.

I hereby certify that José Antonio Valverde López has carried out the experimental work leading to her PhD thesis entitled “P53 and PUMA in Pluripotent Cell Competition” under my supervision at the Centro Nacional de Investigaciones Cardiovasculares (CNIC) in Madrid.

I also declare that the work presented is novel and of great importance in the field, and of sufficient quality to merit to be presented in order to obtain a PhD degree by the Universidad Autónoma de Madrid.

Madrid, 19th December 2020

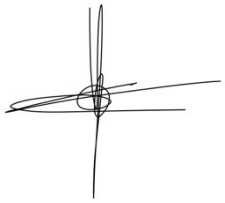

Miguel Torres Sánchez

“I have no special talents, but I am passionately curious”

Albert Einstein

INDEX

Abbreviations

2i: 2 inhibitors
Atg: Autophagy Related Genes
Avl: Avalanche
Bbc3: Bcl-2-Binding Component 3
BMP: Bone Morphogenetic Protein
BSA: Bovine Serum Albumin
Bst: Belly spot and tail
CC: Cell Competition
cCM: Condition Cell Medium
Cdk4: Cyclin-Dependent Kinase4
CHIRON: CHIR99021 (inhibitor)
Dgl: Discs Large
DHE: Dihydroethidium
Dpp: Decapentaplegic
Drp1: Dynamin-Related Protein 1
EDAC: Epithelial Defence Against Cancer
EpiLCs: Epiblast-like Cells
EpiSCs: Epiblast Stem Cells
ERK: Extracellular Regulated Kinase
ESC: Embryonic Stem Cell
FGF: Fibroblast Growth Factor
Fwe: Flower
GSK: Glycogen Synthase Kinase 3
ICM: Inner Cell Mass
iPSC: induced Pluripotent Stem Cell
JAK-STAT: Janus Kinase - Signal Transducer and Activator of Transcription
JNK: c-Jun N-terminal Kinase
KO: Knockout
Lgl: Lethal Giant Larvae
LIF: Leukemia Inhibitory Factor
MAPK: Mitogen-Activated Protein Kinase
MDCK: Madin-Darby Canine Kidney
MEF: Mouse Embryonic Fibroblast
Mfn2: Mitofusin-2

mTOR: Mechanistic Target Of Rapamycin
Myc: Myelocytomatosis oncogene
NAC: N-acetylcysteine
NEM: N-Ethylmaleimide
NOX: NADPH Oxidase
Nrf2: Nuclear factor erythroid 2-related factor 2
nTSG: Neoplastic Tumour Suppressor Genes
pHH V3: Phospho Histone H3
PD03: PD0325901
PI: Propidium Iodide
Rab: Ras Related in the brain
Ras: Rat Sarcoma
ROS: Reactive Oxygen Species
RP: Ribosomal Protein
Scrib: Scribble
Spz: Späetzle
Sparc: Secreted Protein Acidic and Rich in Cysteine
SR: Serum Replacement
Src: Sarcoma
Tsg: Testis Specific GTPase
Ubi: Ubiquitous
Upd: Unpaired-like Protein
Vps: Vacuolar Protein Sorting
Vps25: Vacuolar Protein-Sorting-Associated protein 25
WT: Wild Type
WGA: Wheat Germ Agglutinin
Yki: Yorkie

SUMMARY

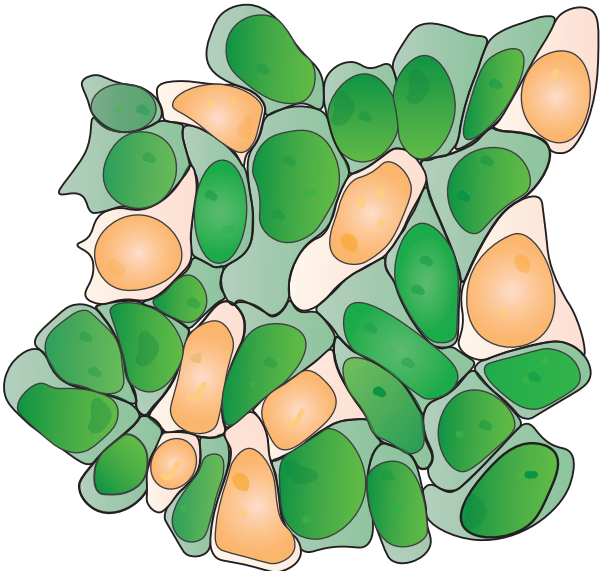

Cell Competition (CC) is a biological process in which viable cells are eliminated by the presence of neighbouring cells with increased fitness. First observed in *Drosophila*, Cell Competition has been described in numerous biological scenarios in metazoans both during embryonic development and in the adult. Cell Competition has been envisioned as a conserved and extended quality control system that eliminates less fit, mispatterned or non-well adapted cells, ensuring homeostasis and proper function of tissues and organs throughout life.

During the early mouse development, the mouse epiblast and its *in vitro* counterpart, mouse embryonic stem cells (ESCs) are subjected to natural Cell Competition. Through this mechanism, suboptimal or potentially harmful cells are removed by the presence of fitter cells, optimizing the pool of cells that will give rise to the new individual. This endogenous CC model correlates with MYC transcription factor expression, so cells with low MYC levels are eliminated by the presence of cells with higher levels (Clavería et al., 2013; Díaz-Díaz et al., 2017; Sancho et al., 2013). This process relies on the interaction and comparison between cells with different fitness, which results in the elimination of less fit cells. However, these molecular mechanisms remain largely unknown, especially in mammals.

Here, we have explored different factors and pathways regulating cell fitness and the execution of loser cell death. We have identified and analysed different candidates of the P53 pathway and propose a model based on increased susceptibility to apoptosis, autophagy and mitophagy induction and reduction of mitochondrial OXPHOS function, accounting, at least in part, for the loser “signature” in pluripotent Cell Competition.

We have found that P53 and PUMA regulate apoptosis susceptibility in ESCs but their function and expression is not restricted to apoptotic cells. We have shown that P53 activity inhibits MYC expression and is strictly required for PUMA expression. P53 and PUMA regulate fitness and induces Cell Competition in ESCs.

P53 regulation of competitive fitness depends on the pluripotency status, with the pathway being activated as the cells progress towards differentiation and their ability to induce Cell Competition is supressed in naïve pluripotency conditions.

We propose a model that integrates the P53 pathway and MYC in the definition of the loser cell fitness “status” and suggests that an alteration in mitochondrial OXPHOS function regulated by P53-PUMA underlies competitive fitness in pluripotent cells.

La Competición Celular (CC) es un proceso biológico por el cual células con menor *fitness* son eliminadas por la presencia de células vecinas con mayor fitness. Observada por primera vez en *Drosophila*, la CC se ha descrito en numerosos escenarios biológicos en todo el reino animal tanto en el desarrollo embrionario como en el organismo adulto. Actualmente, la Competición Celular se considera como un importante mecanismo de control de calidad capaz de eliminar células subóptimas o con un patrón erróneo, asegurando así la homeostasis y el correcto funcionamiento de órganos y tejidos a lo largo de la vida del individuo.

Durante el desarrollo temprano, en el epiblasto de ratón ocurren procesos de Competición Celular, de forma que, las células con menor *fitness* o potencialmente dañinas son eliminadas por la presencia de células más aptas, optimizando el conjunto de células que dará lugar al individuo. Este modelo de CC correlaciona con la expresión del factor de transcripción MYC, de manera que las células con menores niveles de MYC son eliminadas por la presencia de células con niveles más altos (Clavería et al., 2013; Díaz-Díaz et al., 2017; Sancho et al., 2013). Estos procesos también afectan al equivalente *in vitro* de las células del epiblasto, las células madre embrionarias (ESCs). Estos procesos de CC se basan en la interacción y comparación entre células con distinto nivel de *fitness*, que finalmente conduce a la eliminación de las células con menor *fitness* o *loser*. Sin embargo, los mecanismos que regulan y dirigen este fenómeno permanecen en su mayoría desconocidos, especialmente en mamíferos.

En este trabajo, exploramos diferentes factores y rutas de señalización que definen el f*itness* de las células ES, así como aquellos que regulan la eliminación de las células *loser*. Así pues, identificamos y analizamos diferentes factores de la ruta de P53 y proponemos un modelo que explica el estatus de la célula *loser* basado en una mayor susceptibilidad a sufrir apoptosis, la inducción de la autofagia y la mitofagia y la alteración de la función mitocondrial.

P53 y PUMA regulan la susceptibilidad a la apoptosis en ESCs, sin embargo, su patrón de expresión y función no está restringido a células apoptóticas. P53 inhibe la expresión de MYC es necesario para la expresión de PUMA. P53 y PUMA regulan el fitness e inducen Competición Celular en ESCs. Por su parte, el estatus de pluripotencia regula la expresión de P53 y su capacidad para inducir CC.

En resumen, proponemos un modelo sobre el estatus *loser* en células pluripotentes que integra la ruta de P53 y MYC y sugerimos que la alteración en la función mitocondrial podría ser un factor clave en la reducción del *fitness*.

INTRODUCTION

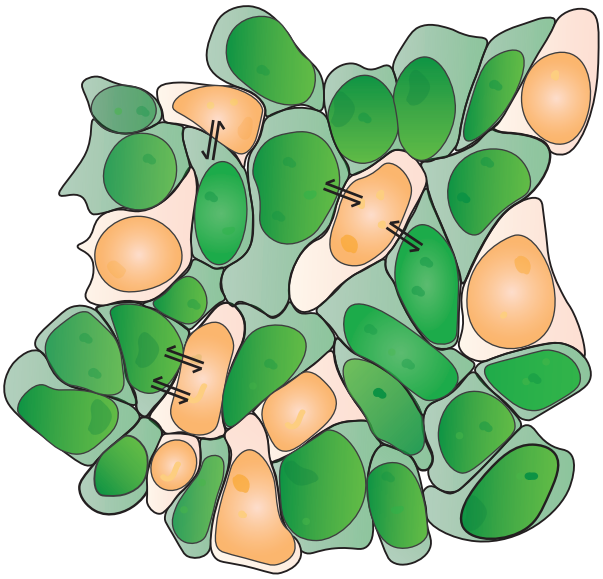

Cells within multicellular organisms would be subjected to evolutionary pressures as animals in the wild, and this pressure could enhance organismal fitness.

(Roux, 1881)

CELL COMPETITION

1 INTRODUCTION. Historical background and relevant discoveries

1.1 Early discoveries in flies. Deciphering the rules of Cell Competition

Cell Competition (CC) was first reported by Ginés Morata and Pedro Ripoll (Morata and Ripoll, 1975), when studying mutant flies for *Minute* genes. Although this mutation is lethal in homozygosity, heterozygous flies ($M^{+/-}$) are viable with just minor abnormalities as shorter and thinner bristles (Brehme, 1939). A principal feature of $M^{+/-}$ flies is a slower embryonic development (Morgan and Bridges, 1923). To test whether this developmental delay was due to a slower cell growth rate, Morata and Ripoll induced $M^{+/-}$ clones in wild type (WT) embryos within the wing imaginal disc[1]. $M^{+/-}$ clones were expected to be smaller than WT clones, however, they completely disappeared, even though $M^{+/-}$ flies are viable and fertile. This effect could not be explained by autonomous differences in proliferation rate and the authors proposed that *Minute* cells were eliminated when growing next to wild type cells. This process was termed as Cell Competition (Figure 1A).

Subsequent observations revealed some main characteristics of this CC model. For instance, only $M^{+/-}$ clones adjacent to WT clones are outcompeted, indicating that close proximity is required for CC. Competitive interactions did not occur when $M^{+/-}$ were induced in abdominal histoblasts[2]. Besides, CC was not effective across compartment boundaries[3] (Morata and Ripoll, 1975). These observations demonstrated that CC is a local but specific process (as cannot be induced in all tissues) that eliminates less-fit cells from a cell population of the same kind. Later, *Minute* cells elimination was also reported in *Drosophila* muscle precursors (Lawrence, 1982), indicating that other tissues apart from wing discs are susceptible to undergo CC.

During 15 years, CC was not a subject of interest, however new discoveries put the field again in the spotlight. For many years, only *Minute* mutants were known to induce CC. More recent works reported that cells mutant for genes affecting cellular growth/proliferation such as *dmyc*, *chico*, *ras* or *dpp* were eliminated by CC (Böhni et al., 1999; Burke and Basler, 1996; Johnston et al., 1999; Prober and Edgar, 2000). Additionally, different studies showed that mutant cells were eliminated by apoptosis (Johnston et al., 1999; Moreno et al., 2002; Prober and Edgar, 2000).

1.2 Supercompetition. Relative nature of cell fitness

Myc proteins are transcription factors involved in cell growth/proliferation, biosynthes is capacity and apoptosis (Eisenman, 2001). Cells carrying hypomorphic versions of *dmyc* were eliminated from a WT environment (Johnston et al., 1999), in a similar way to

[1] Imaginal discs are the precursors of adult insect structures and during developmental patterning they show a simple epithelial morphology (Clavería and Torres, 2015).
[2] Group of cells, precursors of the abdominal epithelium (Roseland and Schneiderman, 1979).
[3] Cell lineage restriction borders (which do not correlate with any morphologically visible landmarks) that separate developing cell populations from different lineages as independent functional units (Irvine and Rauskolb, 2001).

Minute mutants. Two subsequent studies demonstrated that *myc*-overexpressing cells actively eliminate neighbouring non-mutant WT cells (De La Cova et al., 2004; Moreno and Basler, 2004). This process, termed Supercompetition demonstrates that CC relies on the relative comparison of intrinsic cell properties and that competitive fitness could be enhanced over that of wild type cells (Figure 1B).

Notably, overexpression of other components that increase cell growth/proliferation, as Dp110 (PI3K complex) or CyclinD-Cdk4, as well as *Minute* genes failed to induced Super-competition (De La Cova et al., 2004; Hafezi et al., 2012; Simpson, 1979) (Hafezi et al., 2012). This indicates that generating a difference in cell growth/proliferation is therefore not sufficient to trigger CC.

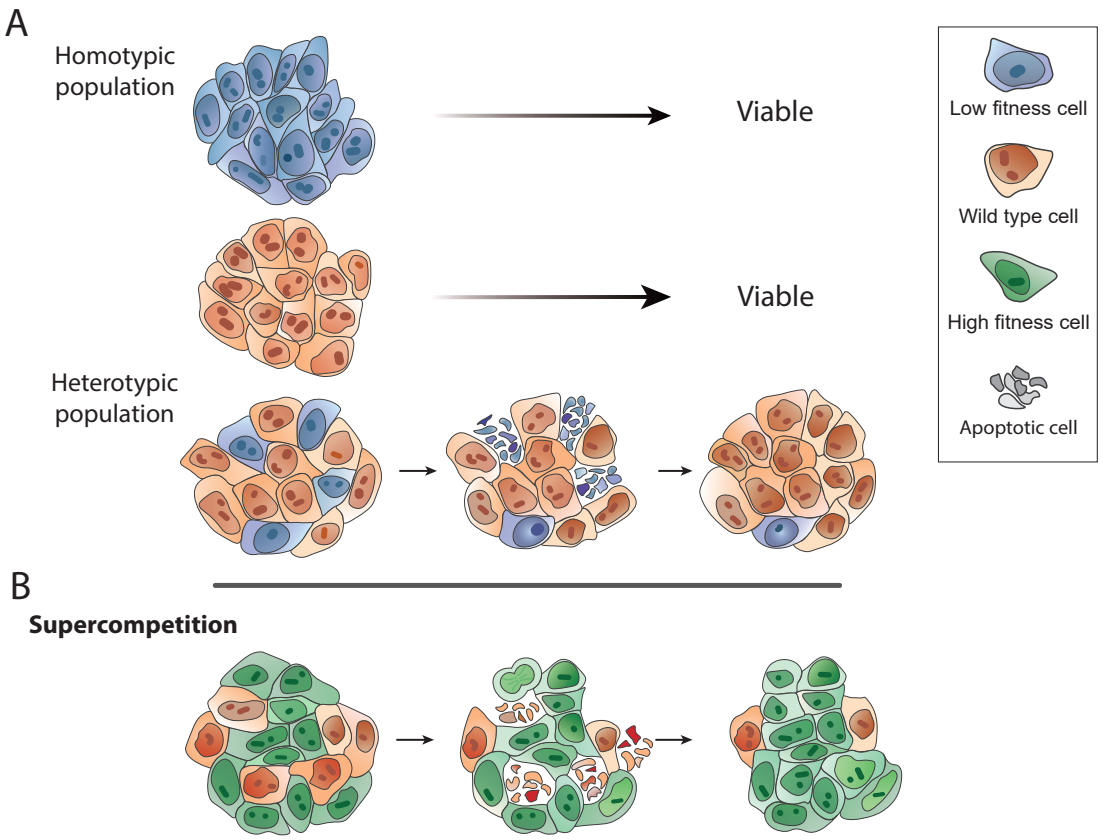

Figure 1. Cell Competition and Supercompetition

A. WT cells and cells with reduced fitness are viable. However in the presence of WT cells, cells with reduced fitness are eliminated. **B.** WT cells population can be eliminated by the presence of cells with increased fitness, which is called Supercompetition.

1.3 Cell Competition in mammals

The mouse *bst* mutation (*Belly spot and tail*), which impairs the ribosomal protein gene *rpl24* is similar to *Minute* mutations in flies, which also affect ribosomal proteins. $Bst^{+/-}$ mice are viable with minor defects. Interestingly, WT cells injected into a $bst^{+/-}$ blastocyst contribute in a larger proportion to the chimeric animals produced that those injected

into a WT blastocyst (Oliver et al., 2004). These experiments suggested competitive interactions in mammals for the first time, although whether this process was due to cell-autonomous differences between *bst*$^{+/-}$ and WT cells or CC was not addressed.

In a later study, Oertel et al. provided new evidences suggesting CC in mammals. They transplanted fetal liver progenitor/stem cells into damaged adult rat livers and fetal liver cells expanded across the liver inducing the elimination of adjacent host hepatocytes for prolonged periods (Oertel et al., 2006).

More recently, two studies described CC in the early mouse embryo and in embryonic stem cells[4] (ESCs). Sancho et al., demonstrated that ESCs with defective BMP signalling, autophagy machinery or tetraploid cells are eliminated by WT cells. They also suggested that MYC acts as a common downstream mediator regulating CC (Sancho et al., 2013). Meanwhile, Clavería el al., established an inducible genetic mosaic system. With this model, they demonstrated that generating a relative difference in MYC levels in the epiblast leads to the expansion of the population with higher MYC levels through the elimination of the one with lower levels by apoptosis, without disrupting mouse development. This process also occurs in ESCs and requires cell contact. Furthermore, in the epiblast, MYC expression shows a natural cell-to-cell heterogeneity in a random distribution. Cells with lower MYC levels are eliminated by natural CC, selecting cells with higher MYC level, which posses more anabolic capacity (Clavería et al., 2013). This work demonstrated for the first time an example of natural CC, without the induction of any genetic alteration.

Since its discovery, different aspects of CC have been reported and are introduced in the following sections.

2 MECHANISMS OF CELL COMPETITION

The Cell Competition process can be subdivided in four steps: (1) Generation of fitness imbalance between cells, (2) fitness comparison, (3) *loser* cell elimination and (4) compensation for *loser* cell elimination by winners.

(1) CC is triggered by a fitness difference between cells. Competitive fitness encompasses a variety of intrinsic cellular properties that affect the competitive behaviour of cells. Different mutations affecting apparently unrelated cellular processes can trigger CC, like apico-basal polarity, cell metabolism and cell proliferation. This suggests that fitness includes many different cellular features and CC is an extended mechanism that function downstream all those features. These pathways alteration could converge into common cellular downstream mechanisms leading to loser outcompetition when in presence of winner cells.

Several scenarios of different complexity are possible to explain the mechanisms of fitness comparison (2) and loser elimination (3):

[4] ESCs are considered the *in vitro* counterpart of the epiblast. During the early development, the epiblast is an epithelium compound of pluripotent cells that give rise to all cell lineages of the whole organism (Sheng, 2015).

a) Difference in fitness between cells is non-autonomously sensed, and as result, a cellular mechanism is triggered. This response to differential fitness level can be triggered directly in loser cells, winner cells or both, eventually leading to loser outcompetition.

b) There is no response to differential fitness level between winner and loser cells. Conversely, intrinsic cellular differences directly lead to loser outcompetition. For instances, loser cells can be eliminated by a toxic signal or by growth factors deprivation, which results from intrinsic differences in sensitivity to a "killing" signal or growth factors deprivation between winner and loser cells.

Eventually, the elimination of loser cells (3) can induce a non-autonomous response in "winner" cells (4) to compensate for "loser" cell elimination.

We will described the main discoveries according to each part.

2.1 Fitness. Pathways Triggering CC

Cell Competition initiates because of a difference in cell fitness between neighbouring cells. Less fit cells or "loser cells" will be eliminated, while "winner cells" induce loser cell elimination and remain in the tissue. We can learn about the nature of competitive fitness from all the reported pathways able to induce CC. Along the last 15 years, the field has exploded revealing a vast set of pathways inducing CC. They comprise many cellular processes, like cell growth/proliferation, signalling transduction, patterning, stress or cell polarity. Among these pathways, complex cross-talk regulation and pleiotropic relationships are established, which makes it difficult to set a clear classification. Nevertheless, we will consider here a Metabolic CC and a Structural CC (Figure 2).

2.1.1 Metabolic Cell Competition

CC can be induced by deficiency in pathways involved in cell growth and biosynthesis, like MYC (Johnston et al., 1999; De La Cova et al., 2004; Moreno and Basler, 2004), genes encoding ribosomal proteins (Rps) (Morata and Ripoll, 1975; Simpson, 1979) or the helicase 25E (which provokes reduced protein synthesis) (Nagata et al., 2019). CC is also induced by pathways implicated in proliferation and signal transduction, like RAS (Karim and Rubin, 1998; Prober and Edgar, 2000), SRC (Enomoto and Igaki, 2013; Kajita et al., 2010), BMP/DPP (Burke and Basler, 1996; Sancho et al., 2013), HIPPO (Tyler et al., 2007; Neto-Silva et al., 2010; Ziosi et al., 2010) or JAK-STAT (Rodrigues et al., 2012). Moreover, pathways related with metabolism and stress can be included in this group, e.g. P53 (Bondar and Medzhitov, 2010; Dejosez, 2013), mTOR (Bowling et al., 2018) or autophagy (Sancho et al, 2013). Alteration of mitochondrial dynamics through DRP1/MFN2 proteins (Lima et al., 2020) or the activation of stress responses as oxidative stress (Kucinski et al., 2017) can also trigger CC.

Alteration of many of these pathways can decrease fitness conferring cells a loser status or increase it, inducing Supercompetition. Moreover some of these pathways have been reported both in *Drosophila* and mammals, arguing for a deep conservation (Amoyel and Bach, 2014; Baker, 2020; Bowling et al., 2019; Clavería and Torres, 2015; Gregorio et al., 2016). Epistatic relationships among these factors suggest they could play a role in a common pathway regulating competitive fitness. In this context, MYC has been proposed as a general downstream fitness reporter. We will here mention some of these

epistatic relationships.

BMP inhibits P53, which in turn inhibits mTOR signalling (Bowling et al., 2018), a principal regulator of autophagy (Kim et al., 2015). Alteration of any of these components can induce CC. Interestingly, the authors proposed that loser cells defective for BMP (*bmpr1a*$^{-/-}$), autophagy (*atg5*$^{-/-}$) or tetraploid cells (4n), show less MYC levels than WT cells when in co-culture (Sancho et al., 2013). RAS and HIPPO also regulate MYC and MYC function is required for HIPPO-driven CC (Prober and Edgar 2000; Neto-Silva et al., 2010; Ziosi et al., 2010). Moreover, *Minute* mutations are enough to block Myc supercompetition (Moreno and Basler, 2004), suggesting that ribosomal proteins function downstream Myc in defining competitive fitness. Interestingly, during *Minute* and Myc-driven CC, loser cells display less BMP/Dpp signalling (Moreno et al., 2002; Moreno and Basler, 2004). Moreover, Dpp upregulation can rescue WT cells during Myc supercompetition. Additionally, *Minute* cells upregulate Nrf2 (key factor inducing oxidative stress response) whose overexpression in the absence of stress is sufficient to induce CC, (Kucinski et al., 2017), demonstrating that *Rp* heterozygosity plays a role in CC beyond protein translation (Lee et al., 2018).

Eventually, some pathways that regulate growth play also a role in patterning, differentiation and cell identity. Thus, mis-patterned cells can be recognised and eliminated by WT neighbouring cells. In this way, CC has been reported by altered BMP/Dpp (Adachi-Yamada et al., 1999; Milán, 2002), Wnt signalling (Akieda et al., 2019; Suijkerbuijk et al., 2016; Vincent et al., 2011) and pathways involved in differentiation such as Notch (Alcolea et al., 2014) or *bam* and *bgcn* (Jin et al., 2008).

2.1.2 Structural Cell Competition

Alteration of some genes involved in apico-basal polarity has been described to induce CC. Apico-basal polarity is controlled by different protein modules as the basolateral complex SCRIB, which is formed by Dlg, Lgl and Scrib proteins. In *Drosophila*, homozygous mutants of these proteins generate neoplastic formations[5] during larval development that eventually kill the animal. For that reason, these genes were called neoplastic tumour suppressor genes, nTSG (Bilder, 2004). Notably, these mutant tumorigenic cells are eliminated when surrounded by WT cells (Brumby and Richardson, 2003; Woods and Bryant, 1991; Menéndez et al., 2010). Other apico-basal components that induce CC are Mahjong (Tamori et al., 2010) and Crumbs (Chen et al., 2010; Hafezi et al., 2012).

Ras^{V12} and Src

Ras^{V12} mutation and v-Src transformation cause tissue overgrowth in epithelia, however, when surrounded by WT cells, mutant cells are eliminated (Enomoto and Igaki, 2013; Hogan et al., 2009; Kajita et al., 2010; Vidal et al., 2006). Although not directly involved in apico-basal polarity, they generate a similar CC model. Upon interaction with WT cells, mutant cells are eliminated by apoptosis, apical extrusion and basal

[5] Abnormal growth in which cells overproliferate, lose normal adhesion, shape and are unable to differentiate. On the contrary, hyperplasia refers to normally shaped, overproliferating cells that remain in the epithelium and differentiate (Bilder, 2004).

protrusion.

Endosomal trafficking

Endosomal transport control recycling or degradation of plasma membrane components. In similarity with some polarity genes, different endocytic genes behave as nTSGs in *Drosophila* (Menut et al., 2007). An explanation could be that endocytic transport can regulates apico-basal polarity by controlling the levels of membrane proteins essential in polarity, as Crumbs (reviewed in Eaton and Martin-Belmonte, 2014). Thus, endocytic mutant cells lose shape and overgrowth but are eliminated in the presence of WT cells. These genes include: *vps25* (Herz et al., 2006), *rab5* (Ballesteros-Arias et al., 2013), *tsg101* (Moberg et al., 2005) or *avl* (Lu and Bilder, 2005). Additionally, defective endosomal transport generate aberrant endosomal structures, in which active receptors continue signalling. In fact, mutants for endocytic genes, show increased Notch signalling.

Notably, in contrast to metabolic CC, in the context of polarity deficient mutants, loser cells are the faster proliferating with tumorigenic potential and CC acts as a tumour suppressor mechanism.

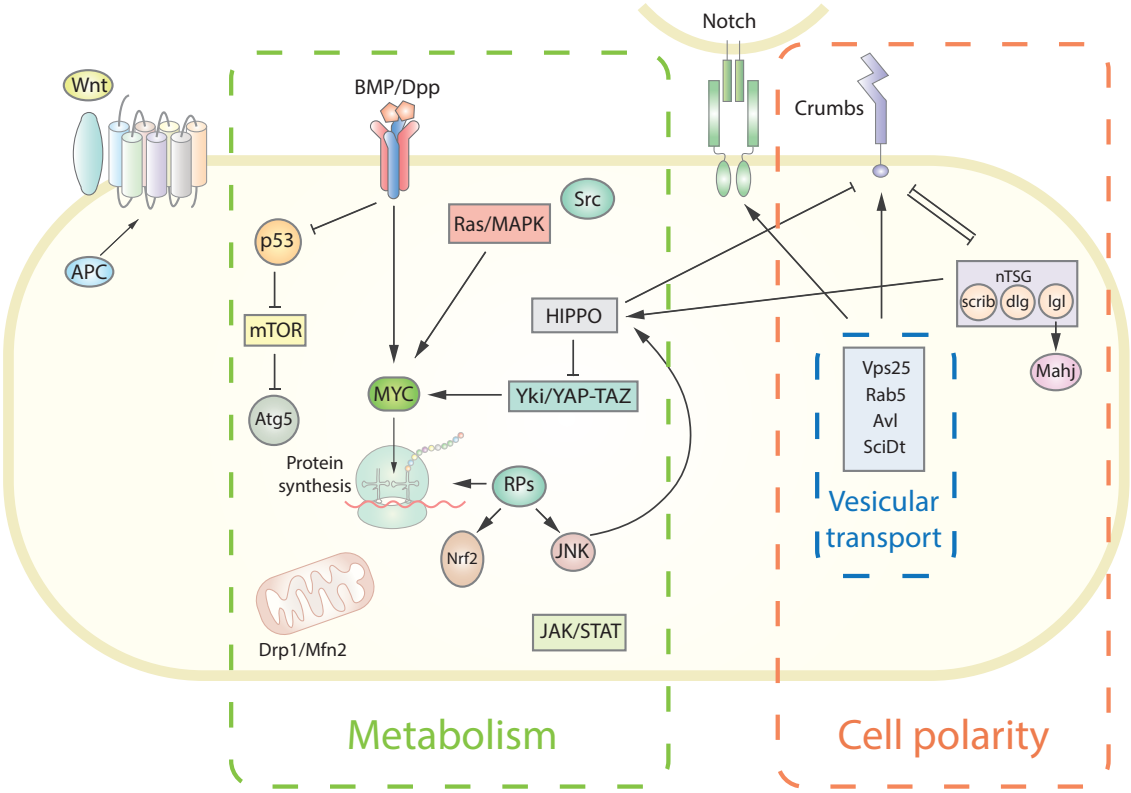

Figure 2. Pathways involved in CC.

Schematic representation of different pathways whose differential activity induce CC. These pathways are divided in growth and metabolic associated pathways and cell polarity related pathways. Some of the crosstalk regulations between factors and pathways are represented (Based on (Clavería and Torres, 2015)).

2.1.3 Polarity and metabolic crosstalk-regulation

Crosstalk-regulation among structural and metabolic pathways have been reported. Indeed, in a homotypic environment, apico-basal impairment increases overgrowth by inhibiting Hippo pathway, which contributes to tumour formation. Remarkably, the confrontation with WT cells reverses the situation and makes mutant cells to downregulate Hippo (Chen et al., 2012; Doggett et al., 2011; Enomoto and Igaki, 2013; Froldi et al., 2010; Grzeschik et al., 2010; Hafezi et al., 2012). In this vein, some polarity deficient clones can be rescued if surrounding by *Minute* cells (Froldi et al., 2010; Grzeschik et al., 2010) or by overexpressing growth/proliferating pathways as Yki or Myc (Chen et al., 2012; Froldi et al., 2010).

2.2 Fitness Comparison Mechanisms

Along the years, different elements reporting fitness and comparison models have been described.

2.2.1 The FLOWER code

Moreno and collaborators have proposed a comparison model based on the expression of the different isoforms of the transmembrane protein Flower.

In *Drosophila*, *fwe* encodes three transmembrane proteins: $Fwe^{ubiquitous\ (ubi)}$, $Fwe^{lose\text{-}A}$ and $fwe^{lose\text{-}B}$. In the wing disc, *lose* isoforms are expressed in loser cells in different models of CC. Indeed, induction of fwe^{lose} is enough to turn WT cells into losers. The authors proposed that Fwe isoforms report cell fitness downstream Dpp signalling, MYC or *Minute* (Rhiner et al., 2010). Notably, overexpression of mouse Fwe isoforms in mammalian cell cultures did not induce CC while they did in *Drosophila* wing disc (Petrova et al., 2012). In humans, two *winner* and two *loser* isoforms were found. $Fwe^{-/-}$ cells overexpressing *loser* isoforms are eliminated by $Fwe^{-/-}$ cells overexpressing *winner* isoforms (Madan et al., 2019).

2.2.2 Mechanical sensing

Differences in mechanical properties such as membrane elasticity or cell attachment ability have been proposed as a fitness-reporting and comparative mechanism. For instance, Ras, Src or Wnt alteration can modify cell attachment and membrane elasticity (Akieda et al., 2019; Vidal et al., 2006). Differences in β-catenin/E-cadherin expression, proteins involved in cell-cell adhesion, have also been shown to trigger CC in *Drosophila* ovaries, zebrafish embryo or mammalian cell culture (Akieda et al., 2019; Jin et al., 2008). Notably, mechanical features can lead to *loser* cell outcompetition (which will be discussed below).

2.2.3 Diffusible signals in fitness comparison

Diffusible signals have been reported as a mechanism to report fitness and induce *loser* outcompetition. Cell culture experiments in which *winner* and *loser* cells are physically separated but share the same culture medium (known as Transwell cell culture system), have shown that *loser* outcompetition only takes place when sharing medium with *win-*

ner cells (Sancho et al., 2013; Senoo-Matsuda and Johnston, 2007).

2.3 *Loser* Cell Elimination

Concerning *loser* elimination, apoptotic cell death is the most broadly observed mechanism so far, although other mechanisms like epithelial extrusion, induction of senescence or differentiation have also been reported (Clavería and Torres, 2015; Gregorio et al., 2016). Most of what is known about the molecular pathways involved in *loser* cell elimination has been studied in *Drosophila*, while in mammals or zebrafish it has been less characterised.

2.3.1 Apoptosis

Activation of the apoptotic machinery has been widely reported in many CC scenarios.

In ***Drosophila***, activation of stress signalling pathways such as JNK or NF-κβ and induction of pro-apoptotic genes, including *hid* and *rpr* have been reported in *loser* cells upon competitive interactions (De La Cova et al., 2004; Meyer et al., 2014; Moreno and Basler, 2004). Additionally, cell stress responses as oxidative stress, proteotoxic stress or autophagy have been reported essential for *loser* cell death (Kucinski et al., 2017; Nagata et al., 2019). In addition, AZOT has been proposed as a specific factor in Cell Competition required for *loser* cell death (Merino et al., 2015). In **mammals**, CASP3 activation in *loser* cells upon competitive interaction has been extensively described (reviewed in Clavería and Torres, 2015; Sancho et al., 2013). Additionally, activation of stress kinases like P38 and stress response factors, such as p53, have been involved in *loser* cell elimination (Díaz-Díaz et al., 2017; Hogan et al., 2009; Wagstaff et al., 2016). Interestingly, the intrinsic apoptotic pathway but not the extrinsic one leads to *loser* elimination in the mouse epiblast (Clavería et al., 2013). In **zebrafish**, Smad2/3 activation leads to ROS production and DNA damage, which induces apoptosis in *loser* cells by downregulating anti-apoptotic factor Bcl-2 (Akieda et al., 2019).

2.3.1.1 Stress sensors: JNK, P53

Here, we highlight the role of JNK and P53 as important stress sensor factors regulating apoptosis in CC.

JNK. In Metabolic-CC, JNK regulates *loser* apoptosis in competition models driven by mutations in *Minute* (Moreno et al., 2002), *Dpp* (Ziv et al., 2009) or *APC* (Suijkerbuijk et al., 2016), but not by Hippo (Tyler et al., 2007) or JAK-STAT (Rodrigues et al., 2012). In MYC-induced CC, some authors described that loser apoptosis is JNK-dependent (Moreno and Basler, 2004), while others found it is JNK-independent (De La Cova et al., 2004). Notably, it has been described that the combination of JNK and autophagy activation in *loser* cells is required to trigger *loser* apoptosis (Nagata et al., 2019).

Concerning Polarity CC, JNK plays a consistent role in *loser* apoptosis in CC models as *lgl* (Menéndez et al., 2010), *scrib* (Chen et al., 2012; Igaki et al., 2009), *src/ras* (Vidal et al., 2006) or endosomal (Herz et al., 2006) induced CC. Interestingly, in *lgl*, *scrib* or *src/ras* induced-CC, JNK promotes tumorigenesis. However, in contact with WT cells, JNK contributes to *loser* cell death. In addition to apoptosis, JNK also inhibits proliferation

in *loser* cells (Kucinski et al., 2017) and increases proliferation non-autonomously in *winner* cells (Chen et al., 2012; Enomoto and Igaki, 2013). Notably, JNK seems to exerts these effects by promoting different Yki expression in *winner* and *loser* cells (Enomoto and Igaki, 2013). Indeed, Igaki and collaborators reported two mechanisms leading to this JNK function switch in mutant cells from tumorigenic (in homotypic conditions) to pro-apoptotic (upon contact with WT cells):

- **Sas-PTP10D.** Sas and PTP10D are transmembrane proteins. In CC, they accumulate in the interface between *winner* and *loser* cells. These proteins interact and inhibit EGFR-RAS signalling in *loser* cells. In homotypic conditions, mutant cells activate EGFR-RAS, which collaborate with JNK to induce overgrowth by Yki activation. However, in contact with WT cells, Sas-PTP10D interaction inhibits EGFR-RAS in mutant cells and JNK displays pro-apoptotic functions (Yamamoto et al., 2017).

- **Serpin5.** Toll signalling activated by Späetzle (Spz) ligand, contributes to *scrib*$^{-/-}$ cells overgrowth in homotypic conditions, via JNK-Yki. However, in contact with WT cells, the secreted protein Serpin5 inhibits Spz and Toll activation in mutant cells, leading to their elimination via JNK (Katsukawa et al., 2018). However, the involvement of EGFR-RAS after Toll inhibition was not explored.

Curiously, JNK modulation does not induce CC, indicating that JNK does not regulate fitness. Instead, it regulates *loser* elimination after fitness comparison has occurred (Kucinski et al., 2017).

In mammals, a function of JNK in *loser* apoptosis is not clear so far. Indeed, in *scrib* induced CC in mammalian epithelia, *loser* apoptosis does not depend on JNK, but other stress sensor proteins as P53 and P38 (Norman et al., 2012; Wagstaff et al., 2016).

P53. In CC, P53 has been involved both in regulating fitness and *loser* elimination upon competitive interactions. In mammals, it has been described in multiple CC scenarios, while its role in *Drosophila* is less clear. For instance, modulation of P53 induces CC in Hematopoietic Stem cells (HSPCs) (Bondar and Medzhitov, 2010; Marusyk et al., 2010), mammalian epithelial cells (Fernandez-Antoran et al., 2019; Wagstaff et al., 2016) or in mouse embryo and fast-proliferating adult tissues (Dejosez et al., 2013; Zhang et al., 2017).

Regarding *loser* apoptosis, P53 is involved in elimination of *scrib*$^{-/-}$ cells in mammalian epithelium and mouse ESCs (Díaz-Díaz et al., 2017; Wagstaff et al., 2016). Indeed, P53 disruption rescues tetraploid and *Bmp*-deficient *loser* cells from CC in the mouse epiblast and ESCs (Bowling et al., 2018).

Notably, in the bone marrow and cultured mammalian epithelial cells *p53* deficiency appears insufficient to induce Supercompetition but mild P53 activation through radiation or Nutlin-3 treatment is required for WT cells to be eliminated by *p53*-deficient cells (Bondar and Medzhitov, 2010; Wagstaff et al., 2016). In ESCs, it is necessary to initiate differentiation to induced CC b etween *p53*-deficient and WT cells (Bowling et al., 2018; Dejosez et al., 2013). In contrast, in the mouse epiblast, *p53*-deficient cells outcompete WT cells without treatment, probably because it is subjected to a natural differentiation process (Dejosez et al., 2013).

In *Drosophila*, *p53*$^{-/-}$ cells did not outcompete WT cells (De La Cova et al., 2004), however, P53 activation via radiation or Nutlin-3 was not performed. Additionally, *Minute*$^{+/-}$ cells were outcompeted in a null *p53* background, indicating that P53 is not required for *loser* elimination in this model of competition (Kale et al., 2015).

2.3.1.2 Innate immunity

Jonhston and collaborators proposed that unfit cells are eliminated by components of the innate immunity, in a similar way to infected or altered-self cells. They found that during Myc-induced and Minute-induced CC, Toll-related receptors (TRR) are more expressed in *loser* cells and they are activated by the ligand Spätzle, leading to NF-κβ activation and apoptosis in *Drosophila* wing disc (Alpar et al., 2018; Meyer et al., 2014). In a later study (Germani et al., 2018), this type of TRR-mediated competition was found to depend on the septic status of flies, indicating that a systemic response to infection is required for TRR-mediated cell competition.

In contrast to the involvement of TRR signalling in these models, in *scrib*$^{-/-}$ induced CC, Toll activation turns *loser* cells into *winners* via Yki activation (Katsukawa et al., 2018).

2.3.1.3 Diffusible signals in loser cell death

Medium from a co-culture of *winner* and *loser* cells (also referred as "conditioned cell medium, cCM") can induce the death of naïve *loser* cells and stimulate proliferation of naïve *winner* cells. Notably, *loser* and *winner* cells receiving cCM never interacted before between them (De La Cova et al., 2014; Senoo-Matsuda and Johnston, 2007). These experiments indicate that in this model the mechanisms leading to *loser* cell elimination and winner compensation are triggered by diffusible factors secreted to the medium by competing cells. In contrast to the "transwell experiments" previously described, here comparative interactions (if they occur), could be contact-dependent. Notably, the proposal of secreted killing signals implies interaction with intrinsic features of *winner* and *loser* cells that determine their differential response.

On the other hand, different works reported no effects in *loser* or *winner* cells when using conditioned medium or setting up transwell experiments (Clavería et al., 2013; Penzo-Méndez et al., 2015; Wagstaff et al., 2016). Indeed, in most cases it has been reported that only *loser* cells at or very close to the boundary between *winner* and *loser* cells are eliminated by CC and that CC requires cell contact (Enomoto and Igaki, 2013; Li and Baker, 2007; Penzo-Méndez et al., 2015; Simpson and Morata, 1981; Tamori et al., 2010; Villa del Campo et al., 2014).

Here we describe some secreted signals involved in *loser* cell apoptosis:

- **Notum.** In Wnt-supercompetition in *Drosophila*, Notum is proposed to be expressed in *winner* cells and inhibit Wnt signalling in surrounded *loser* cells. This increases Wnt signalling differences between *winner* and *loser* cells, which is required for *loser* cell death (Vincent et al., 2011).

- **Serpin5.** In *scrib*$^{-/-}$ induced-CC in *Drosophila* eye wing, Serpin5 is secreted by WT winner cells, which inhibits Toll signalling in loser cells. Toll inhibition contributes to

scrib$^{-/-}$ elimination through JNK (Katsukawa et al., 2018).

- **SPARC.** In contrast with the previous factors, SPARC is secreted by loser cells and provides certain protection against apoptosis in different models of CC in *Drosophila* (*Minute*, Myc-supercompetition, *lgl*$^{-/-}$ or Dpp induced-CC) (Portela et al., 2010).

2.3.1.4 Azot

Moreno and collaborators reported Azot as a protein specifically induced in suboptimal viable cells that are eliminated by CC. Azot is expressed in loser cells in different CC models in *Drosophila* (Myc-supercompetition, Dpp, Wg, JAK-STAT, *Minute* or *Fwe*^{lose} induced-CC) but not in others, like polarity-CC or CC induced by *src* deficiency. Azot is required for loser cell elimination, although its overexpression is not sufficient to induced cell death in the wing disc. Irradiation can induce Azot, however is not induced upon the activation of pro-apoptotic factors like Hid, Eiger, Bax or JNK, and it is not inhibited by P35, Bcl-2 or the P53 apoptotic pathway. Additionally, it can be blocked by Fwe-lose downregulation or Sparc activation in Myc-supercompetition (Merino et al., 2015). These observations suggest Azot is upstream apoptotic pathway but downstream Fwe and Sparc.

2.3.1.5 Elimination of dead cells

Once loser cells are dead, they are cleared from the tissue. In Myc-supercompetition in the *Drosophila* wing disc, loser cells are basally extruded and removed by hemocytes (Lolo et al., 2012). Additionally, loser dead cells have been reported to be engulfed by neighbouring cells. An interesting case is when intact-live cells are engulfed (process termed "entosis" (Overholtzer et al., 2007) and loser death is triggered upon engulfment. This has been described in *Drosophila* in *scrib* induced-CC (Ohsawa et al., 2011) and in *Minute*-CC (Li and Baker, 2007), although data in *Minute*–CC have not been reproduced in (Lolo et al., 2012). In the mammalian epiblast and ESCs CC, engulfment of intact cells has also been reported (Clavería et al., 2013).

2.3.2 Mechanical Cell Competition

Loser cells can be eliminated by mechanical compaction and extrusion from epithelia. For instance, in *ras*^{V12} induced CC and Myc-supercompetition, loser cells are delaminated upon mechanical compaction from the epithelium (Levayer et al., 2015; Levayer et al., 2016).

Additionally, *src* and *ras*^{V12} mutant cells are extruded by WT cells in the zebrafish gastrula (Kajita et al., 2010), mammalian cultures (Hogan et al., 2009; Kon et al., 2017) and in the mouse intestine (Kon et al., 2017) in a process called Epithelial Defense Against Cancer (EDAC). Interestingly, *ras*^{V12} loser cells previously to be extruded undergo a reduction of mitochondrial function driven by the PDK (Kon et al., 2017). Furthermore, this metabolic switch is required for cell extrusion.

Scrib$^{-/-}$ mutant cells are also extruded from the *Drosophila* eye disc and mammalian epithelial cell cultures (Vaughen and Igaki, 2016; Wagstaff et al., 2016). At least in *Drosophila*, this process is controlled by the Slit-Robo2-Ena pathway and E-cadherin upon interaction with WT cells (Vaughen and Igaki, 2016). In cultured mammalian epithelial

cells, WT cells are also extruded by *p53*$^{-/-}$ cells upon mild P53 activation (Wagstaff et al., 2016).

2.3.3 Cell displacement

Additional outcompetition mechanisms rely on loser cell displacement instead of cell death. This takes place in stem cell-sustained tissues by the selective differentiation or senescence of loser cell lineages, so that loser cell self-renewal is prevented.

In *Drosophila* ovaries, less fit germline stem cells (GSCs) are pushed out from the niche (Jin et al., 2008; Rhiner et al., 2009). Less-fit cells undergo differentiation in CC in mouse oesophageal epithelium (Alcolea et al., 2014; Fernandez-Antoran et al., 2019; Snippert et al., 2014). In the mammalian adult bone marrow and embryo, *p53*$^{-/-}$ cells can also outcompete WT cells by reducing WT proliferation or inducing their senescence (Bondar and Medzhitov, 2010; Zhang et al., 2017).

2.4 Winner Compensation Fitness.

Despite the elimination of loser cells, CC does not show a big influence in tissue size or morphology (De La Cova et al., 2004; Morata and Ripoll, 1975; Simpson, 1979; Villa del Campo et al., 2014). This suggests the existence of mechanisms that stimulate winner cells to compensate for loser cell elimination.

Increased proliferation in winner cells due to CC has been described in different CC models (Bowling et al., 2018; Sancho et al., 2013; Senoo-Matsuda and Johnston, 2007) but not in others (Clavería et al., 2013). A proposed mechanism is that loser cells when undergoing CC-induced apoptosis secrete growth factors that enhance non-autonomous proliferation in winner cells (Ballesteros-Arias et al., 2013; Takino et al., 2014). In fact, the production of proliferative signals seems to be a general feature of apoptotic cells (Pérez-Garijo et al., 2004; Ryoo et al., 2004). Other models propose that loser cells enhance winner stimulation through different signalling pathways, like Upd/Dome, Yki or P53 (De La Cova et al., 2014; Kolahgar et al., 2015; Kucinski et al., 2017; Takino et al., 2014).

Interestingly, in the postmitotic follicular epithelia, winner cells undergo hypertrophy instead of proliferation to compensate loser outcompetition (Tamori and Deng, 2013).

3 ROLES OF CELL COMPETITION

The characterization of the physiological roles of CC relies on the identification of endogenous CC models, as well as the specific inhibition of CC without affecting other cellular processes. Although these aspects still represent a challenge, relevant roles have been proposed for CC.

3.1 Quality Control

CC eliminates viable cells, suggesting that CC optimizes tissues by selecting the best available cells and eliminating those that could compromise tissue performance.

Azot was described in *Drosophila* as a CC-specific component in loser cells that promotes their elimination. *Azot* null flies develop malformations in the wings and are less resistant to radiation. In addiction, they display age-associated features in the adult brain tissue and present a reduced lifespan (Merino et al., 2015). This suggests that CC eliminates suboptimal cells ensuring tissue health and lifespan. On the other hand, the addition of three *azot* extra copies improves irradiation resistance, reduces neurodegenerative vacuoles in the adult brain and prolongs lifespan (Merino et al., 2015). A subsequent study showed that *azot* is upregulated in a model of Alzheimer´s diseases in *Drosophila,* while an extra copy of azot contributes to the elimination of less fit neurons, which improved brain function (Coelho et al., 2018).

CC has been described to eliminate stressed cells in different models. For instance, in the epiblast, loser cells exhibit different stress indicators including altered mitochondrial function or high P53 expression (Díaz-Díaz et al., 2017; Lima et al., 2020; Zhang et al., 2017). Moreover, in the adult, CC eliminates cells displaying oxidative stress, proteotoxic stress or active P53 response in *Drosophila* (Bondar and Medzhitov, 2010; Kucinski et al., 2017; Wagstaff et al., 2016; Zhang et al., 2017; Baumgartnert el al., 2021).

Furthermore, CC has been proposed as a mechanism to removed cells carrying chromosomal abnormalities (Bradley et al., 2014; Kale et al., 2015; Sancho et al., 2013), mispatterned or undesired differentiating cells (Díaz-Díaz et al., 2017; Rhiner et al., 2009).

3.2 Regeneration

CC has been reported to contribute to the removal of damaged cells after injury in the *Drosophila* brain (Coelho et al., 2018; Moreno et al., 2015). Additionally, in tissues such as the heart, the hematopoietic system or the liver CC can function as a mechanism by which a fitter population expands (Bondar and Medzhitov, 2010; Menthena et al., 2011; Oertel et al., 2006; Villa del Campo et al., 2014).

3.3 Tumour Formation

CC has been described either as a tumour suppressor or as an oncogenic mechanism depending on the context.

3.4.1 Tumour suppressor

Tumorigenic mutant cells for polarity genes (*lgl*, *dlg*, *scrib*), are eliminated by WT cells. Indeed, if associated in large-enough groups, they still can induce tumours as just mutant cells at the border of the clone are subjected to CC and the mutant clone overgrowth (Ballesteros-Arias et al., 2013; Menéndez et al., 2010).

Cells overexpressing ras^{V12} or *src*, which can generate tumours, are normally extruded apically from the epithelia by a process called EDAC (Hogan et al., 2009; Kajita and Fujita, 2015; Kon et al., 2017; Vidal et al., 2006). However, the extrusion can also take place basally, in which case, the mutant cells are retained in the tissue and this could contribute to tumour formation. Interestingly, high-fat diet attenuates apical elimination of ras^{V12} transformed cells in mouse intestinal and pancreatic epithelia and promoted basal extrusion and tumour formation (Sasaki et al., 2018). This demonstrates how environ-

mental conditions, the diet in this case, can modify CC.

In the immune system, T cells precursors of the thymus are constantly replaced by younger bone marrow precursors by CC. When the income of bone marrow progenitors is prevented, the aged thymic T-cell precursors autonomously renovate the thymus and produce tumours (Martins et al., 2014).

3.4.2 Tumour promoter

A set of Supercompetition models are based on alterations in signalling pathways and transcription factors involved in cell growth, patterning or metabolism such as *myc*, *p53* or *notch*. Mutant cells for these genes eliminate WT cells and expand through the tissue. Although these Supercompetition models do not directly generate tumours, CC can extend oncogenic mutations facilitating the phenomenon of field cancerization and increasing the chances that a second hit initiates tumour formation (Rhiner and Moreno, 2009). For instance, overexpression of ras^{V12} or *notch* in $scrib^{-/-}$ or $lgl^{-/-}$ isolated cells restores their neoplastic capacity (Brumby and Richardson, 2003; Menéndez et al., 2010) and *p53* mutant cells, normally eliminated in a WT background, persist in the tissue in a ras^{V12} background (Watanabe et al., 2018).

Evidence from the role of cell competition factors in oncogenesis came also from the discovery that *flower*-deficient mice show decreased susceptibility to papilloma (Petrova et al., 2012). Additionally, in different types of human tumours, cancer cells express Fwe winner isoforms, while neighbouring WT cells express loser isoforms. In fact, inhibition of *fwe* reduces tumour growth (Madan et al., 2019). Additionally, in a model of intestinal competition, $apc^{-/-}$ cells or cells overexpressing *egfr* and *miR-8* outcompete WT cells generating tumours (Eichenlaub et al., 2016; Suijkerbuijk et al., 2016).

EMBRYONIC STEM CELLS AND PLURIPOTENCY

Pluripotency is the capacity of cells to generate all embryonic lineages but not the complete set of extraembryonic tissues (Nichols and Smith, 2009a). In the early mouse embryo between day 3.5 and 6.5 of development (E3.5-E6.5), this characteristic corresponds to a group of cells in the blastocyst called epiblast cells. Pluripotency must be understood not as a single status, but as a set of complex and dynamics stages that evolve in a continuum manner during early development. Different stages can be distinguished by differences in gene expression, epigenetic landscape, signal transduction or metabolic profile (Nichols and Smith, 2009a; Sperber et al., 2015).

Previous to implantation in the uterus, at E3.5, epiblast cells present a pluripotency state termed “naïve” or “ground” (Hackett and Surani, 2014). This state is characterized by homogenous expression of pluripotent transcription factors and the elimination of gametic epigenetic silencing, which generates a hypomethylated “open” chromatin. As the mouse embryo develops from pre-implantation to post-implantation, pluripotent epiblast

[6] Group of pluripotent cells in the blastocyst at E3.5, previous to the segregation into the epiblast and the primitive endoderm (Nichols and Smith, 2009a).

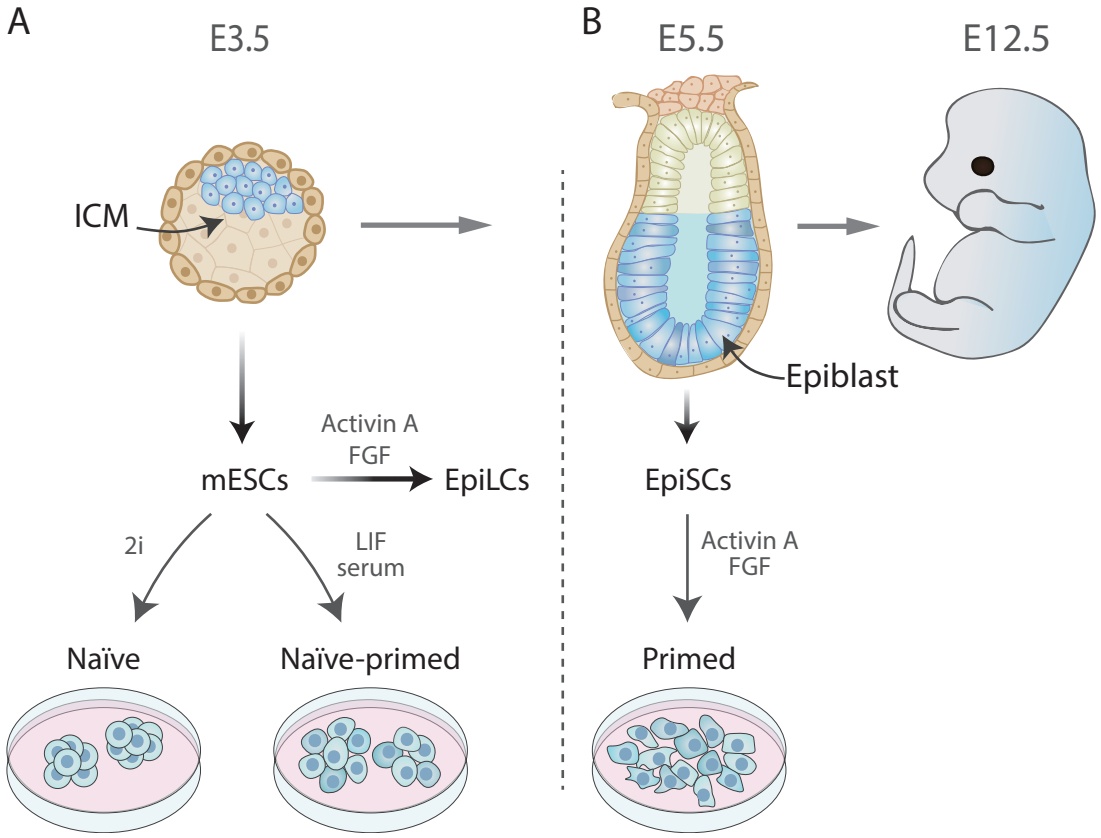

Figure 3. Types of pluripotent stem cells

A. mESCs are derived from the Inner Cell Mass (ICM) at E3.5. mESCs can be maintained in more naïve pluripotent status with the addition of "2i" into the medium. By using the conventional medium "serum + LIF" mESCs exhibit a more cell-to-cell heterogeneous status of pluripotency. Alternatively, mESCs can be maintained in medium containing Activing A and FGF to obtain EpiLCs. **B.** From the epiblast cells of the mouse embryo at E5.5, EpiSCs can be derived, which exhibit a primed status of pluripotency and are maintain in medium containing Activin A and FGF.

cells evolve in a continuum manner and transit from a "naïve" towards a "primed" pluripotent status. Although both states of pluripotency are characterized by the expression of a set of "core" pluripotent transcription factors (including OCT4, SOX2 and NANOG), some differences have been reported. For instance, naïve cells express some specific transcription factors such as REX1 and KLF4, while expression of FGF5 and OTX2 have been reported exclusively in primed cells. Another differential aspect is the inactivation of one X chromosome in female cells in primed status (Nichols and Smith, 2009a; Tosolini and Jouneau, 2016). Eventually, pluripotency finishes between E6.5-E7.5, when epiblast cells differentiate into the three germ layers during gastrulation (Posfai et al., 2014).

Pluripotent cells possess a specific metabolic profile reflecting their rapid proliferation. Proliferation requires energy and significant amounts of nucleotides, amino acids and lipids to assemble the two daughter cells. Pluripotent cells divert part of the glucose to the generation of precursors for fatty acid, amino acids, and nucleotides synthesis,

conferring them a highly glycolytic metabolism (Vander Heiden and DeBerardinis, 2017; Varum et al., 2011). Interestingly, as the epiblast transits from the pre-implantation to the post-implantation stage, it undergoes a metabolic remodelling characterized by a decreased in oxygen consumption and increased glucose uptake, which is converted into lactate (Sperber et al., 2015). In fact, the highest rate of proliferation ever reported in mammalian cells takes place in cells at the onset of gastrulation.

1. PLURIPOTENCY *in vitro*

Different pluripotency states can be recreated *in vitro*. Typically, two kind of pluripotent stem cells can be derived from early mouse embryos.

Mouse embryonic stem cells (mESCs) are derived from the inner cell mass[6] of the blastocyst (Evans and Kaufman, 1981) or from the naïve epiblast, after epiblast-primitive endoderm segregation (Brook and Gardner, 1997) (Figure 3A). mESCs can be propagated indefinitely and differentiate into all three germ layers *in vitro*. When undifferentiated ESCs are returned to the preimplantation embryo, they integrate into the epiblast and contribute to the entire adult organism, including the germ line (Bradley et al., 2014).

The originally described ESCs culture medium results in a heterogeneous mixture of cells with different pluripotentcy status. This conventional medium includes fetal bovine serum, which contains factors that prevent differentiation (e.g. BMP4), but also FGF or activin-like activities which promote the exit from naïve pluripotency. Additionally, it contains leukemia inhibitory factor (LIF), which is required for ESCs proliferation and maintenance of pluripotency in the absence of mouse embryonic fibroblast (MEFs) (Smith et al., 1988; Williams et al., 1988). This “serum + LIF” condition generates a certain cell-to-cell heterogeneity in the pluripotency status (Boroviak et al., 2014; Ying et al., 2008). Notably, by adding the inhibitors PD03 and CHIRON to the medium, mESCs are maintained in a more homogenous naïve-state that resembles the E3.5 pre-implantation epiblast. PD03 inhibits the FGF/ERK signalling, while CHIRON inhibits GSK3, two important differentiating pathways. This medium was is known as “2i” culture conditions (Sato et al., 2004; Ying et al., 2008) (Figure 3A).

Another pluripotent cell type, known as epiblast stem cells (EpiSCs), are derived from the postimplantation epiblast at around E5.5-6.5 (Figure 3B). These pluripotent cells contribute to all three germ layers and the germ line when transplanted into postimplantation embryos but not when transplanted into the preimplantation epiblast (Huang et al., 2012). The medium used to maintain EpiSCs contains Activin A and Fibroblast Growth Factor (FGF) (Brons et al., 2007; Tesar et al., 2007). Additionaly, mESCs maintained under similar cultured conditions acquire an pluripotent state comparable to the primed E5.5 epiblast, and are called epiblast-like cells (EpiLCs) (Yamamoto et al., 2011) (Figure 3A).

ESCs and EpiSCs, although both originated from the epiblast lineage, represent different developmental stages. Thus, naïve ESCs correspond with a more immature state of pluripotency (E4.0), whereas EpiSCs resemble the primed state (E5.5-E6.5). In similarity to *in vivo* stages, both cell types share the expression of essential pluripotent factors (OCT4, SOX2 and NANOG). However, they differ in chromatin state, expression profile or X-chromosome inactivation (Hackett and Surani, 2014). Regarding metabolism, mouse naïve-to-primed ESC transition is characterized by an increase in glycolysis and a decrea-

se in mitochondrial oxidative phosphorylation (OXPHOS) activity. Notably, while naïve ESCs show a wide range of energy substrate usage, primed cells can only use glucose. (Mathieu and Ruohola-Baker, 2017; Sperber et al., 2015; Tsogtbaatar et al., 2020).

P53 AND BCL-2 PROTEINS

1. P53

P53 was originally discovered as a 53kD protein bound to the viral SV40 T antigen, while studying tumour-inducing viruses, (Lane and Crawford, 1979; Linzer and Levine, 1979). Subsequent studies established P53 as the most frequent mutated tumour suppressor gene in human cancers (Baker et al., 1990).

P53 is an important transcription factor. Its most studied functions are the ability to promote cell cycle arrest, senescence and apoptosis in response to DNA damage, preventing the propagation of mutations. For that reason, P53 is known as the "guardian of the genome" (reviewed in Jain and Barton, 2018; Kastenhuber and Lowe, 2017). Indeed, *p53*$^{-/-}$ mice mayor phenotypes are an increased rate of tumour formation and resilience to radiation-induced apoptosis (Donehower et al., 1992).

P53 is post-translationally regulated by a set of proteins, the most important of which is MDM2, an ubiquitin ligase that facilitate P53 degradation (Haupt et al., 1997). Additionally, a wide range of posttranslational modifications control P53 activity, such as phosphorylation, acetylation, or methylation, as well as, SUMOylation or glycosylation (Kumari et al., 2014).

Apart from its traditional roles, P53 is currently known to regulate different processes like autophagy, metabolism, ROS production, cellular plasticity or differentiation. The biological output exerted by P53 depends on factors such as cell type, differentiation status or stress conditions (Kastenhuber and Lowe, 2017). Additionally, P53 has been described to exert non-transcriptional functions like centrosome duplication, apoptosis induction or inhibition of autophagy (reviewed in Green and Kroemer, 2009).

Importantly, excessive activation of P53 can lead to a decline in stem cell populations required for tissue homeostasis. This results in degeneration and age-associated diseases, such as neurodegenerative diseases (Kastenhuber and Lowe, 2017).

2. P53 IN PLURIPOTENT STEM CELLS

P53 plays important functions during embryonic development, for example, *p53*$^{-/-}$ mice present developmental abnormalities in the neural tube, eyes and testes at low penetrance (Danilova et al., 2008). Maintaining genomic stability is critical for pluripotent stem cells (PSCs), as they give rise to all the cells in the organism. It has been suggest that P53 is critical to maintain genome integrity and prevent mutations expansion through cell division (Song et al., 2010). Efforts to study the role of P53 in cell cycle arrest, apoptosis and senescence have generated controversial results and recent studies indicate that P53 function is modulated as pluripotent stem cells develop through different pluripotent stages (Jaiswal et al., 2020; Ter Huurne et al., 2020). On the other hand, it has

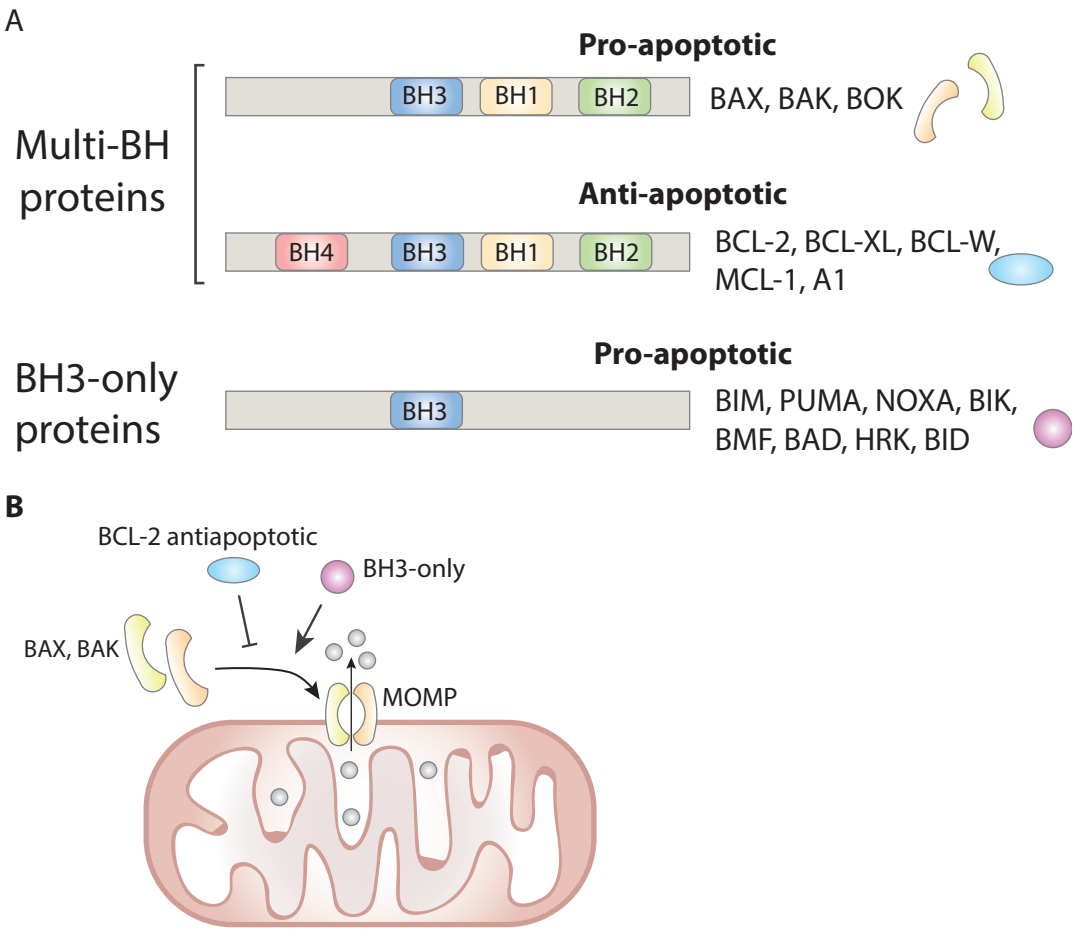

Figure 4. BCL-2 proteins

A. BCL-2 proteins are classified in multi-BH domains proteins that can be pro-apoptotic and antiapoptotic and BH3-only proteins, which are pro-apoptotic. **B.** Multi-BH pro-apoptotic proteins can oligomerize and form pores in the mitochondrial outer membrane, which is known as mitochondrial outer membrane permeabilization (MOMP). This allows the exit of pro-apoptotic factors (here represented as grey spheres), which trigger apoptosis. BH3-only proteins promotes MOMP, while antiapoptotic BCL-2 protein prevent it.

been proposed that P53 restricts cellular self-renewal, limits cellular plasticity and inhibits epigenetic reprogramming (Kastenhuber and Lowe, 2017). Indeed, P53 induces differentiation in PSCs upon genotoxic or oncogenic stress, as a mechanism to ensure the genomic stability (Jain et al., 2012; Li et al., 2012; Lin et al., 2005; Zhang et al., 2014). Additionally, P53 has been shown to regulate PSC metabolic status by inhibiting OXPHOS (Kim et al., 2019) and to induce anti-oxidant genes in response to oxidative stress (Liu and Xu, 2011).

3. BCL-2 PROTEIN FAMILY

B cell lymphoma-2 (BCL-2) family proteins are important components of apoptosis. Apoptosis is considered a controlled, energy-dependent mechanism by which damaged

or infected cells that may interfere with the normal functioning of the organism are eliminated. During apoptosis, activation of caspases leads to the cleavage of essential cellular components, such as cytoskeletal and nuclear proteins, causing cell shrinking and chromatin condensation. Eventually, these apoptotic corpses are removed by phagocytic cells without generating harm to the surrounding tissue (Yacoubian and Standaert, 2009). According to the stimulus inducing apoptosis, this process can be classified as extrinsic or intrinsic apoptotic pathway. While, extrinsic apoptosis relies on death-inducing ligands binding to cell surface receptors, which in turns activate the caspase cascade, intrinsic apoptosis depends on intracellular factors such as cellular stress and is executed through mitochondrial permeability regulation (Kroemer et al., 2009). In fact, mitochondria contains different pro-apoptotic factors such as Smac/DIABLO, apoptosis-inducing factor (AIF) and cytochrome c (cyt c), which are released upon apoptotic stimuli. BCL-2 family proteins are important factors regulating mitochondrial permeability and pro-apoptotic factors release (Siddiqui et al., 2015).

Different pro- and anti-apoptotic BCL-2 proteins have been described so far. Upon apoptotic stimuli, pro-apoptotic BCL-2 proteins BAX, BAK and BOK can oligomerize generating the "mitochondrial outer membrane permeabilization complex" (MOMP complex), which allows the formation of pores in the outer layer of the mitochondria and the release of different factors as cyt c, leading to apoptosis. BAX and BAK oligomerization is tightly regulated by the balance between the remaining pro- and anti-apoptotic BCL-2 proteins, which promotes or inhibits MOMP. Thus, this balance is essential to regulate the sensitivity to undergo apoptosis (Certo et al., 2006).

At structural level, all BCL-2 family proteins possess a conserved "BCL-2 homology (BH) domain. Indeed, they are classified as multi-BH BCL-2 proteins, which include anti-apoptotic (BCL-2, BCL-XL, BCL-W, MCL-1, A1, BCL-B) and pro-apoptotic (BAX, BAK, BOK) proteins. Additionally, there are BCL-2 proteins with a single BH domain, "BH3-only proteins" which exert a pro-apoptotic role (BIM, BAD, tBID, BMF, BIK, NOXA, PUMA, HRK). Two mechanisms have been suggested to explain BCL-2 proteins function. The "displacement" model proposes that BH3-only proteins lead to the release of BAX and BAK from the anti-apoptotic BCL-2 protein to initiated MOMP (Figure 4). The "direct activation" mechanism suggests that, additionally, some BH3-only proteins can also directly activate BAK and BAX through conformational changes (Certo et al., 2006). Although this family is widely regulated at the transcriptional level, proteins of the family can also be post-translationally activated by phosphorylation or cleavage. NF-κβ, c-MYC or P53 have been described as important regulators of BCL-2 proteins (Siddiqui et al., 2015). The balance between pro- and anti-apoptotic BCL-2 family proteins regulates susceptibility to MOMP. This mechanism, known as "mitochondrial priming", determines how close a cell is to undergoing MOMP (Certo et al., 2006). This mechanism allows the adaptation of apoptotic sensitivity appropriately. For example, pluripotent stem cells have been described to be highly sensitive to DNA damage due to "mitochondrial priming", which lowers the threshold to apoptosis triggering. (Heyer et al., 2000; Liu et al., 2013; Pernaute et al., 2014). Lie et al., also demonstrated that P53 cytosolic function is enough to induce apoptosis in hESCs. Additionally, Pernaute et al., identified several miRNAs in mESCs controlling apoptotic threshold by regulating Bim expression (Pernaute et al., 2014).

Notably, BCL-2 family proteins have been described to perform additional non-apoptotic roles such as metabolic regulation, autophagy or cell cycle (reviewed in Siddiqui et al., 2015). For instance, they interact with mitochondrial proteins, such as VDAC, glucokinase, mitochondrial pyruvate import channels and ATP synthetase (Danial et al., 2003; Kim et al., 2019; Perciavalle et al., 2012), while thay can also regulate endoplasmic reticulum Ca2+ homeostasis and interact with cytosolic P53 regulating its function (Tasdemir et al., 2008).

OBJECTIVES

Cell Competition can be described as a process by which cells with different fitness interact and as a result, less fit cells are non-autonomously outcompeted.

Understanding the pathways and factors that define fitness and induce Cell Competition is therefore of high relevance. This includes the autonomous intrinsic differences that determine the cell competitive "status" and eventually whether a cell will stay in a tissue or be outcompeted by neighbouring cells. Identifying these factors, their crosstalk relations and whether they are common in different CC models would pave the way for a better understanding of the Cell Competition phenomenon. Moreover, in most CC models, after competitive interaction, loser cells are eliminated by apoptosis. Understanding the specific pathways regulating the execution of loser cell death would allow us to identify specific CC components and block CC, exposing its role.

Thus, the main goals of this thesis are:

- Identify cellular stresses, pathways and factors involved in the execution of loser cell death during MYC-driven Cell Competition in mammalian pluripotent cells.

- Identify pathways and factors determining competitive fitness in mammalian pluripotent cells and integrate them in a model that describes loser cell status.

- Propose cellular mechanisms involved in the definition of competitive fitness.

MATERIALS & METHODS

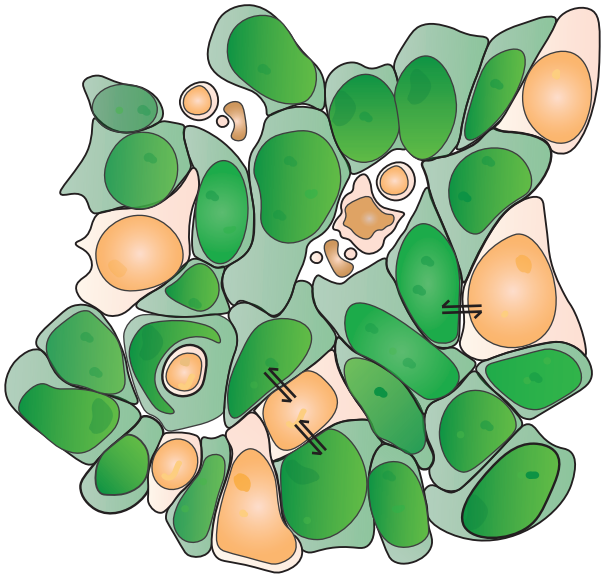

1. EXPERIMENTAL MODELS

1.1 mESCs Lines

- GFP-Myc reporter (Díaz-Díaz et al., 2017; Huang et al., 2008) and *iMOS*$^{T1\text{-}MYC}$ line (Clavería et al., 2013) has been previously described.

- *p53, puma, noxa* and *myc* knockout ESCs lines were generated by CRISPR-CAS9 technology. Generation of *p53, puma, noxa* KO cell lines is explained below. *myc-KO* ESCs line was generated in our lab (Li et al., unpublished).

- *Wt, p53*$^{-/-}$ and *puma*$^{-/-}$ ESCs lines expressing the *Grx1-roGFP*$_2$ construction were generated by lentiviral transfection, which is further explained below.

1.2 Animals

- CD1 strain WT mice.

- *p53*$^{-/-}$ mice were generated by crossing heterozygous *p53*$^{tm1b/+}$ mice, previously described (Jacks et al., 1994) http://www.informatics.jax.org/allele/MGI:6120822. *p53*^{tm1b} animals were genotyped using DreamTaq Green (ThermoFisher) as indicated below. Primers are included in (Table 1).

p53 genotyping PCR

DreamTaq	10µl
P. Forward	0,2µl
P. Forward	0,2µl
P. Reverse	0,4µl
DNA	1µl
	20µl

PCR program

Initial denat.	94	3min	
Denaturalization	94	30sec	35 x
Annealing	60	30sec	
Elongation	72	1min	
Final elongation	72	10min	

2. EMBRYO HARVEST

Mice were mated during the afternoon and pregnant females were checked every morning for the presence of vaginal plugs. Midday of the day in which vaginal plug was detected was considered gestational day 0.5 (E0.5). Pregnant females were euthanized by CO_2 inhalation and the uterus was extracted through an incision in the abdominal cavity and transferred to DMEM media # 41965-039 (ThermoFisher) at 37ºC.

2.1 E5-E7 Embryos

Working under the scope, and using precision forceps (Dumont #55 0.05x0.02mm) (FST), muscular uterine walls was carefully ripped. After that, both the decidual layer and the Reichert´s membrane were removed and embryos were fixed in paraformaldehyde (PFA) (Merck) 2% in PBS overnight at 4ºC. After fixation, embryos were washed in PBS several times.

2.2 E3.5 Embryos

Working under the scope and using precision forceps and scissors, adipose tissue was

removed and the uterus was cut next to the oviducts. Blastocysts were extracted by flushing them out of the uterus using a 1ml syringe with 23-G needle. Oviducts were also carefully removed from the ovaries and blastocysts were flushed out thorugh the infundibulum. Blastocyst were then transferred to KSOM media MR-101 (Merk) with a mouth pipette. Tyrode´s solution #T1788 (Merk) was used during a few seconds to dissolved zona pellucida. Blastocysts were washed in PBS 1% FBS and fixed in PFA 2% in PBS 1% FBS for 15 minutes at 4ºC. Eventually, blastocysts were washed in PBS + Triton-X100 0,1% 1% FBS.

3 CELL CULTURE ROUTINE

3.1 Mouse Embryonic Fibroblasts (MEFs)

MEFs are used as a feeder layer for the ESCs. Fibroblasts were previously extracted from E10.5 CD1 embryos by the Pluripotent Cell Technology (PCT) unit at CNIC. Over 5 million fibroblast were plated on a 100mm plate. Medium was changed after 24h. Two days after plating, MEFs were passaged to three 150mm-plate. Upon 3-4 days, MEFs were inactivated using mitomycin C # M4287 (Sigma) for 2.5h and then washed 3 times with PBS, trypsinized (Trypsin-EDTA 10x, Gibco) and frozen (0.6 million in 500µl volumen and 1,2 millions in 1ml freezing media). For cell freezing, cells were resuspended in MEFs media (50% final volume) and then freezing media was carefully added (50% final volumen) to get a final DMSO concentration of 10%. Vials are kept in a freezing container (Nalgene®) at -80ºC and transfered to liquid nitrogen 24h later.

Upon inactivation, MEFs were plated on 0,1%-gelatin coated plates.

3.2 Mouse embryonic stem cells (mESCs)

Approximatelly, $1x10^6$ ESCs contained in one cryovial (Nalgene) were plated on a 35mm-plated previously covered by mitomycin-C inactivated MEFs ($0.3x10^6$). Medium was changed every day and cells were passaged every 2 days.

For ESCs expansion, they were passaged to a 100mm-plate with inactivated MEFs ($1.2x10^6$) and after 2 days, cells were trypsinized, counted and freeze 1.2 millions in 1ml volume per vial following the same procedure to freezing MEFs.

To perform experiments, ESCs were thawn over inactivated MEFs. After 2 days, MEFs depletion is performed and ESCs are transfered to a 0,1%-gelatin coated new plate. For MEFs depletion, after trypsinized, cells are plated in a 0,1%-gelatin coated plate and after 1 or 2 hours, MEFs are attached while ESCs do not. ESCs can then be transfered to a new plate. Approximatelly, 700.000 cells were passaged to a 35mm-plate and 180.000 cells in the case of 12-wells plates.

3.3 Cell Culture Medium

mESCs medium: High glucose DMEM #41965 (LifeTech). 1% Sodium pyruvate, 1% non-essential aminoacids, 1% penicillin/streptomycin (10,000U/ml) and 0,1% β-mercaptoethanol were added. mESC medium also contained:

- Serum. Fetal Bovine Serum (FBS), previously tested for mESCs cultured by the PCT unit was used. Alternatively, KnockOut™ serum replacement (here referred as SR) #10828 (Invitrogen) was used when indicated.

- Leukemia inhibitor factor (LIF). LIF was provided by the PCT unit and used 250x. LIF was removed to induce mESC differentiation.

- 2i. The inhibitors CHIR99021 #04-0004-02 (Stemgent) and PD0325901 #04-0006 (Stemgent) were added to the mESCs medium at 0.1µM and 0.3µM, respectively, to obtain "2i medium".

MEFs medium: High glucose DMEM (LifeTech), 15% Fetal Bovine Serum (FBS), 1% sodium pyruvate (100x), 1% Penicillin/Streptomycin (10,000U/ml; 100x), 0,2% 2β mercaptoethanol (50mM).

Freezing media: 55% (MEFs or ESCs Medium), 25% FBS, 20% DMSO (Sigma)

4. MUTANT ESCs LINES GENERATION

4.1 *p53*$^{-/-}$, *puma*$^{-/-}$ *and noxa*$^{-/-}$ ESCs Generation

p53, puma and *noxa* knockout lines were generated by using CRISPR-CAS9 technology. Two crRNA sequences were employed per gene to generate a deletion in the gene sequence. crRNAs are indicated in Table 1. CRISPOR web tool (http://crispor.tefor.net/crispor.py) was used for crRNAs design. In the case of *p53*, the targeted region included the DNA binding domain, the nuclear localization sequence and the oligomerization domain. Regarding *puma*, it covers the majority of exons 1 and 2, including BH3 domain and Ser96 and Ser106 residues, recently described important for PUMA-metabolic functions (Kim et al., 2019). In case of *noxa*, removed region consisted in exons 2 and 3, including BH3-1 and 2 domains.

crRNAs and tracrRNA were acquired from IDT while CAS9 protein was expressed and purified by the PCT unit at CNIC. To generate each knockout line, 2x10^6 GFP-MYC cells were electroporated with the ribonucleoprotein (RNP) complex formed by the guide RNA (crRNA + tracrRNA) and the CAS9. Cells were electroporated with Neon Transfection System. A *tdTomato*-expressing plasmid was used as a reporter, so that 24h later, tdTomato positive cells were sorted by FACS to select those cells in which electroporation generated pores so *tdTomato* plasmid could enter into the cell. Then, individual cells were expanded into single colonies and knockouts clones were screened by PCR.

p53 and noxa genotyping PCR

DreamTaq	10µl
P. Forward	0,2µl
P. Reverse	0,2µl
DNA	20ng
	20µl

puma genotyping PCR

Buffer (MyTaq)	4µl
P. Forward	0,6µl
P. Reverse	0,6µl
MyTaq	0,2µl
DNA	100-200ng
	20µl

PCR program

Initial denat.	95	3min	
Denaturalization	95	30sec	35 x
Annealing	63	30sec	
Elongation	72	2min	
Final elongation	72	10min	

p53 and *noxa* screening PCRs were performed using DreamTaq Green and MyTaq™ HS (Bioline) in the case of *puma*. PCR reactions were performed under the same conditions. *P53* and *puma* KOs clones were also checked by immunofluorescence.

OLIGONUCLEOTIDE	FORWARD /REVERSE	SEQUENCE (5'-3')
Oligomers for crRNA		
crP53 #1		GGACAAGCCGAGTAACGATC AGG
crP53 #2		TCTCGAAGCGTTTACGCCCG CGG
crPUMA #1		TCGCGGGCTAGACCCTCTAC GGG
crPUMA #2		CAACGCGCAGTACGAGCGGC AGG
crNOXA #1		GGATGTGCTAATTTGCGAGT AGG
crNOXA #2		AAGGAAGTTCCGCCGGTTGA TGG
Primers for KO screening		
P53 #1	Forward	TTCCCACCCTCGCATAAGTTT
P53 #1	Reverse	GAGGTCTGGGTAGAGCACCA
P53 #2	Forward	AGGGGACGTGGAACTCTCTT
P53 #2	Reverse	GCAGCCCTAAGCATCTAGCA
PUMA #2	Forward	TTTGCTACAAACCCCAGACG
PUMA #2	Reverse	GCATCCAGCAGATCCATTCCTT
PUMA #5	Forward	CCTGGTGGGTTTTGCTACAA
PUMA #5	Reverse	TAGCCCGGGATATAGGAGCC
NOXA #1	Forward	AGGAGGGCATAAATGGGCAA
NOXA #1	Reverse	ACTTCCCTAGCTCCACGACT
NOXA #3	Forward	GAGGGGTACCAGAACAACCA
NOXA #3	Reverse	CAAACGACTGCCCCCATACA
Primers for Gibson assembly		
Grx1-roGFP$_2$	Forward	TTCTTCCATTTCAGGTGTCGTGAGGAATTG-GATCCCCGGGATGGCCTCCACTCGTGTC
Grx1-roGFP$_2$	Reverse	ACAAATTTTGTAATCCAGAGGTTGATTGTCGAC-GAATTCGTTACTTGTACAGCTCGTCCATG
Primers for *p53*$^{-/-}$ mice		
p53f_12B7	Forward 1	TGGTTTGTGCGTCTTAGAGACAGT
pPNTf_2B5	Forward 2	CCAGCTCATTCCTCCCACTCA
p53r_1B3	Reverse	AAGGATAGGTCGGCGGTTCAT

Table 1. crRNA and primers sequences.

4.2 *Grx1-roGFP$_2$* ESCs Generation

Grx1-roGFP$_2$ construction was cloned into a lentiviral vector under the EF1 promoter. For that, "pLPCX mito Grx1-roGFP2" plasmid from Tobias Dick (Gutscher et al., 2008)

(Addgene plasmid # 64977) was used and the *Grx1-roGFP*$_2$ sequence cloned into the lentiviral plasmid "pCDH-EF1" from Kazuhiro Oka (Addgene plasmid # 72266) using Gibson assembly technology, (primers described in Table 1).

This construction was packaged into lentiviral particles by the Viral Vectors Unit at CNIC. Finally, lentiviral particles (MOI between 5 to 10) were used to infect 100.000 ESCs cells overnight in a 24-well plate. After ESCs expansion, GFP positive cells were sorted by FACS.

5. COMPETITION ASSAYS

Upon one passage using inactivated MEFs and the posterior MEFs depletion, 180.000 cells were plated in co-culture or separated conditions in 12-well plates using FBS medium without LIF to induced differentiation. For each time point, cells were trypsinized and counted using a Newbauer chamber (Sigma-Aldrich). The percentage of fluorescent and non-fluorescent cells in the co-cultures was determined by flow cytometry.

6. RT-PCR

RNA extraction. Cells were resuspended in TRI Reagent (Invitrogen), (approx 4x10^6 cells/ml), 5min at RT. Then, we added (1:1) ethanol (95-100%) volume and vortex. "Direct-zol RNA Miniprep kit" R2051 was used to extract RNA and we proceed as indicated by the manufactures. Finally, RNA was stored at -80ºC.

cDNA reverse transcription. 1µg of RNA was used to perform the retrotranscription reaction using "High Capacity cDNA Reverse Transcription" Kit 4368814 (ThermoFisher).

qPCR. "Sybr Green" #4472903 (Invitrogen) was used to perform the qPCR reaction. Primers for the qPCR reaction were adquired from "KiCqStart® SYBR® Green Primers" (Sigma-Aldrich). *gadph* was used as a control.

7. IMMUNOFLUORESCENCE

7.1 Whole-mount Embryo Immunofluorescence

E3.5 whole-mount immunostaining was performed using 4-well plates and a mouth pipette. Triton X-100 0,1% and FBS 1% was added to PBS and blocking solutions to avoid blastocyst getting attached to the plate.

E5.0-E7.5 immunofluorescent was performed using 35mm plates and/or round bottom 2ml Eppendorf tubes using a micro-pipette with end-cut tips to avoid excessive pressure when transfering the embryos.

Both E3.5 and E5.0-E7.5 embryos were permeabilized using 0,5% PBT (PBS + Triton X-100 0,5%) for 20min. Embryos were washed in PBT 0,1% and blocked using 10% goat serum (Gibco-BRL Life-Technologies) in 0,3% PBT 1 hour at RT. Embryos were incubated with primary antibodies overnight using blocking solution at 4ºC. Embryos were washed several times with PBT 0,1% and then incubated with the secondary antibodies, Wheat Germ Agglutinin (1:500) (ThermoFisher) to stain plasma membrane and DAPI (1:1000) using blocking solution for 1 hour at RT. Finally, embryos were washed several times and

embbebed in mounting media. To avoid the embryos to collapse due to the different density between 0,1% PBT solution and mounting media, mounting media was diluted in serial dilutions using 0,1% PBT, (25, 50, 80 and 100% mounting media concentration) and the embryos were transferred through the different dilutions.

For E.5.0-E7.5 embryos , we used VectaShield mounting media (Vector Laboratories) while, for E3.5, liquid Abberior mounting media was used.

7.2 mESCs Immunofluorescence

For confocal microscopy adquisition, 180.000-250.000 ESCs were plated into 35mm-glass bottom dishes (MatTek). Previous, MatTek plates were coated using human fibronectin #354008 (Corning) overnight at RT. Two days after plating, cells were washed with PBS and fixed overnight using PFA 2% at 4ºC. Immunostaining was then performed similar to the embryo immunostaining described above. For ESCs, permeabilization was reduced to 10 minutes. Vectashield is used as a mounting media.

Primary and secondary antibodies were incubated in a 100µl volume. To avoid evaporation during primary antibody overnight incubation, plates were kept inside a humidity chamber.

For BECLIN1 (BECN1 H-300) detection, cells were permeabilized with -20ºC-cold methanol for 10min.

For aCASP3 (Asp175) (D3E9) (Alexa Fluor 594 Conjugate) #8172, used in the double aCASP3-PUMA immunostaining, we proceed as described in the Cell Signaling Tech Protocol Id: 182 [https://www.cellsignal.com/products/antibody-conjugates/cleaved-caspase-3-asp175-d3e9-rabbit-mab-alexa-fluor-594-conjugate/8172?_=1576109130770&Ntt=casp3%20594&tahead=true].

To generate P53 activation, ESCs were treated with 40µM etoposide (Sigma) during 10 hours or 5-30µM Nutlin-3 (BioVision) during 12 hours previous to immunostaining.

7.3 Cell Suspension Immunostaining

For immunostaining of suspension ESCs, they were trypsinized and fixed with 2% PFA in PBS for 1 hour at 4ºC. Then, we permeabilized and blocked cells with 10% serum goat in PBS containing 0,1% saponin for 1 hour at RT. Subsequently, ESCs were incubated with the primary antibody in blocking solution overnight at 4ºC. After that, cells were washed with PBS-0,1% saponin and incubated with the secondary antibodies in blocking solution for 1 hour at RT. Finally, we washed cells and resuspended them in 200µl of PBS and analyse by flow cytometry. Primary and secondary antibodies were incubated in 100-200µl volume.

7.4 Antibodies

- All the primary antibodies used and their concentrations are summarized in Table 2.

- Secondary antibodies were diluted at a ratio 1:500.

ANTIBODY	HOST	DILUTION	BRAND	REFERENCE
Alpha tubulin (TU-02)	mouse	1:1000	Santa Cruz	sc-8035
ARTS	mouse	1:300	Merk	A4471
BECN1 (H-300)	rabbit	1:100	Santa Cruz	sc-11427
Cleaved Caspase-3 (Asp175)	rabbit	1:100	Cell Signaling	9661
Cleaved Caspase-3 (Asp175) (D3E9) (Conjugate- Alexa Fluor® 594)	rabbit	1:75	Cell Signaling	8172
GFP	chicken	1:500	Aves lab	AB_2307313
GLUT1	rabbit	1:300	Merk	07-1401
MYC	rabbit	1:300	Merk	06-340
NOX4	rabbit	1:150	Ajay Shah' lab	
NOXA	mouse	1:50	Novus	NB600-1159
NOXA	mouse	1:50	Santa Cruz	sc-56169
P53 (1C12)	mouse	1:500	Cell Signaling	2524
Phospho-Histone H2A.X	mouse	1:500	Merk	05-636
Phospho-Histone H3 (Ser10)	mouse	1:500	Cell Signaling	9706
Phospho-p44/42 MAPK (Erk1/2) (Thr202/Tyr204) (D13.14.4E)	rabbit	1:200	Cell Signaling	4370
Phospho-S6 (Ser240/244) (D68F8)	rabbit	1:800	Cell Signaling	5364S
Phospho-SAPK/JNK (Thr183/ Tyr185)	mouse	1:200	Cell Signaling	9255
PUMA (D7L9L)	rabbit	1:400	Cell Signaling	24633
TOM20	rabbit	1:500	Santa Cruz	

Table 2. Primary antibodies.

8. METHODS BASED ON MOLECULAR PROBES

8.1 ROS Measurements

DHE (Invitrogen) was used for H_2O_2 and $O^{\bullet -}$ measurement. ESCs were incubated with 2µM DHE for 15min at 37ºC. Then, cells were washed and analysed in "live" by confocal microscopy. 0,2% H_2O_2 was used as a positive control while "cold-ice incubation" with DHE was used as a negative control.

8.2 Mitochondrial Membrane Potential

TMRM was used to measure membrane potential. Cells were incubated with TMRM (D-1168, Invitrogen) was incubated at 25nM for 20min at 37ºC. WGA 633 (1:500) and Hoescht 33342 (Invitrogen) (1:2000) were used as membrane and nuclear markers respectively. Then, cells were washed with PBS and analysed "in live" by confocal microscopy. Cells pre-incubation with 2µM oligomycin (Sigma-Aldrich) for 3 hours was used as,

while pre-incubation with 50µM FCCP (Sigma-Aldrich) for 30min was used as a negative control. Oligomycin and FCCP treatment were also maintained during incubation with TMRM.

8.3 Apoptosis Measurement

FLICA™ 660 Caspase-3/7 (BIORAD) was used to measure apoptosis according to manufacturers. Additionally, apoptosis was determined by immunostaining against Cleaved Caspase-3 (Asp175), according to procedures described in "6. Immunofluorescence".

8.4 Cell Cycle

Propidium iodide (PI) was used to determine cell cycle. For that, 200.000 cells were trypsinized and resuspended in 500µl of 70% ethanol at -20ºC, drop by drop and stored during 24h at -20ºC. Then, cells were washed in PBS twice, resuspended in 200µl of PBS containing 50µg/ml PI and analysed by flow cytometry. Data were analysed using Dean-Jett-Fox model in FlowJo.

For flow cytometry data analysis, FACSDiva and FlowJo softwares were used.

9. MITOCHONDRIAL REDOX STATUS

ESCs mitochondrial REDOX status was studied by "in live" analysis of the *Grx1-roGFP*$_2$ cells lines through confocal microscopy.

Additionally, *Grx1-roGFP*$_2$ cells were fixed and immunostained. To avoid REDOX status alteration caused by 2% PFA fixation, cells were incubated with 20mM N-etilmaleimida (NEM) (Sigma) 5min previous to fixation. NEM is a thiol-blocking agent that protects against thiol oxidation mediated by paraformaldehyde fixation (Albrecht et al., 2011). To induced maximun oxidation or reduction, cells were pre-incubated with 100µM H_2O_2 or 20mM DTT for 10min before the NEM treatment.

10. IMMUNOBLOT

Cells were lysed with RIPA buffer containing (25x) protease inhibitor (Roche) for 30min at 4ºC. Approximately $1.5x10^6$ cells were lysed at a concentration of $3x10^6$ cells/ml. Protein concentration was measured using BSA (Sigma-Aldrich) serial dilutions and the "DC™ Protein Assay" kit (BioRad). Absorbance was measured at 690nm using a microplate spectrophotometer. Proteins were separated via 12% SDS-PAGE under reducing conditions and transferred to a polyvinylidene difluoride (PVDF) membrane using "Wed blotting system" (BioRad). After incubation with primary and secondary antibodies, protein signal was detected via chemiluminescence using the "Pierce ECL Western Blotting Substrate" kit (Thermo-Fisher).

11. EQUIPMENT

11.1 Microscopy

Leica TCS SP8 coupled to a DMi8 inverted confocal microscope Navigator module equipped with white light laser was used for imaging. A HC PL Apo CS2 40x/1.3 oil objective

and 1024x1024 pixels, A.U. set to 1 were commonly used.

For Super-resolution microscopy, a Leica gated STED-3X- WLL SP8 and a HC PL APO CS2 100x/1.40 oil objective was used. Alexa Fluor 514 and Alexa Fluor 568 secondary antibodies were used for this technique.

11.2 Flow Cytometry

ESCs suspensions were analysed in a BD LSRFortessa™ Special Order Research Product (laser wavelengths 405, 488, 561, 633).

ESCs were sorted by FACS using a BD FACSAria™ II and Synergy 4L cell sorter.

12. IMAGE ANALYSIS

Confocal images were analysed using FIJI (https://imagej.net/Fiji).

12.1 Nuclear Signal

For nuclear signal quantification, nuclei were segmented by DAPI/TO-PRO-3™ staining. Nuclei masks were created applying the “default Threshold tool” and they were manually corrected to ensure that segmented objects correspond to individual cells and discard mis-located, apoptotic or mitotic cells. Then, “Analysed particle” tool was used to identify the regions of interest (ROIs) corresponding to nuclei. Finally, ROIs were were used to measure the nuclear signal.

12.2 Cytoplasmic Signal

For cytoplasmic signal quantification, we first segmentated the whole individual cells using WGA as a membrane marker. Then, we substracted the nuclear area (obtained as described above) from the whole cell region.

For whole cell segmentation, we applyed a “Gausian Blur” filter (scaled units 2) to the WGA signal and used the “Find Maxima” tool (Find Maxima configuration: output type, segmented particles; light background) to create a mask. Afterwards, manual correction was performed to ensure that segmented objects correspond to individual cells. Finally, “Analysed particles” was used to identify the ROIs corresponding to whole cells.

To couple the whole cell ROIs with the nuclear ROIs from the same cell, a macro was designed with the help of CNIC Microscopy Unit based on ROIs position within the image (Anexo 1). This macro generated the “cytoplasmic” ROIs that were used to measure the cytoplasmic signals.

12.3 Foci Number

To detect foci number, each ROI corresponding to a nucleus was selected and processed using the “Find maxima” tool. Configuration was output=count. Noise was manually adjusted. A macro was used to generate a loop for counting foci in all the ROIs corresponding to the nuclei of the capture (Anexo 1) .

12.4 Whole-mount Embryo Immunofluorescence Analysis

To study PUMA positive cells - MYC correlation at E6.5, MYC levels were normalised per Z slice and embryo to avoid depth-dependent loss of signal and variation among different embryos. Statistical analysis was performed using linear mixed models using lme4 R library, p value=$6.81x10^{-10}$.

This type of analysis was also performed for the P53-PUMA correlation at E3.5, p=0.105 and P53-MYC correlation at E3.5. Embryo was set as random variable and either P53, PUMA or MYC-classification and Z-position as covariates to simultaneously adjust for the two factors. Coefficients represent either the quantitative increase in the response variable (log_2(MYC)) per unit increase in the independent variables (either log_2(P53) or PUMA-classification variables) and their associated p-values show the significance of such coefficients under the null hypothesis of them being 0.

13. RNASEQ ANALYSIS

RNAseq data described in (Díaz-Díaz et al., 2017) were analysed to identify apoptotic-related factors. Apoptotic-related genes were screened using "Genering Gene ontology (GO) term finder" (https://go.princeton.edu/cgi-bin/GOTermFinder) and "The Gene Ontology (GO) Project" tools (http://www.informatics.jax.org/mgihome/GO/project.shtml). Potential downstream P53 candidates were manually selected from those genes.

14. STATISTICAL ANALYSIS

Parametrical T student test was performed to compare two groups of data. For comparisons with more than two groups of data One –way ANOVA multiple comparison was used. One-sample test (Wilcoxon test) was used to compare a group of data with a hypothetical mean. Comparison and graphs were made with Graph Pad Prism 8.4.3 statistical analysis software. Adjusted values of P<0,05 were considered statistically significant.

RESULTS

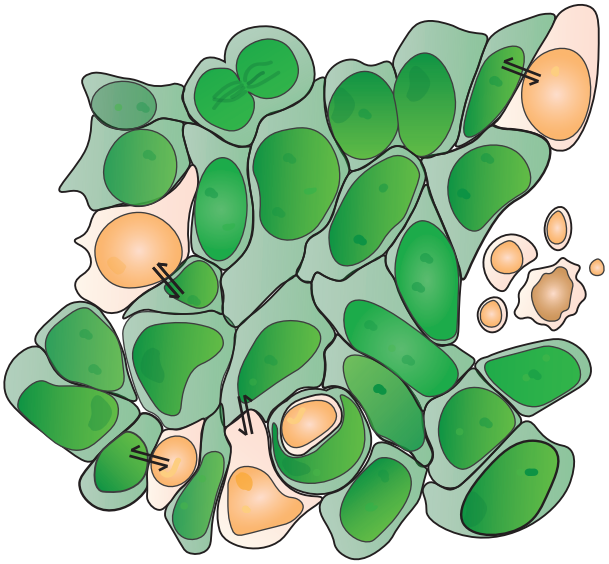

"Equipped with his five senses, man explores the universe around him and calls the adventures Science "

Edwin P. Hubble

1. CELL STRESS IN LOW-MYC CELLS

Live analysis in ESCs shows that loser elimination occurs in low MYC cells after the accumulation of random contacts with high MYC cells for around 10h (Díaz-Díaz et al., 2017). We wondered whether the persistent random contacts of prospective loser cells with MYC-high cells could generate some cellular stress in low MYC cells leading to apoptosis.

GFP-MYC reporter ES cell line was used to measure MYC levels(Figure 5A, A') (Díaz-Díaz et al., 2017) and we analysed the levels of the stress-activated protein kinase p-JNK1/2, which were higher in low MYC cells, supporting this idea (Figure 5B-B''). Therefore, we analysed a number of candidate mechanisms and factors potentially involved in loser cell stress.

1.1 DNA DAMAGE

Maintenance of genome integrity is essential for ESCs. These cells acquire abundant

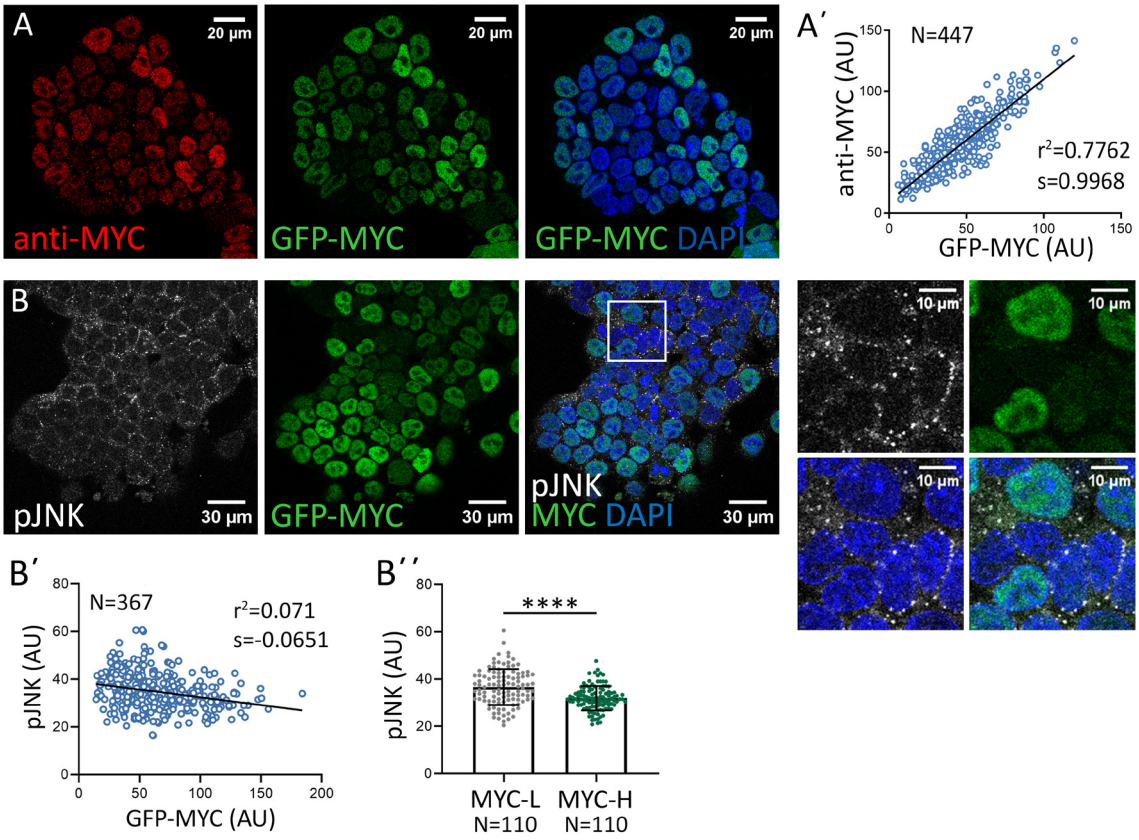

Figure 5. GFP-MYC reporter line and pJNK expression in ESCs.

A. Confocal images of anti-MYC antibody and endogenous GFP-MYC signal. **A'.** Quantification of GFP-MYC and anti-MYC, p<0.0001. **B.** Confocal detection of pJNK and GFP-MYC. **B'.** Correlation between MYC and pJNK, p<0.0001. **B''.** Quantification of pJNK levels in MYC-Low and MYC-High populations (MYC-L group represents the 30% population of cells with lowest MYC levels while MYC-H group represents the 30% of the population with highest MYC levels).

DNA lesions, probably due to a high proliferation rate and shortened G_1 cell cycle phase. However, they accumulate mutations at low rates (10 times less than differentiated counterparts) because of a more robust and efficient DNA Damage Response (DDR) mechanisms (Vitale et al., 2017).

When DNA damage is unresolvable, ESCs undergo Regulated Cell Death (RCD) or lose pluripotency. ESCs are particularly prone to suffer RCD, as they display constitutive mitochondrial priming. In other words, the balance between anti- and pro-apoptotic members of BCL-2 protein family is close to threshold for apoptotic induction (See Introduction). Indeed, ESC are hypersensitive to genotoxic stress (Li and Huang, 2010; Vitale et al., 2017) .

DNA lesions include a wide range of alterations such as single base modification (alkylation, deamination and oxidation), nucleoside hydrolysis, distorting lesions, single strand

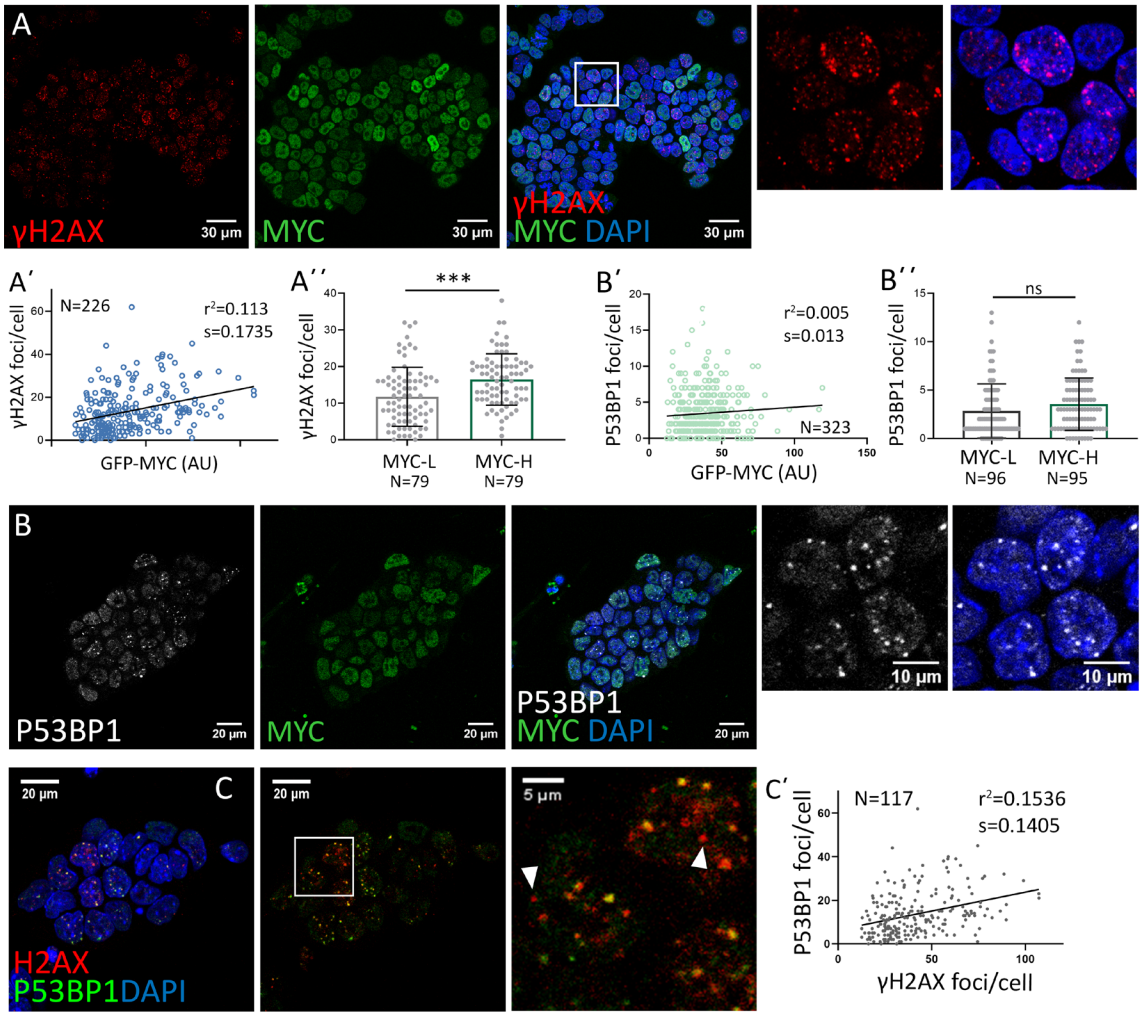

Figure 6. Double strand breaks in MYC-low ESCs.

A. Confocal images of γ-H2AX and GFP-MYC. **A'.** Correlation between MYC and γ-H2AX, p<0.0001. **A''.** Quantification of γ-H2AX levels in MYC-Low and MYC-High populations. **B.** Confocal images of P53BP1 and MYC levels and quantification **(B', B'')**. **C.** Double immunostaining of γ-H2AX and P53BP1 and **(C')** quantification.

breaks or double strand breaks.

Double Strand Break (DSB) is considered the most harmful form of DNA damage and the major type incurred physiologically during cellular proliferation (Fu et al., 2017). Upon DSB, histone H2AX is phosphorylated (modification termed γ-H2AX), which constitutes an extended early indicator of DSBs. Additionally, γ-H2AX has been reported to be particularly high in ESCs (Dickey et al., 2009). Therefore, we wanted to explore the correlation between DSBs and MYC levels. Unexpectedly, we identified a positive correlation between MYC levels and γ-H2AX foci number, so that there are more γ-H2AX foci in cells with higher MYC levels (Figure 6A- A'').

Curiously, a function of γ-H2AX in maintaining self-renewal, independent of DNA damage in ESCs, has been proposed (Turinetto et al., 2012). Given that MYC levels correlates with pluripotency, so naïve ESCs express higher MYC levels than more differentiated ones (Díaz-Díaz et al., 2017), this suggests that in undamaged ESCs, γ-H2AX could be reporting pluripotency status instead of DNA damage.

Thus, we analysed P53BP1 foci number, an important mediator of DSBs repair machinery (Panier and Boulton, 2014). In this case, we found no correlation with MYC levels (Figure 6B-B''). Double γ-H2AX and P53BP1 immunostaining showed more γ-H2AX foci per cell than P53BP1 (15.68 versus 4.45, N=117 cells) (Figure 6C). However, P53BP1 co-localized with γ-H2AX foci and they positively correlate (Figure 6C'). These observations support the notion that γ-H2AX could be playing a role in pluripotency asides its function in DSBs repair.

Although, we cannot reject a role of DNA damage in ESCs Competition, due the broad variety of DNA lesions, DSB (the most dangerous form of DNA damage) is not associated with MYC-low cell stress in Cell Competition.

1.2. OXIDATIVE STRESS

Reactive Oxygen Species (ROS) perform an important role in cell signalling. However, an excess of ROS can damage cellular macromolecules and lead to apoptosis. In ESCs, ROS, which are maintained at very low levels, have been reported to play important role in stress and differentiation (Bigarella et al., 2014). Therefore, we explored the potential role of oxidative stress in ESCs during Cell Competition.

1.2.1 ROS Detection with Dihydroethidium (DHE)

DHE has been widely used to quantify cellular $O_2^{\cdot-}$ and H_2O_2 (Wang and Zou, 2018). In ESCs, DHE showed a cytoplasmic and a nucleolar signal (Figure 7A). H_2O_2 1%, used as a positive control, reduced cytoplasmic signal, while induced an elevation of the nucleolar signal. On the other hand, ice-cold cell pre-incubation as a negative control efficiently inhibited DHE staining (Figure 7B).

Double staining of DHE and mitochondrial marker "Mitotracker Deep Red" indicated that cytoplasmic DHE signal corresponds to a mitochondrial pattern (Figure 7C). Quantification of MYC and DHE signal indicated that neither nuclear nor cytoplasmic DHE levels correlated with MYC levels (Figure 7D, E). Similar results were obtained regarding MYC

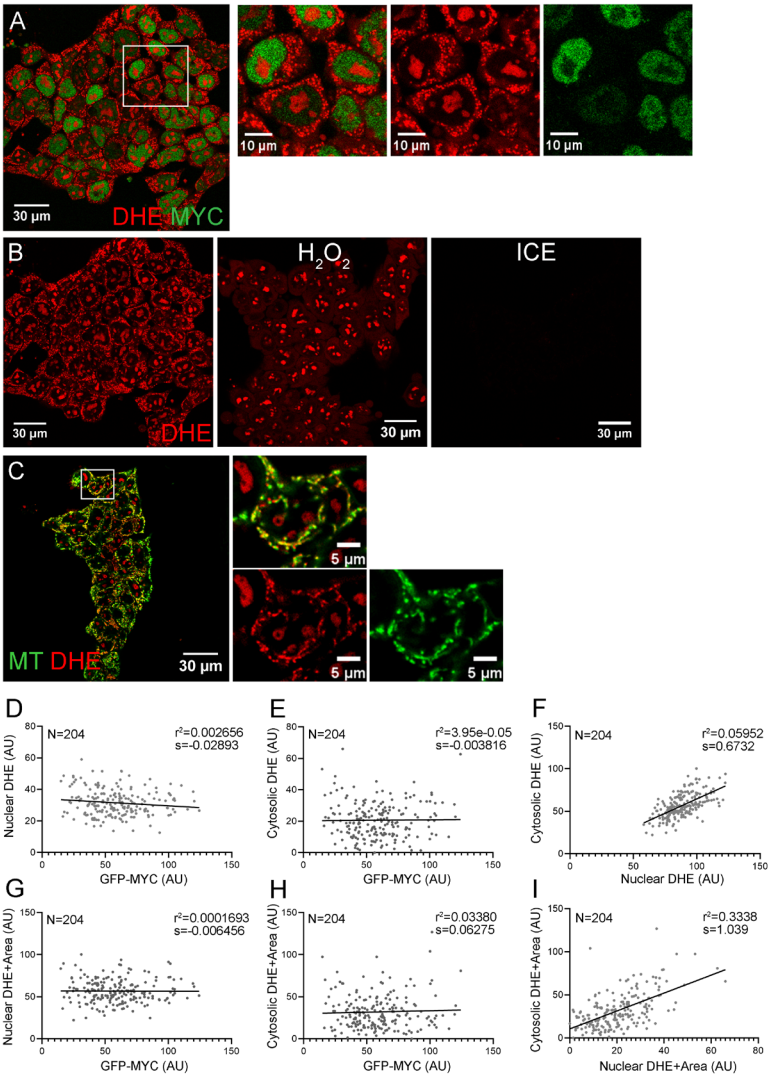

Figure 7. DHE analysis in ESCs.

A. Confocal images of DHE signal in ESCs. **B.** Positive (+ H_2O_2) and negative (ice-cold pre-incubation) DHE staining controls. **C.** Confocal detection of double Mitotracker deep red and DHE immunostaining. D, E. Quantification of nuclear and cytosolic DHE levels, p<0.0001 and **(G, H)** DHE positive area. **F, I.** Quantification of nuclear and cytosolic DHE levels and area, p<0.0001.

levels and total DHE-positive area (Figure 7G, H). Cytoplasmic and nucleolar DHE levels and areas positively correlated (Figure 7F, I).

1.2.2 NOX4

The NADPH Oxidases (NOX) are a group of transmembrane proteins able to transport electrons from NADPH to reduce oxygen producing ROS ($O_2^{\cdot-}$ and H_2O_2). In ESCs, NOX4 has been associated to different processes, such as differentiation (Crespo et al., 2010; Maraldi et al., 2015). Thus, we wanted to explore a potential role for NOX4 in ESCs stress. NOX4 staining showed a cytoplasmic dotted-like signal probably corresponding to membrane organelles such as mitochondria and endoplasmic reticulum and a nucleolar signal

(Figure 8A). We found neither the nuclear nor the cytosolic NOX4 levels correlated with MYC intensity levels (Figure 8B, C). However, the area occupied by NOX4 signal in the nucleus and more significantly in the cytosol positively correlated with MYC levels (Figure 8D-G), although the differences between Myc-high and Myc-low cells were mild.

In some ESCs colonies, we could find cells with a higher cytosolic NOX4 signal than the rest of their neighbours (Figure 8H). However, MYC levels in these cells were not significantly different from that in the general population (Figure 8I).

Collectively, neither detection of two important ROS as $O_2^{\cdot -}$ and H_2O_2 through DHE staining nor expression of ROS- producing NADPH-oxidase NOX4 suggest a role of ROS or oxidative stress in MYC-low stress during CC.

1.3 MITOCHONDRIAL STATUS

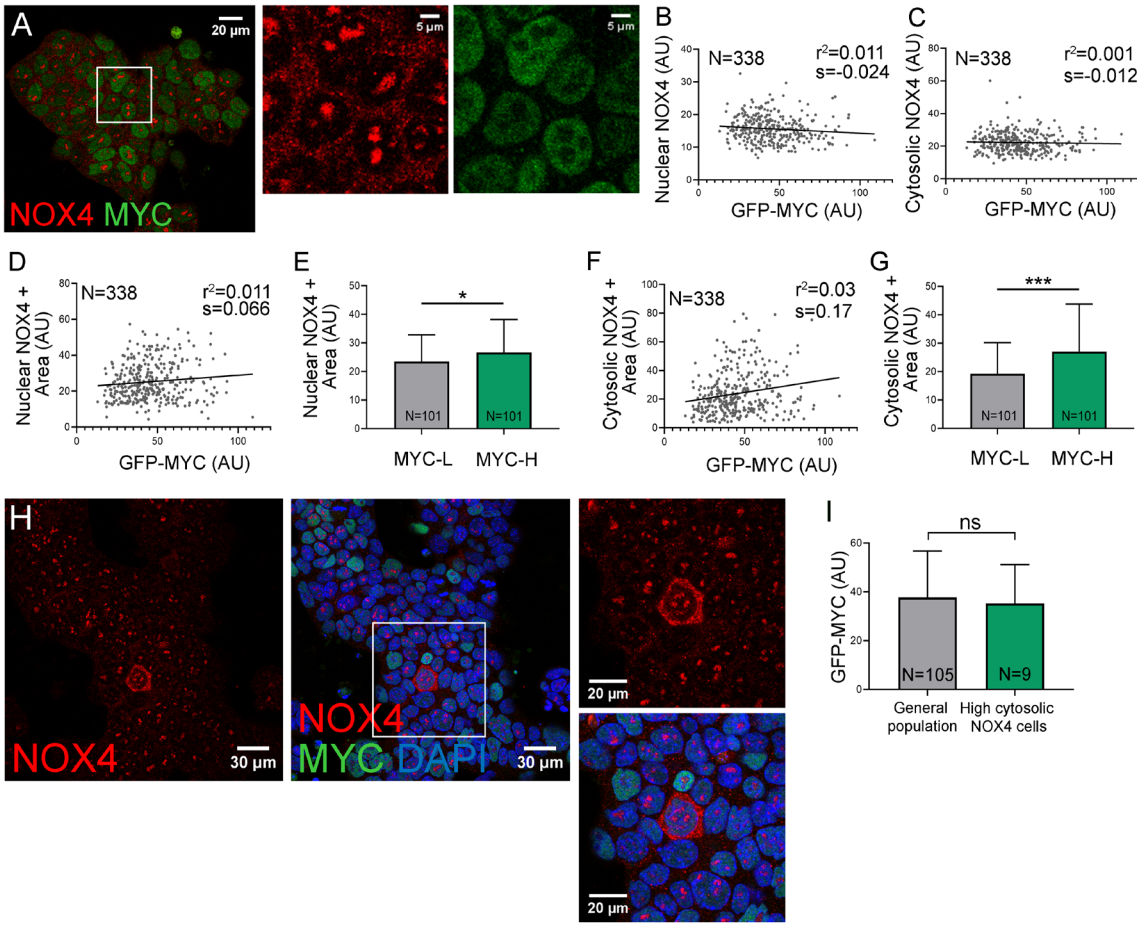

Figure 8. NOX4 analysis in ESCs.

A. Confocal images of NOX4 expression in ESCs. **B, C.** Quantification of MYC and nuclear and cytoplasmic NOX4 levels. **D, F.** Quantification of MYC levels and nuclear and cytosolic NOX4 positive area. **E, G.** Quantification of nuclear and cytosolic NOX4 positive area in MYC-L and MYC-H cells. **H.** Confocal acquisition showing a cell with a high cytosolic NOX4 level. **I.** MYC levels of the general population versus cells with a high cytosolic NOX4 levels.

Mitochondria has a key role in metabolism and homeostasis. Different features as mitochondrial mass, mitochondrial architecture, or mitochondrial membrane potential (MtMP) contribute to cellular adaptation to energy demand and other cellular processes. Altered mitochondrial number or MtMP could be an indicator of metabolic stress (Duarte et al., 2015). Thus, we decided to explore the mitochondrial status in MYC-low cells during Cell Competition.

1.3.1 Mitochondrial Content

TOMM20, a mitochondrial outer membrane protein was used as a mitochondrial marker. We found a weak positive correlation between MYC levels and mitochondrial mass (Figure 9A, B). No significant changes were found in a direct comparison between MYC-L and MYC-H populations (Figure 9C).

1.3.2 Mitochondrial Membrane Potential

MtMP is a central mechanism for ATP production through OXPHOS and it is considered a key parameter for evaluating mitochondrial function and cell health. To evaluate MtMP, we used TMRM, a cationic fluorescent dye sequestered by active mitochondria (Creed and McKenzie, 2019). First, TMRM staining was validated by flow cytometry. As a positive control, we used oligomycin, which blocks the V-ATPase and induces proton accumulation within the intermembrane space. As a negative control, we used the proton uncoupler FCCP, which disrupts proton gradient (Figure 10A). The olygomicyn control indicates that ESC mitochondria are near their maximum capacity of MtMP. Then, we analysed the relationship between TMRM and MYC levels in ESCs by confocal microscopy (Figure 10B). We found a positive correlation between MYC and TMRM levels and

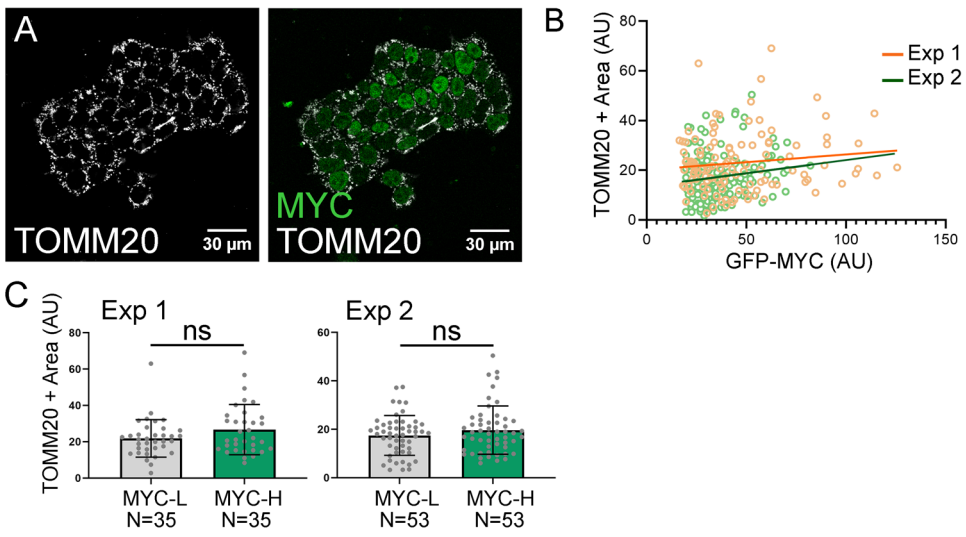

Figure 9. Mitochondrial content and MYC levels in ESCs.

A. Confocal captures of TOMM20. **B.** Quantification of TOMM20 positive area and MYC levels in two independent experiments. Experiment 1: r^2=0.01707, s=0.06204, p=0.1640. N=115. Experiment 2: r^2=0.02277, s=0.1056, p=0.045, N= 177. **C.** Quantification of TOMM20 positive area in MYC-L and MYC-H population.

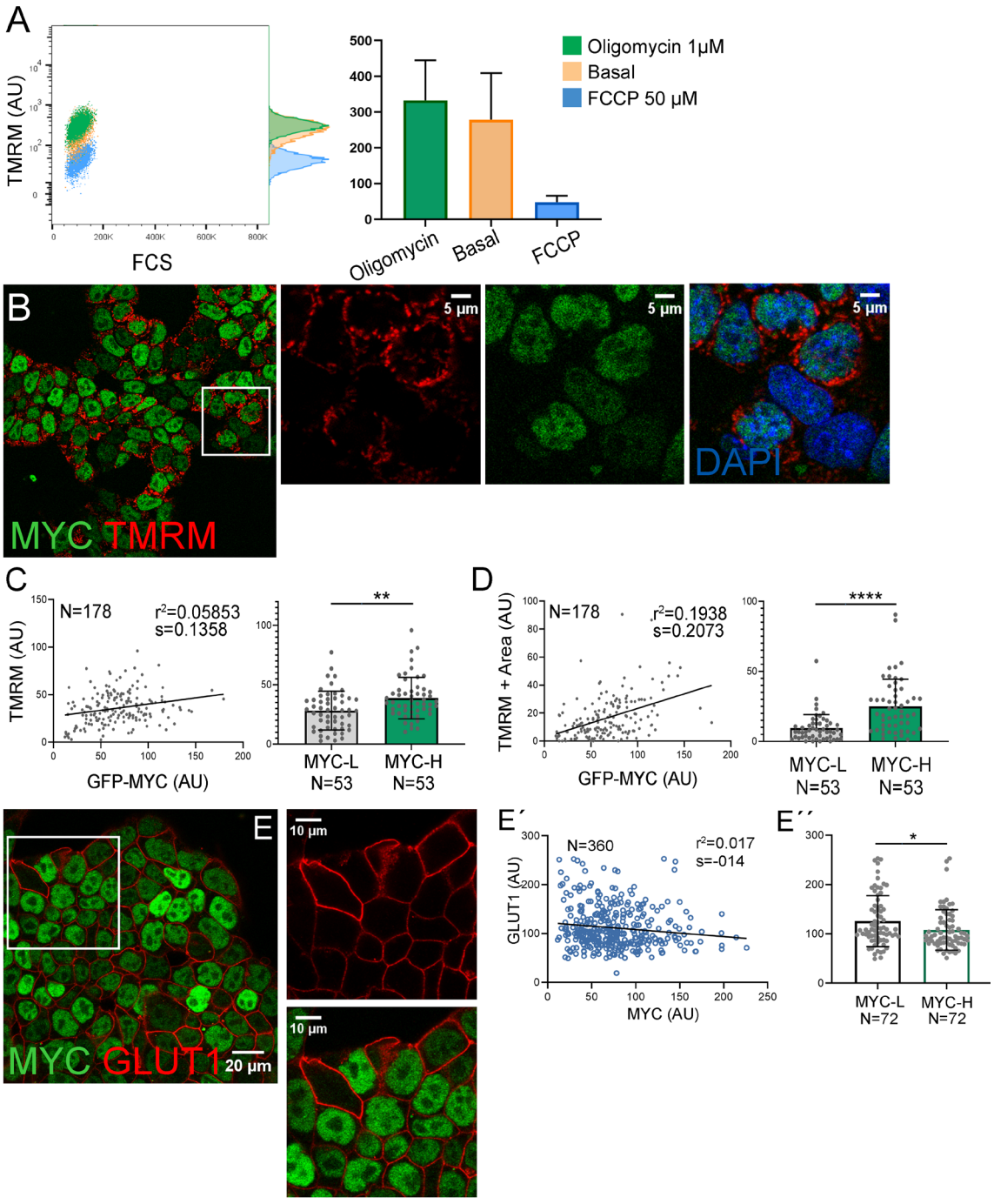

Figure 10. Mitochondrial membrane potential (Ψm) in ESCs.

A. Flow cytometry profile of ESCs stained with TMRM, TMRM + oligomycin (positive control), TMRM + FCCP (negative control) and bar plot. **B.** Confocal images of TMRM in ESCs. **C, D.** Quantification of MYC and TMRM levels and positive area, p<0.01 and bar plot showing TMRM levels and positive area in MYC-L and MYC-H populations. **E.** Confocal images of GLUT1 in ESCs and **(E, E')** quantification.

a more significant correlation between MYC levels and TMRM positive area, indicating that MYC low cells present a lower MtMP (Figure 10C, D).

ESCs experience a metabolic switch as they commit into a more differentiated status, from OXPHOS to glycolysis (Tsogtbaatar et al., 2020). As MtMP is an indicator of the potential to obtain ATP through OXPHOS, these results suggest that MYC-low cells display a lower oxidative metabolism. This is also supported by the fact that the glucose transporter, GLUT1 (one of the main transporters for glucose uptake in ESCs) (Heilig et al., 2003), is expressed at higher levels in low-MYC cells (Figure 10E-E'').

Collectively, our results suggest that MYC-low cells have a more glycolytic metabolism than Myc-high cells.

1.4 ARTS AND HTRA1 PROAPOPTOTIC PROTEINS

We next explored the role of recent described pro-apoptotic proteins in MYC-low cells death during CC.

1.4.1 ARTS

ARTS/SEP4_2 is a pro-apoptotic protein located at the outer membrane of the mitochondria. It has been generally thought that mitochondrial outer membrane permeabilization (MOMP) precedes caspase activation. However, after apoptotic stimuli, ARTS initiates a first wave of caspase activation before MOMP, by translocating to the cytosol where it degrades XIAP and BCL-2. This contributes to MOMP enhancing apoptosis (Edison et al., 2011; Edison et al., 2017). Interestingly, ARTS is induced by P53 and has a role in stem

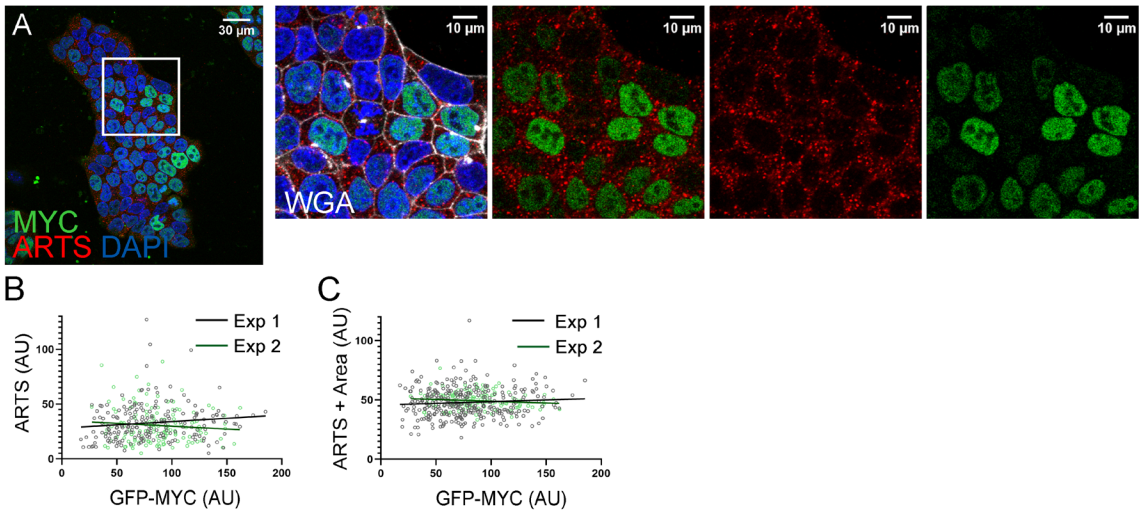

Figure 11. ARTS and MYC levels analysis.

A. Confocal capture of ARTS in ESCs. **B.** Quantification of ARTS and MYC levels in two independent experiments. Exp 1: r^2= 0.0058, s=0.028, N=328, p=0.167. Exp 2: r^2= 0.0137, s=-0.029, N=138, p=0.1702. **C.** Quantification of ARTS positive area and MYC levels in two independent experiments. Exp 1: r^2= 0.0021, s=0.0266, N=328, p=0.399. Exp 2: r^2= 0.0086, s=-0.0526, N=138, p=0.2792.

cells apoptosis (Fuchs et al., 2013; Hao et al., 2020).

In ESCs, ARTs displayed a dotted-cytoplasmic pattern compatible with a mitochondrial localisation (Figure 11A). However, we did not find any correlation between MYC levels and ARTS levels or ARTS positive area (Figure 11B, C). We conclude that, although ARTS is probably involved in ESCs apoptotic execution machinery, it does not play a role in loser cell apoptosis due to CC.

1.4.2 HTRA1

HTRA1 is serine protease involved in apoptosis. Although it is mainly secreted into the extracellular space, a fraction remains within the cytosol. HTRA1 plays different functions such as extracellular matrix re-organization, cell signalling or cell migration. Additionally, it is involved in apoptosis by degrading the caspase inhibitor XIAP (Chien et al., 2009; Hara et al., 2009; He et al., 2012; Klose et al., 2019; Tiaden and Richards, 2013; Zurawa-Janicka et al., 2017).

In ESCs, HTRA1 is present in the cytoplasm. By STED- Super-resolution microscopy using the mitochondrial marker TIM23, we confirmed HTRA1 is localized in the mitochondria (Figure 12B). However, we did not observe any correlation between HTRA1 and MYC

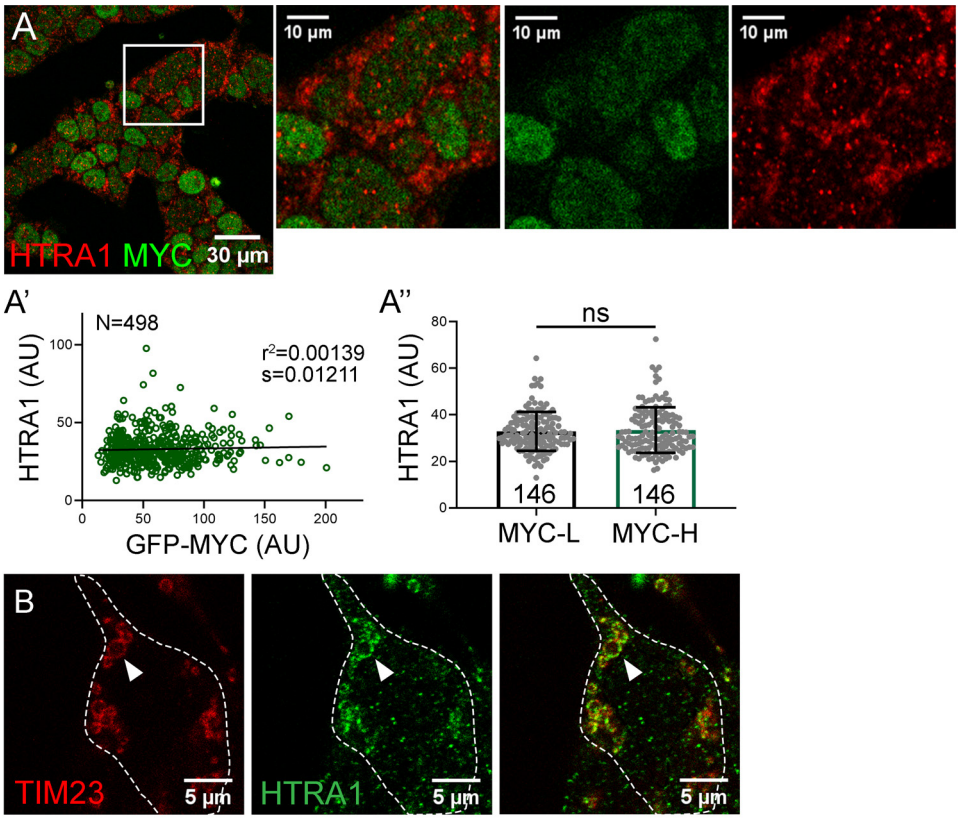

Figure 12. HTRA1 in ESCs.

A. Confocal images of HTRA1. **A', A''.** Quantification of HTRA1 levels. Cell number analysed is indicated inside the bars. **B.** STED-Super-resolution microscopy for HTRA1 and mitochondrial marker TIM23. Arrowheads indicated TIM23 and HTRA1 co-localisation.

levels (Figure 12A-A''). HTRA1 mitochondrial localization has not been described so far, in contrast to HTRA2/OMA protein, which also plays a role in apoptosis inhibiting XIAP (Zurawa-Janicka et al., 2017). These results could indicate a new undescribed location for HTRA1 in ESCs or lack of specificity of the HTRA1 antibody. Nonetheless, these results indicate that although HTRA1 could play a role in apoptosis in ESCs, we didn´t identify a relation between HTRA1 with "loser" cell death during MYC-driven CC.

In summary, our data did not suggest an important role for the candidate stresses and factors analysed as important elements in loser elimination downstream the fitness comparison. Therefore, in order to identify specific pathways related to "loser" cell status and death in an unbiased manner, we took advantage of transcriptomic data obtained in the lab from the GFP-MYC ES cell line (Díaz-Díaz et al., 2017).

2. LOSER CELL STATUS AND DEATH. ANALYSIS OF THE TRANSCRIPTOME

Since GFP-MYC cell line reports natural heterogeneous MYC levels, cells with different MYC levels were sorted by FACS according to GFP expression, obtaining a MYC-LOW ("loser"), MEDIUM and HIGH ("winner") population (Figure 13A, B).

Molecular Signature Database analysis (MSigDB) between MYC-HIGH and MYC-LOW transcriptome identified P53 pathway upregulated in MYC-L cells (Díaz-Díaz et al., 2017). Indeed, CASP3-positive cells, which express low MYC levels, show high P53 levels (Díaz-Díaz et al., 2017). Moreover, the whole MYC-L population, without including the CASP3-positive cells, expressed higher P53 levels than the MYC-H population, although this difference is less strong (Figure 14) (Díaz-Díaz et al., 2017). These data suggest P53 involvement in ESCs Cell Competition, both in the execution of loser cell death and in the stress associated to the loser status. Thus, we decided to focus on genes involved in stress/apoptosis downstream of P53.

Among the genes upregulated in MYC-L population, we found several members of the BCL-2 family (See Introduction) such as the pro-apoptotic BH3-only genes *puma, noxa, bik* and *bnip3*. On the other hand, the pro-survival BCL-2 gene *bcl-xl* was downregulated in MYC-L population. We also identified other P53-downstream genes highly upregulated in the MYC-L population such as *ddit4*, *perp*, *tp53inp1* or *sesn3* (Figure 13C).

- *ddit4* is expressed upon stress stimuli as hypoxia or DNA damage by P53, P63 or HIF-1. It functions as an inhibitor of MTORC1. *ddit4* has been also associated metabolism, autophagy and ROS production (Tirado-Hurtado et al., 2018).

- *tp53inp1* is induced after stress stimuli by P53 and P73. In a "steady-state" stress condition has a protective role and is located in the cytoplasm where induces autophagy (especially mitophagy), alleviating ROS and regulating REDOX metabolism. At a certain stress level, autophagy can display a pro-apoptotic role and TP53INP1 can translocate into the nucleus enhancing P53 and P73 transcriptional function in a positive feedback loop (V).

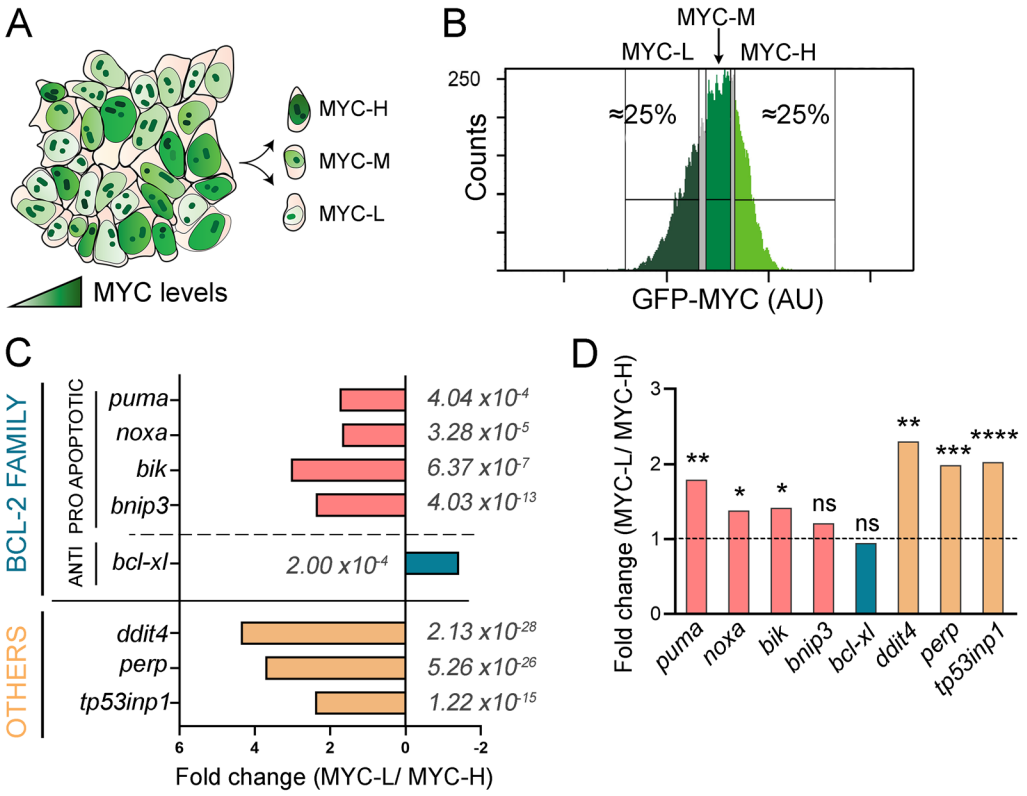

Figure 13. P53 downstream candidates

A. Schematic representation of the GFP-MYC ES cell line. **B.** Histogram showing MYC-H, M and L populations sorted by FACS. **C.** Fold change expression of candidate genes between MYC-L and MYC-H populations (RNAseq data). Grey numbers next to each bar indicate the adj. p-value. **D.** Fold change expression between MYC-L and MYC-H of candidate genes (qPCR data). One sample t and Wilcoxon test was used for statistical analysis.

- *perp* encodes a plasma membrane protein involved in apoptosis and cell adhesion. It is induced upon cell stress by P53 and P63 and can establish a positive feedback loop with P53. It can mediate both extrinsic and mitochondrial apoptotic pathway. PERP has been described to interact with endoplasmic reticulum Ca^{2+} pump, SERCA2b, promoting apoptosis. It also interacts with desmosomes, favouring cell adhesion (McDonnell et al., 2019).

Then, we further validated these candidates by qPCR analysis. Similar results to RNAseq were obtained, although lower differential expression between MYC-L and MYC-H populations was observed for some genes, being not significant in the case of *bnip3* and *bcl-xl* (Figure 13D).

2.1 P53

First, we wanted to check the correlation between P53 and MYC levels as well as the apoptotic function of P53 in MYC-L cells. P53 immunostaining showed a nuclear heterogeneous pattern in ESCs. P53 signal efficiently increased upon etoposide treatment (a

P53 activator through DNA damage generation) (Figure 14A). Per-cell quantification of P53 and MYC levels indicated an inverse correlation between the levels of the two proteins (Figure14 B-D).

To check the apoptotic role of P53 in ESCs, we used an antibody against cleaved CASP3 and looked for cells still maintaining perfect cellular morphology (early apoptotic cells).

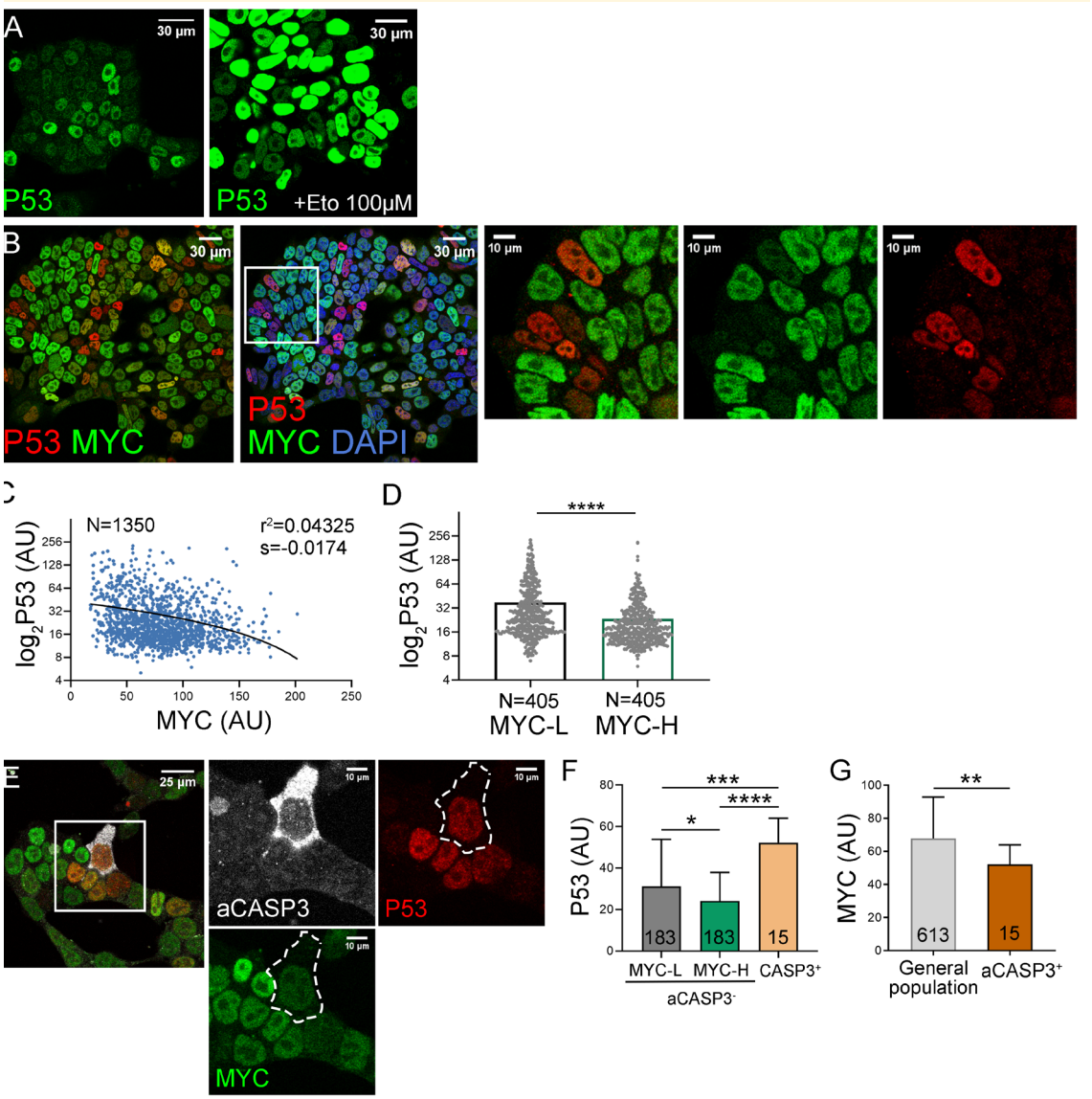

Figure 14. P53 in ESCs.

A. Confocal images showing P53 immunostaining in control and etoposide treated (100µM, 6h) ESCs. **B.** Confocal captures of P53 and MYC signals. **C.** Quantification of P53 and MYC levels, p<0.0001. **D.** P53 levels in MYC-L and MYC-H populations. **E.** Confocal captures showing aCASP3, MYC and P53 **F.** Quantification of P53 levels in MYC-L, MYC-H and aCASP3 positive cells. Quantified number of cells for this experiment is indicated inside the bars. **G.** Quantification of MYC levels in aCASP3 positive cells and the general population.

Early apoptotic cells expressed low levels of MYC and high levels of P53. MYC-low cells (without including apoptotic cells) also expressed higher P53 levels although this difference is lower (Figure14 E-G). These results suggest a role of P53 in both the execution of loser cell death and in *loser* fitness status.

Then, we moved to validate at the protein expression level some of the candidates involved in apoptosis, acting downstream P53.

2.2 BH3-ONLY PROTEIN PUMA

Regarding BCL-2 family, we performed an immunostaining of PUMA, one of the most important apoptotic factors downstream P53 (Yu and Zhang, 2008).

We show that PUMA was expressed in almost all the cells, showing a heterogeneous cytosolic pattern. Quantification of PUMA and MYC levels by confocal microscopy revea-

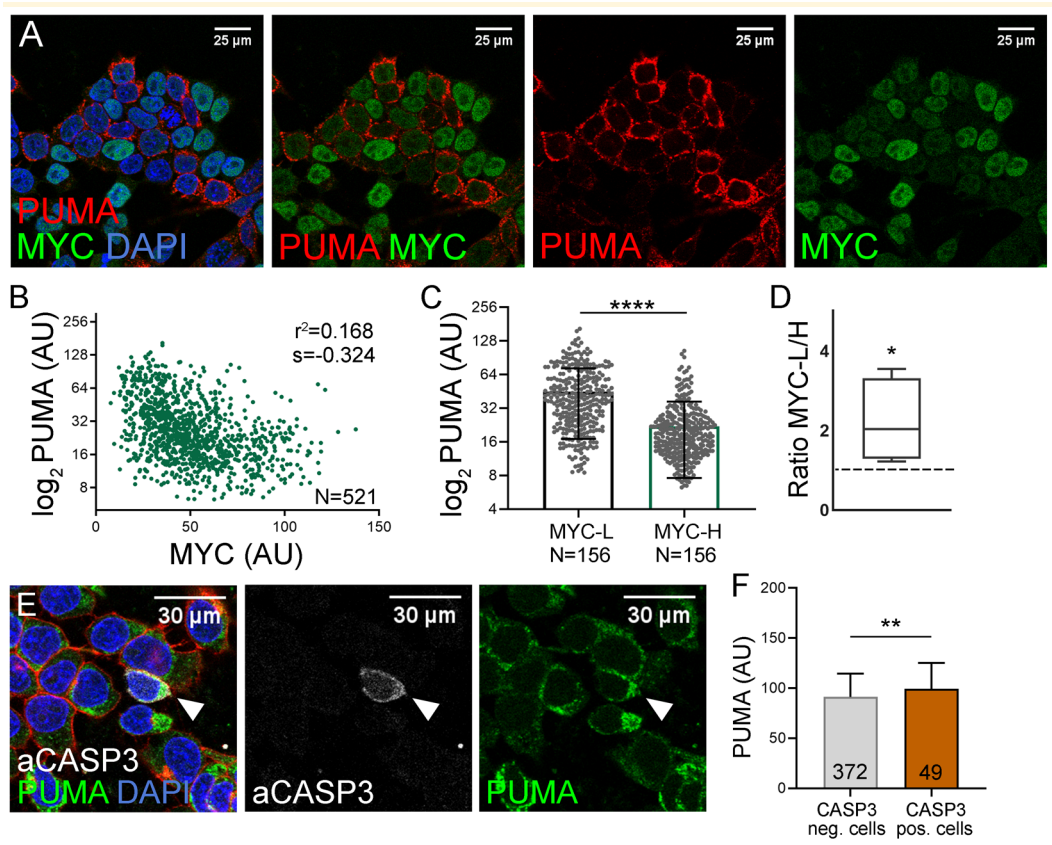

Figure 15. PUMA analysis in ESCs

A. Confocal images showing PUMA and MYC in ESCs. **B.** Quantification of PUMA and MYC levels, p<0.0001. **C.** Quantification of PUMA levels in MYC-L and MYC-H populations. **D.** Ratio of PUMA expression in MYC-L and MYC-H populations by immunoblot. Boxplot represents a set of four independent experiments. **E.** Confocal images of aCASP3+ and PUMA immunostaining. A CASP3 positive cell is indicated with a white arrowhead. **F.** PUMA levels in aCASP3 positive cells and the general population. Cell number quantified for this experiment is indicated inside the bars.

led a strong inverse correlation, which was confirmed by immunoblot (Figure 15A-D). Apoptotic cells expressed moderately higher PUMA levels than the general population (Figure 15E, F).

2.3 mTOR AND BECLIN1

Another potential candidate was DDIT4. As DDIT4 is an important inhibitor of mTORC1, we evaluated mTOR function by measuring pS6 levels, a widely used marker of mTOR

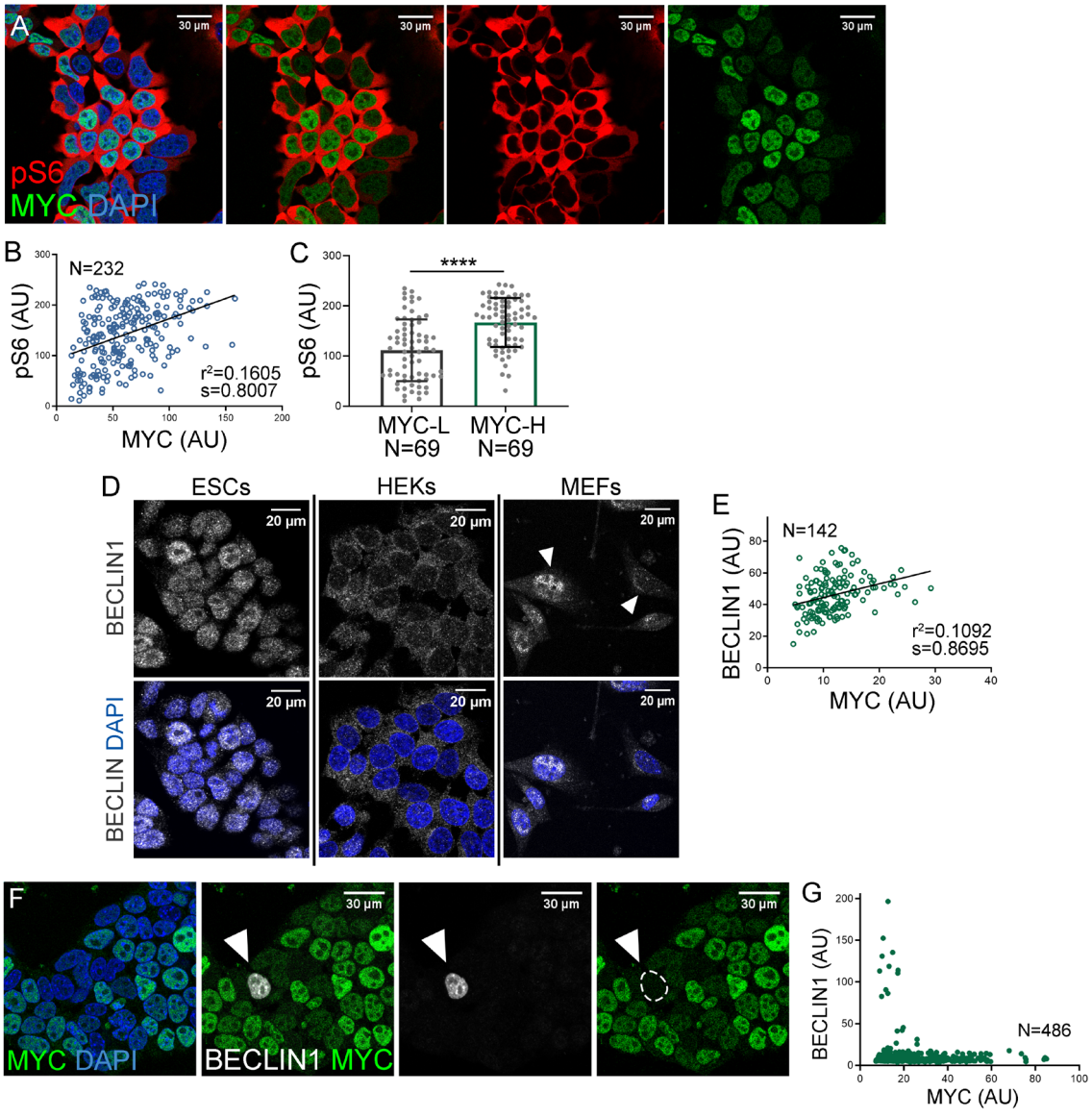

Figure 16 . mTOR activity and BECLIN1 in ESCs.

A. Confocal images showing pS6 and MYC levels. **B.** Quantification of pS6 and MYC levels, p<0.0001 and **(C)** pS6 in MYC-L and MYC-H populations. **D.** Confocal images showing BECLIN1 in different cell types. **E.** Quantification of BECLIN1 and MYC levels, p<0.0001. **F.** Confocal captures of cells with a high nuclear Beclin1 signal and quantification **(G)**.

activity. We found a positive correlation between pS6 and MYC levels (Figure 16A-C).

mTOR inhibition is a critical factor for autophagy initiation (Schmeisser and Parker, 2019). Additionally, TP53INP1 has a role inducing autophagy, especially mitophagy. These two candidates could indicate a function for autophagy in loser status/cell death. To evaluated autophagy, we measured the levels of BECLIN1, a central factor in the formation of the autophagosomes (Kang et al., 2011). In ESCs, BECLIN1 showed a nuclear pattern in the majority of the cells instead of a cytosolic pattern. We assessed BECLIN1 location in other cell types and found a cytosolic signal in HEK cells and a predominantly nuclear pattern in MEFs (Figure 16D). Quantification of BECLIN1 and MYC levels in ESCs indicated a positive correlation (Figure 16E). Further observation of BECLIN1 staining allowed us to identify few ESCs with a considerably high nuclear-signal, which all corresponded to cells with very low MYC levels (Figure 16F, G).

In summary, transcriptional upregulation of *ddit4* and *tp53inp1* suggest a role for autophagy in loser status/cell death. This is supported by the inhibition of mTOR in MYC low cells. Nuclear localization of the autophagy marker BECLIN1 has been previously described although its function is not clear and completely unknown in ESCs (Xu et al., 2017). Therefore, we cannot discard that in this case BECLIN1 is performing a different role from autophagy. However, the fact that it is highly upregulated in cells with very low MYC levels suggest that could be part of the loser cell death execution machinery in ESCs. A similar role for BECLIN1 has been suggested during cardiomyocyte competition in the adult heart (Villa del Campo et al 2014).

2.4 WORKING MODEL

In CC, P53 has a function in both defining cellular fitness and the execution of loser cell death. Here, by transcriptomic analysis we have identified different candidates that could account for these functions downstream P53 (Figure 17).

On one hand, we have identified several BH3-only proteins upregulated in loser cells. These proteins have been involved in apoptosis by inducing MOMP. Moreover, they are linked to metabolism and decreased mitochondrial function through different mechanisms e.g. promoting Ca^{2+} released from the ER (which also can contribute to apoptosis) or interacting with factors involved in mitochondrial fusion and fission or the β subunit of the F0/F1-ATP synthase (Vervliet et al., 2016). Recently, PUMA has been described to block mitochondrial pyruvate carriers (MPCs), preventing OXPHOS and promoting glycolysis (Kim et al., 2019). On the other hand, we have identified *ddit4* and t*p53inp1* genes upregulated in low MYC cells. DDIT4 is a potent inhibitor of mTOR. Inhibition of mTOR can induce autophagy and alter metabolism (Dossou and Basu, 2019). Moreover, TP53INP1 has been related to mitophagy (Saadi et al., 2015)we have provided evidence that Tumor Protein 53-Induced Nuclear Protein 1 (TP53INP1. Finally, PERP, which can be induced by autophagy, prompts apoptosis upon interaction with the ER calcium channels SERCA2b (McDonnell et al., 2019; Roberts and Paraoan, 2020).

In summary, we can propose a signature that reports competitive cell fitness in ESCs based on the levels of P53, its targets PUMA/NOXA, mTOR and MYC. This signature correlates with the status of MTMP and presumably OXPHOS activity. While MYC and mTOR

correlate positively with competitive fitness, P53 and its targets correlate negatively.

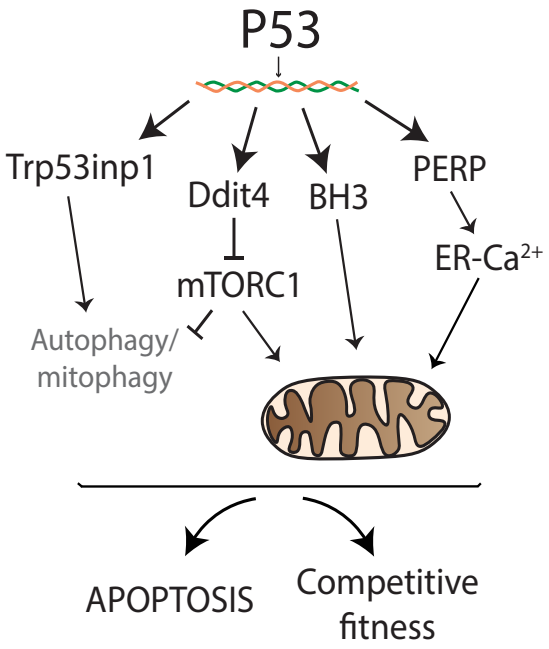

Figure 17. WORKING MODEL.

P53 activates its targets DDIT4, TP53INP1, PERP and some BH3-only proteins. TP53INP1 and DDIT4 (through mTOR inhibition) are important autophagy/mitophagy inducers and can modulate metabolism and mitochondrial function. BH3-only proteins can reduce mitochondrial function by different mechanisms and contribute to apoptosis promoting MOMP. PERP can also contribute to apoptosis by interacting with ER Ca^{2+} channel SERCA2b. Therefore, P53 induces the expression of target genes that can lead to a reduced mitochondrial function (Loser metabolism) and contribute to loser apoptosis via mitochondria.

From all these candidates, we decided to focus on the study of PUMA and its possible function in fitness and CC.

3. P53 AND PUMA IN PLURIPOTENT CELL COMPETITION

Puma has been described as one of the most potent apoptotic inducers of the BH3-only protein (Yu and Zhang, 2008). However, we found that PUMA is expressed in almost every ES cell, suggesting that it is playing a role in ESCs different from apoptosis induction. Together with the fact that PUMA inversely correlates with MYC levels and the recent described functions of PUMA in metabolism (Kim et al., 2019; Siddiqui et al., 2015), suggests that PUMA could contribute to regulate fitness. Thus, we wanted to characterize PUMA in ESCs, its regulation and its function in CC.

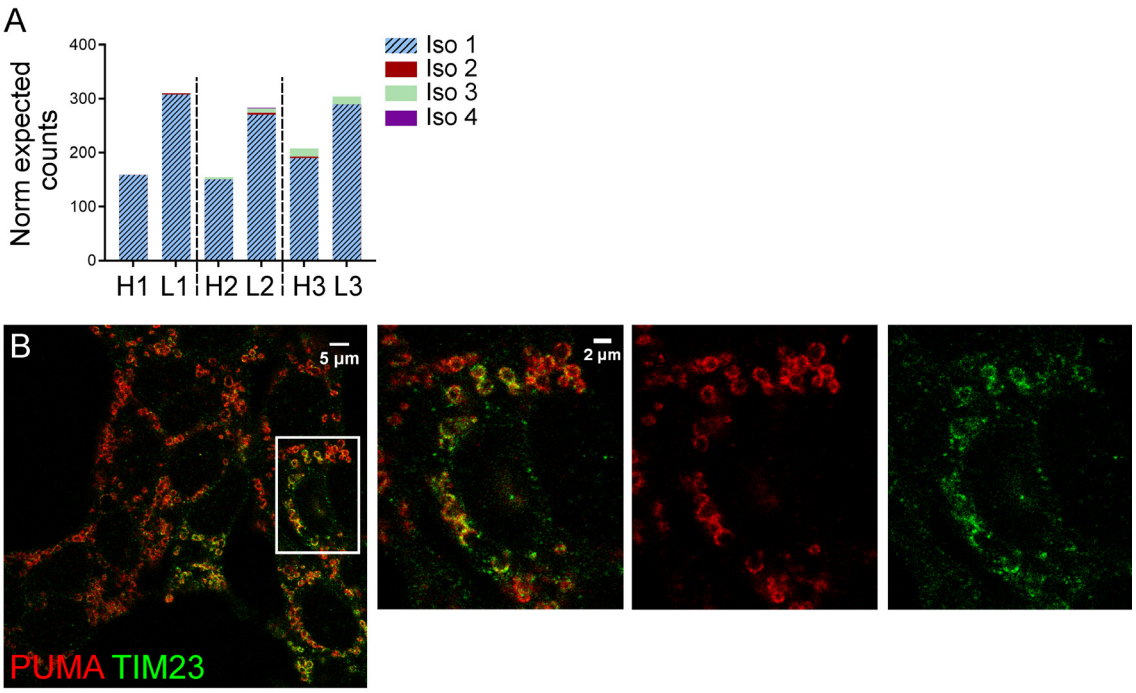

Figure 18. PUMA isoforms and mitochondrial localization

A. Normalized expected counts of PUMA isoforms in MYC-H (H) and MYC-L (L) populations. Numbers 1, 2, 3 next to H or L refer to three biological replicates. **B.** STED-Super-resolution microscopy images showing PUMA and TIM23 levels.

3.1 P53 AND PUMA REGULATION

3.1.1 PUMA Isoforms and Localization

Four isoforms have been described for *puma* gene in the mouse [ensemble.org (2020, Nov)]. We wanted to explore the relevance of these isoforms in PUMA expression in ESCs. Analysis of the counts obtained for each isoform in the RNAseq data showed that the isoform 1 is the principal isoform expressed in ESCs (Figure 18A).

3.1.2 P53 Is the Main Regulator of PUMA in ESCs and the Early Mouse Embryo

Then, we wanted to explore PUMA regulation by P53. We confirmed a positive correlation between P53 and PUMA in ESCs and an inverse correlation between these two proteins and MYC expression (Figure 19A- A'').

Aside from P53, PUMA can be regulated by different factors independently of P53 such as P73, FoxO3a, CHOP, glucocorticoids or ischemia-reperfusion (Futami et al., 2005; Ming et al., 2008; Wu et al., 2007; You et al., 2006; Yu and Zhang, 2008). To determine the relevance of P53 in the regulation of PUMA in ESCs, we checked PUMA expression in *p53*$^{-/-}$ cells. Interestingly, in the absence of P53, we observed no detectable PUMA signal (Figure 19B). On the other hand, P53 activation by using etoposide or Nutlin3 resulted in PUMA upregulation (Figure 19C-D).

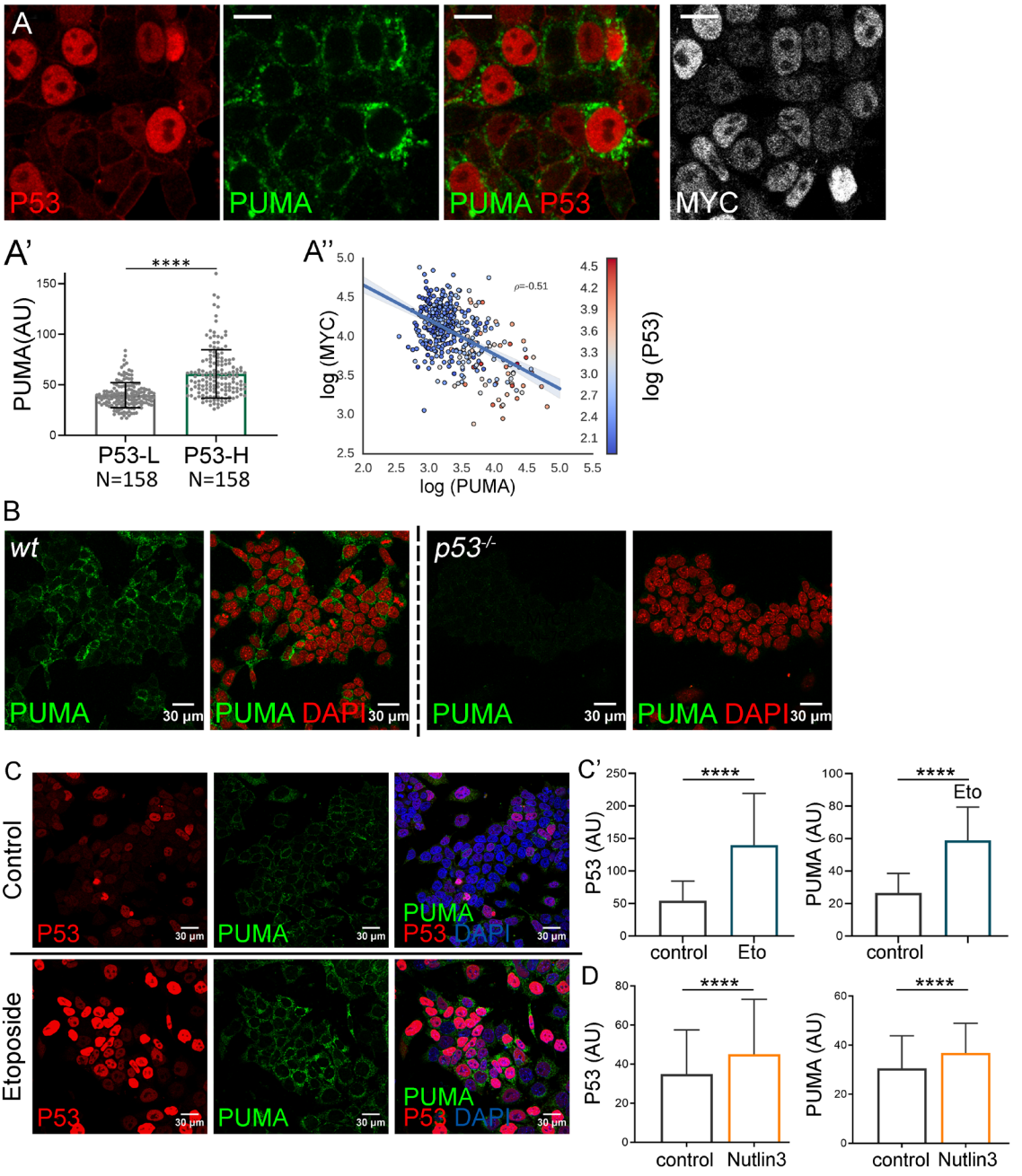

Figure 19. P53 is essential for PUMA expression

A. Confocal images showing P53, PUMA and MYC in ESCs. **A'.** Quantification of PUMA levels in P53-L and P53-H populations. **A''.** Quantification of P53, PUMA, and MYC levels, N=384, PUMA-MYC (r^2=-0.506, p=2.09x10-26), P53-MYC (r^2=-0.457, p=2.09x10-21), P53-PUMA (r^2=0.669, p=3.50x10-51). **B.** PUMA expression in *wt* and *p53*$^{-/-}$ cell line. **C, C'.** P53 and PUMA expression after etoposide treatment and quantification. **D.** Quantification of P53, PUMA levels after Nutlin3 treatment. Scale bar **(A)**, 20µm.

These data indicate that P53 is essential for PUMA expression in ES cells and suggest that, similarly to PUMA expression, P53 activity is widespread in ES cells and not just restricted to stressed or apoptotic cells.

We next moved to study P53, PUMA and MYC expression *in vivo*. We used 6.5dpc mouse embryos given that MYC-driven CC, as well as other CC models, have been described at this stage (Bowling et al., 2018; Clavería et al., 2013; Díaz-Díaz et al., 2017; Lima et al., 2020; Sancho et al., 2013).

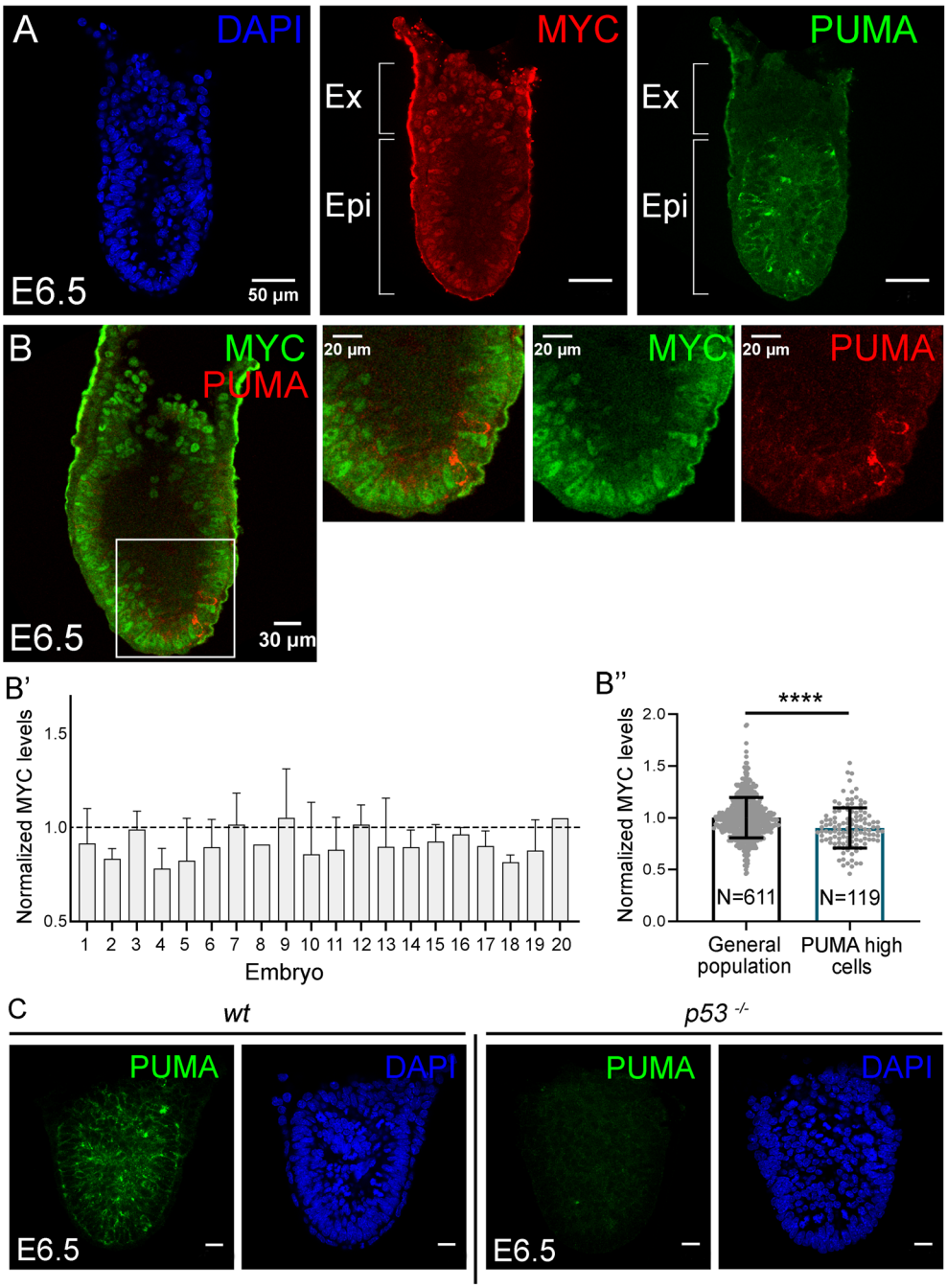

Figure 20. PUMA and MYC inversely correlate in the epiblast.

A, B. Confocal images showing PUMA and MYC expression in an E6.5 mouse embryo (Ex, extraembryonic ectoderm; Epi, epiblast). **B'.** Quantification of normalized MYC levels of high PUMA-expressing cells per embryo. **B''.** Quantification of normalized MYC levels in the general cell population and high PUMA levels. **C.** Confocal images showing PUMA expression in *wt* and *p53*$^{-/-}$ E6.5 embryos. Scale bar **A-C**, 20µm.

Consistent with the observations in ESCs and in similarity to MYC expression pattern, epiblast cells expressed widespread heterogeneous levels of PUMA. In contrast to the epiblast, the extraembryonic ectoderm (Ex) did not show detectable PUMA expression and MYC is strongly expressed here (Figure 20A). We found that epiblast cells with high PUMA levels expressed lower MYC levels than the general population (Figure 20B-B''). Additionally, we found no detectable PUMA signal in *p53*$^{-/-}$ E6.5 embryos (Figure 20C) indicating that P53 is essential for PUMA expression in the embryo.

Then, we wanted to explore P53 expression in the epiblast and its correlation with PUMA and MYC. Although P53 is present and functional at E6.5, we detect almost no P53 positive cells, even after inducing P53 activation with Nutlin-3 (data not shown).

Thus, we moved to a previous stage, E3.5, where Cell Competition has also been described (Hashimoto and Sasaki, 2019). At this stage, P53 immunofluorescence showed a nuclear pattern similar to that obtained in ESCs. We observed a positive correlation between P53 and PUMA in the blastocyst (Figure 21A, A'). However, no correlation was found between P53 and MYC (Figure 21B, B').

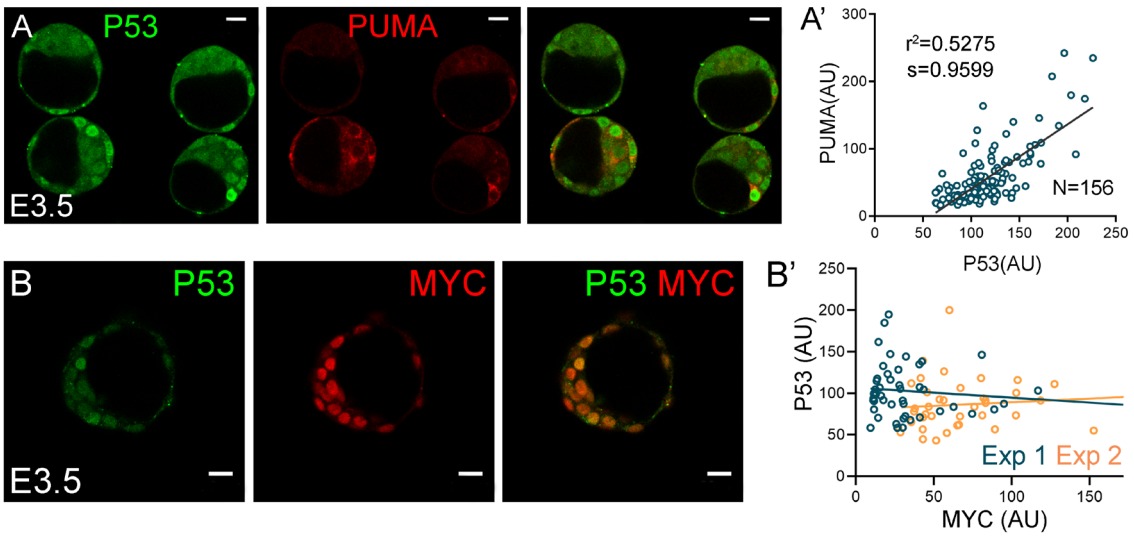

Figure 21. P53-PUMA and MYC expression in the early mouse embryo.

A. Confocal images showing P53 and PUMA levels in E3.5 mouse embryos and quantification **(A')**, p<0,0001. **B.** Confocal captures of P53 and MYC levels in E3.5 embryos. **B'.** Quantification of MYC and P53 levels in the blastocysts of two different litters (Exp 1: r^2=0.0087, s=-0.122, N=46, p=0.53 ; Exp 2: r^2=0.011, s=0.087, N=85, p=0.41).

3.1.3 P53-PUMA and MYC Regulation

We have reported an inverse correlation between MYC and P53-PUMA, so high P53 and/or PUMA cells are exclusively MYC-low cells (Figure 19). To understand whether these observations derive from cross-regulatory interactions between MYC and P53/PUMA, we studied the expression patterns of P53 and PUMA in *myc*-KO cells. We found that elimination of *myc* neither increased P53 nor PUMA expression, but rather we observed a slight non-significant downregulation (Figure 22A-B'). These results indicate that MYC does not regulate P53-PUMA expression.

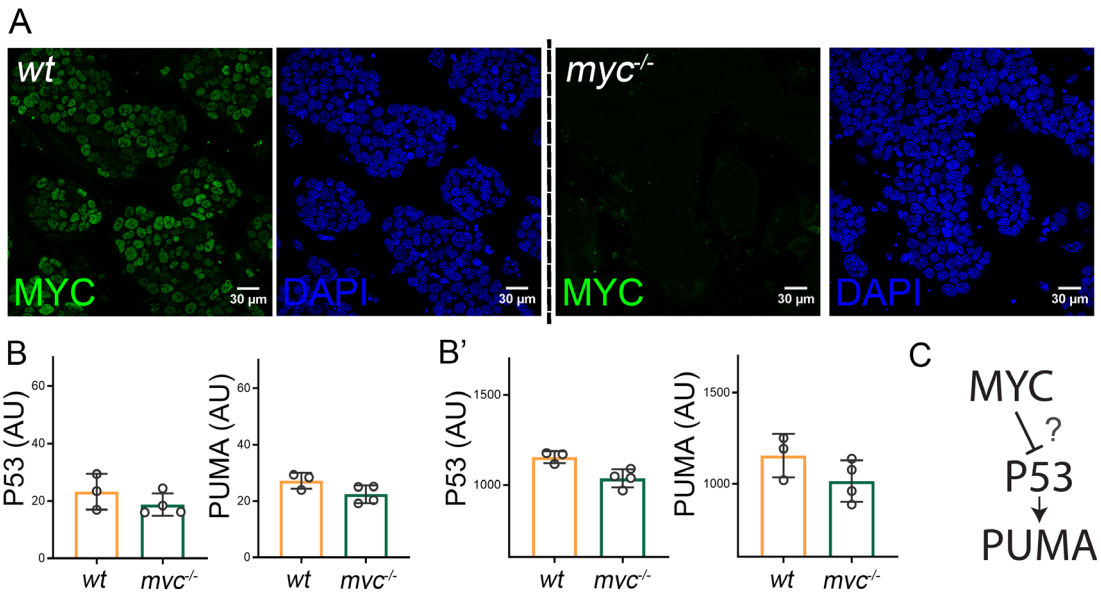

Figure 22. P53-PUMA expression in *myc*$^{-/-}$ cells.

A. Confocal captures showing MYC levels in *wt* and *myc*$^{-/-}$ ES cells. **B.** Quantification of P53 and PUMA levels in *wt* and *myc-/-* clones by confocal microscopy and **(B')** by flow cytometry. **C.** Model representing a hypothetical regulation of P53-PUMA by MYC.

We next measured MYC levels in *p53*, *puma* and *noxa* KO cells. We observed MYC upregulation in *p53*$^{-/-}$ cells (Figure 23A-B). Additionally, P53 activation with Nutlin3 induced MYC downregulation (Figure 23D-F).

We observed a non-significant upregulation of Myc in *puma*$^{-/-}$ cells. *Noxa* elimination does not affect MYC expression (Figure 23A).

Then, we were interested into explore MYC upregulation in *p53*$^{-/-}$ early mouse embryos. We did not observed differences in MYC levels between *p53* KO E6.5 embryos from two litters and their *wt/het* littermates (Figure 24A-B). Same result was observed preliminarily in one E3.5 litter (Figure 24C, C').

3.1.4 P53-PUMA and MYC Are Regulated by Pluripotency

As the mouse embryo develops from pre-implantation to post-implantation before gastrulation starts at E6.5, pluripotent epiblast cells evolve in a continuum manner from a "naïve" pluripotency or "ground state" to a "primed" pluripotency before they commit into a particular fate (see Introduction) (Nichols and Smith, 2009b). The different pluripotency states can be recreated *in vitro* in ESCs by using different culture conditions (Boroviak et al., 2014). MYC is described to be downstream pluripotency and determine competitive ability (Díaz-Díaz et al., 2017).

Thus, we were curious about P53 and PUMA expression dynamic in ESCs along different pluripotent stages. To study this, we used different media: FBS, SR and 2i media, which increasingly promote the naïve state.

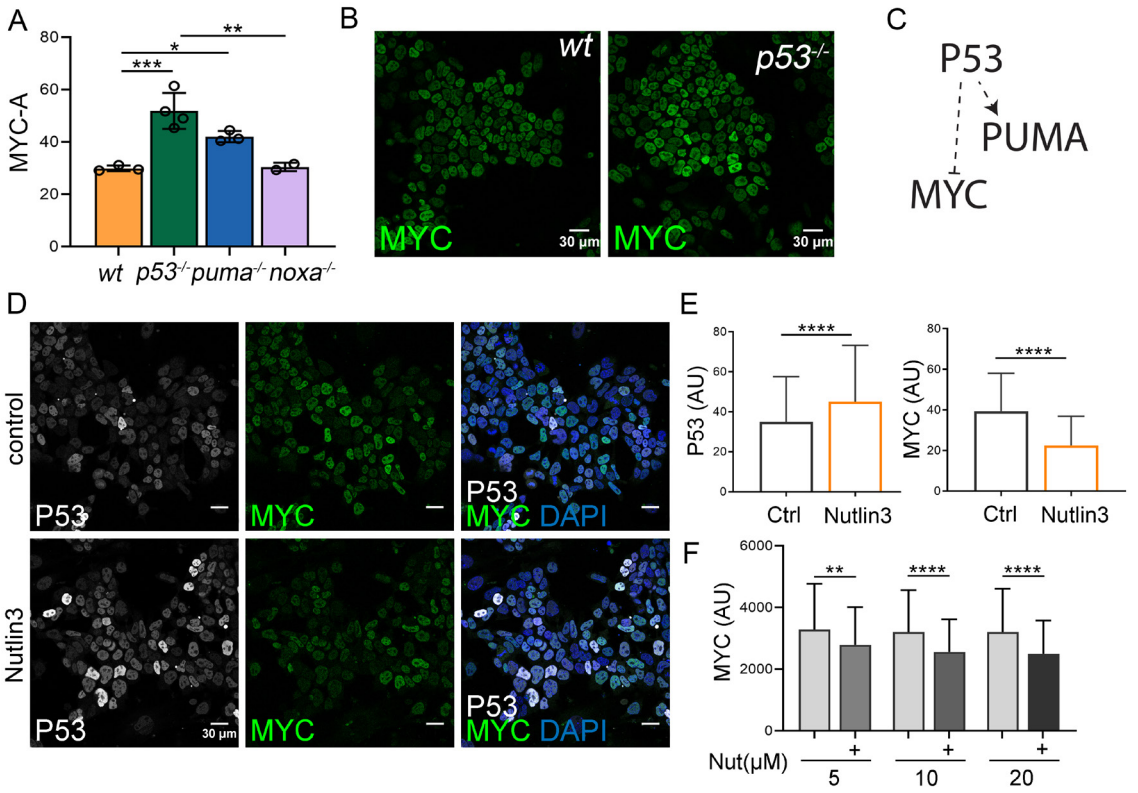

Figure 23. MYC expression in *wt*, *p53*, *puma* and noxa KO ESCs.

A. Quantification of MYC levels in *wt*, *p53*, *puma* and *noxa* KO ES cells. **B.** Confocal images showing MYC levels in *wt* and *p53*$^{-/-}$ cells. **C.** Model representing MYC regulation by P53 and PUMA. **D.** Confocal images showing P53 and MYC levels in cells treated with Nutlin3 and control and quantification **(E)**. **F.** MYC levels upon treatment with increased concentration of Nutlin3 measured by flow cytometry.

- "Serum + LIF medium". Here referred to "FBS medium", is a conventional medium to counterbalance differentiation stimuli. These conditions allow the presence of cells with either a more naïve or a more primed status.

- "SR medium". SR, knockout serum replacement, is a chemically defined formula that can substitute serum. It has been described that maintains a more pluripotent status than conventional serum (Cheng et al., 2004).

- "2i media". Based on PD03 and CHIRON molecules added to conventional media, promotes the "naïve" pluripotent state.

We found that P53 and PUMA levels correlated with the pluripotent state, in similarity with the behaviour of MYC. P53 and PUMA levels were low in 2i medium and they increased in SR and even more in FBS medium (Figure 25A). This indicates that naïve pluripotent cells maintain low levels of P53 and PUMA, whereas, the acquisition of the primed status activates P53 and PUMA. Additionally, naïve pluripotent cells also maintain low levels of MYC. As media conditions allow cells the transit to more prime state, MYC levels and variance increased (Figure 25A) (Díaz-Díaz et al., 2017). On the other hand, we allowed differentiation by removing LIF, which is necessary to maintain ESCs without

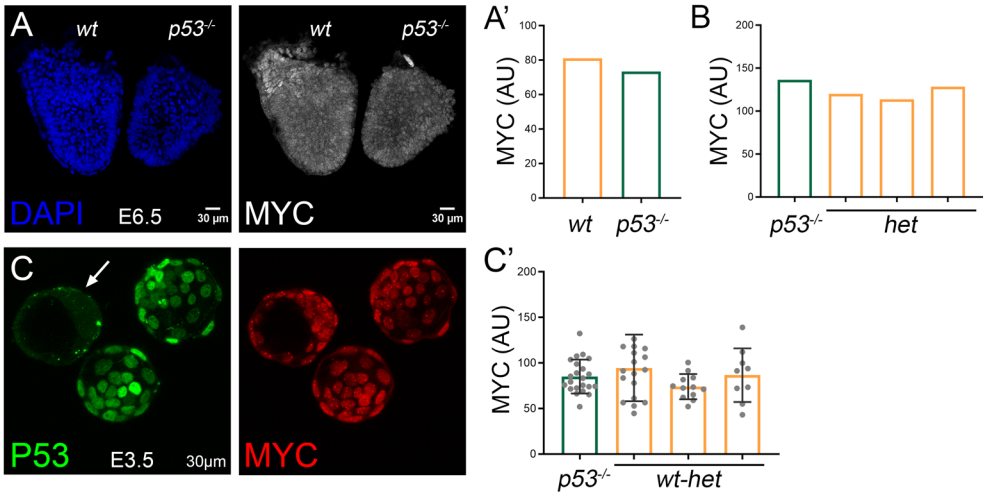

Figure 24. MYC expression in *p53*$^{-/-}$ early mouse embryos.

A. Confocal images of MYC levels in a *wt* and a *p53*$^{-/-}$ 6.5dpc mouse embryo and quantification **(A)**. **B.** Quantification of MYC levels in *p53*$^{-/-}$ or heterozygous 6.5dcp embryos from a different litter. **C.** Confocal captures showing P53 and MYC levels in 3.5dpc mouse embryos and MYC level quantification **(C')**. White arrow in **C** shows a *p53*$^{-/-}$ blastocyst.

MEFs. In these conditions, MYC levels decreased while PUMA augmented (Figure 25B, B'). Collectively, these results indicate that P53 and PUMA expression are regulated by pluripotent conditions and they increase as cells progress towards differentiation.

We were also interested in knowing about PUMA expression pattern during early embryo development. PUMA is first detected at E3.5 and is expressed at high levels in some specimens. From E5 to E6.5, PUMA is heterogeneously expressed in the epiblast. However, when gastrulation starts, PUMA decreases in the gastrulating cells of the primitive streak (Figure 24C).

3.2 CHARACTERIZATION OF *p53, puma* AND *noxa* KNOCKOUT ESCs

P53 is well known to induce cell cycle arrest, senescence and apoptosis in response to DNA damage and other stress stimuli. However, P53 has been related to other functions as regulation of autophagy, metabolism or pluripotency (Kastenhuber and Lowe, 2017). BCL-2 proteins such as PUMA and NOXA are involved in apoptosis, although other non-apoptotic functions as regulation of metabolism have been described (Siddiqui et al., 2015). In ESCs, P53 function in apoptosis and cycle arrest is not clear and recent works suggest that P53 functions change depending on ESCs pluripotent status (Fu et al., 2020; Hao et al., 2020; Jaiswal et al., 2020). On the other hand, less is known about PUMA and NOXA function in ESCs. Thus, we characterized apoptosis, cell cycle and proliferation in *p53, puma* and *noxa* knockout ESCs, using conventional medium (serum + LIF).

To study apoptosis, we performed an immunostaining against active CASP3 (aCASP3) and analysed it by flow cytometry. We observed a reduction of the proportion of cells with active CASP3 in *p53, puma* and *noxa* knockout ESCs, being this reduction stronger in *p53* KO cells (Figure 26A, B). Additionally, to assess caspase activation we used a com-

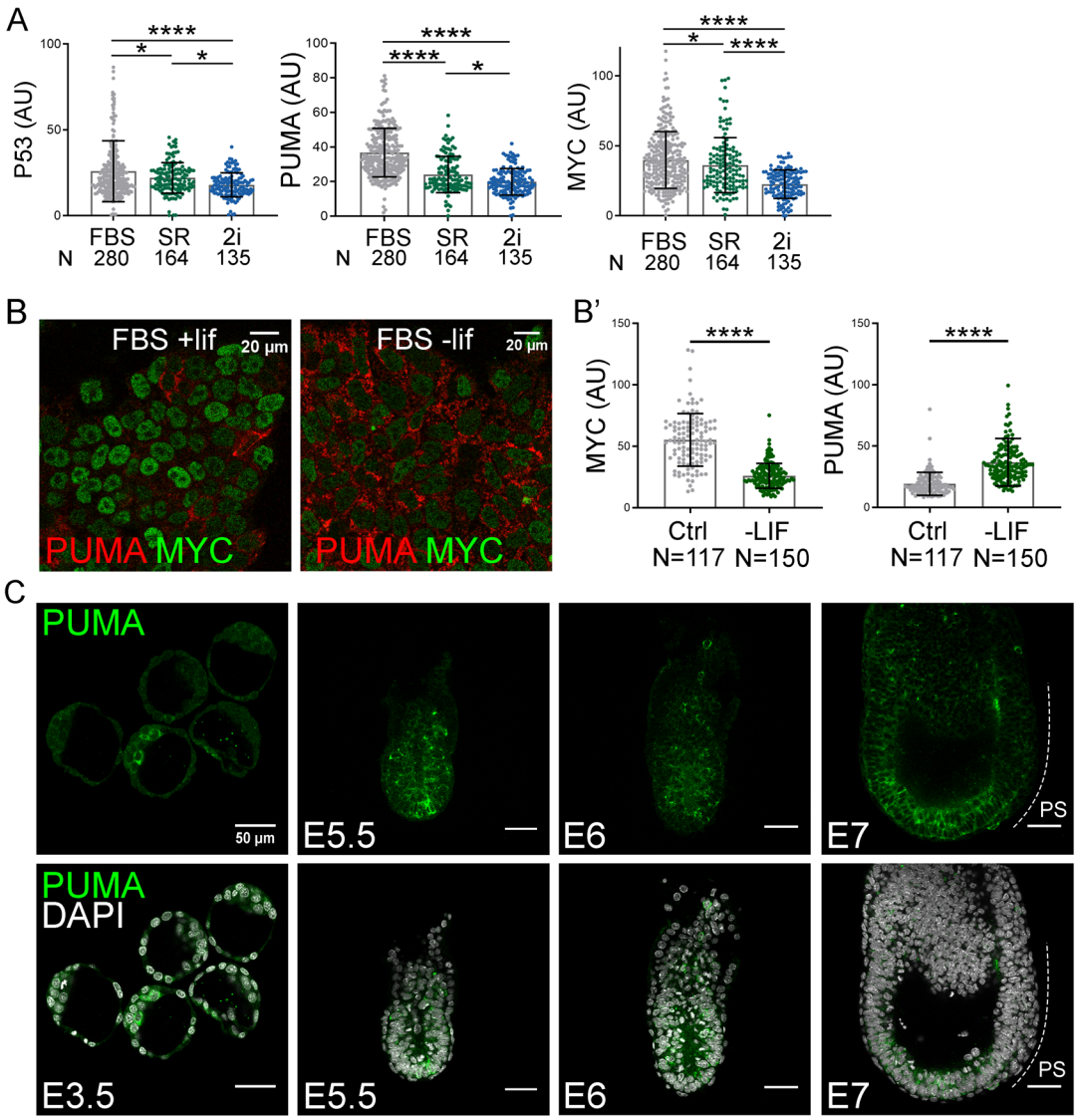

Figure 25. Regulation of P53, PUMA and MYC by pluripotent condition.

A. Quantification of P53, PUMA and MYC levels in FBS, SR and 2i conditions. **B.** Confocal images of PUMA and MYC levels in FBS media with LIF or without LIF and quantification **(B')**. **C.** Confocal images showing mouse embryo at different stages.

mercial reagent (FLICA™). This reagent is based on the CASP3/7 target sequence (DEVD) and a fluorescent dye, so that upon caspase cleavage, it emits fluorescence. By this assay, we also observed a reduction in caspase activity in *puma, noxa* and especially, *p53* KO cells (Figure 26C).

We then examined proliferation by detecting phospho-Histone 3, pH3, (which labels condensed chromosomes during mitosis) and analysed by confocal microscopy and flow cytometry. No significant changes in the proportion of pH3 positive cells were observed in the knockout lines (Figure 26D-E'). To assess a role in cell cycle for *p53*, *puma* or *noxa*, we used propidium iodide and analyzed by flow cytometry and found no significant alteration of cell cycle in the mutant cell lines (Figure 26F, F').

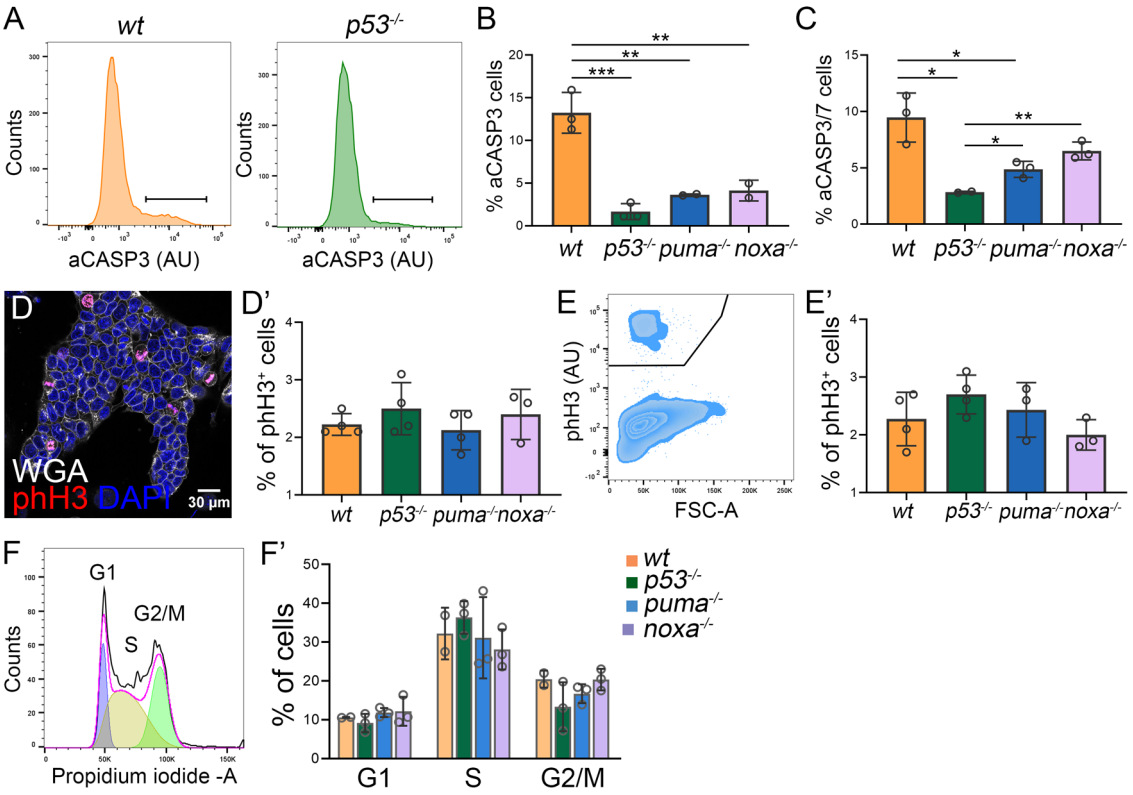

Figure 26. Apoptosis, proliferation and cell cycle in *p53*, *puma* and *noxa* KO ESCs.

A. Histograms showing aCASP3 staining in *wt* and *p53*$^{-/-}$ cells. **B.** Quantification of the percentage of aCASP3+ cells. **C.** Quantification of the percentage of aCASP3/7 positive cells using FLICA™. **D.** Confocal image showing pH3 positive cells and quantification **(D')**. **E.** Zebra-plot of pH3 staining. pH3 positive population is located in the left upper part, gated by a black contour. **E'.** Quantification of the percentage of pH3 positive cells. **F.** Histogram showing cell cycle and quantification **(F')**.

P53 has a function inducing differentiation and restricting plasticity in stem cell populations (Jain and Barton, 2018). In ESCs, different works relate P53 to differentiation. Many of these works are performed after induction of DNA damage or by inducing differentiation. P53 differentiating function in ESCs in normal condition is less described, although it has been suggested in a work in human ESCs (Kastenhuber and Lowe, 2017).

Thus, we wanted to study the differentiation status in the KO cell lines, by detecting p-ERK, which is described to suppress self-renewal and induce differentiation (Deathridge et al., 2019). We performed p-ERK immunostaining and observed higher levels in *p53*$^{-/-}$ cells (Figure 27A, B).

3.3. CELL COMPETITION

Then, we wanted to check whether *p53*, *puma* and *noxa* have a role in regulating fitness, by studying whether their elimination promotes the winner phenotype. To do so, we confronted *tdTomato*-expressing WT cells with *p53, puma* or *noxa* knockout cells and other non-fluorescent WT cells[7] as a control. To account for clonal variation, including

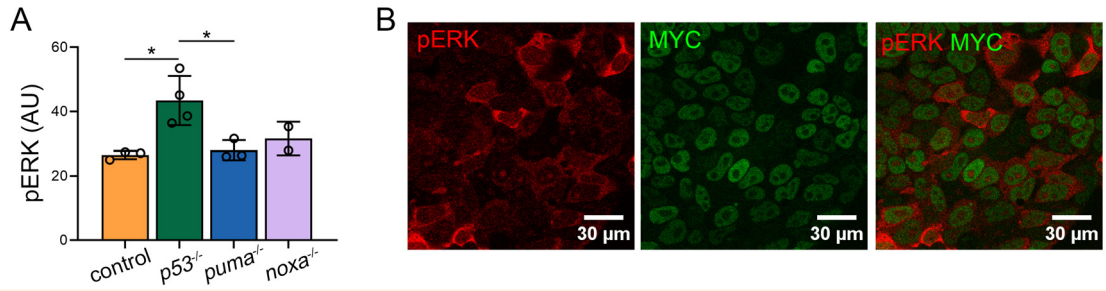

Figure 27. Differentiation in *p53*, *puma* and *noxa* KO ESCs.

A. Bars graph showing p-ERK quantification in mutant cell lines. **B.** Confocal images of p-ERK in ESCs.

possible off-target mutations, we used for each gene at least three mutant and three WT sister clones. According to the literature referring to similar Competition assays, these experiments were performed in differentiating conditions (Dejosez et al., 2013; Lima et al., 2020; Sancho et al., 2013).

In these CC assays, we compared the evolution of *tdTomato*-WT cells in co-culture with WT or the different KO cell lines (Figure 28A, B). *Tomato*-WT cells were eliminated when co-cultured together with *p53*$^{-/-}$ cells but not when they were co-cultured with WT cells (Figure 28C, left). The population of *tomato*-WT cells was also reduced when confronted with *puma*$^{-/-}$ cells, although this effect was less pronounced than in the case of *p53*$^{-/-}$ cells (Figure 28D, left). Similar experiments with *noxa*$^{-/-}$ resulted in a non-significant tendency towards a reduced growth of the confronted *tomato-WT* cells (Figure 28E, left). These differences in cell population growth can be also observed by the ratio between the final and initial cell numbers for each population (Figure 28C, D, E). Some of these assays were repeated with similar results (Figure 28C', C'', D').

These results indicate that *p53* and *puma* can regulate Competitive fitness in ESCs in such a way that higher levels of P53/PUMA results in lower fitness. Additionally, we observed that *p53* KO cells increase their number faster than WT. This also occurs in *puma* KO cells.

3.3.1 CC and Pluripotency

CC induced by BMP-signalling deficient cells occurs in differentiating conditions but this does not take place if naïve pluripotency is enforced in 2i condition (Lima et al., 2020; Sancho et al., 2013). Regarding P53-induced CC, Dejosez et al., showed that *p53*$^{-/-}$ cells seem to outcompete WT cells in the early mouse embryo and in ESCs in differentiating conditions, although it is not clear whether this is due to an autonomous behaviour or to CC. In contrast, in the same work, when cells are maintained in naïve pluripotent status, WT cells outcompete *p53* KO cells, although they show a similar growing rate when separated. (Dejosez et al., 2013).

Thus, we wanted to confirm whether *p53*$^{-/-}$ cells switch their status from winner to loser depending on pluripotency. *p53*-KO cells were not outcompeted by WT cells in 2i me-

[7] *Wt* clones were obtained during the same knockout-generation process than *p53*, *puma* and *noxa*.

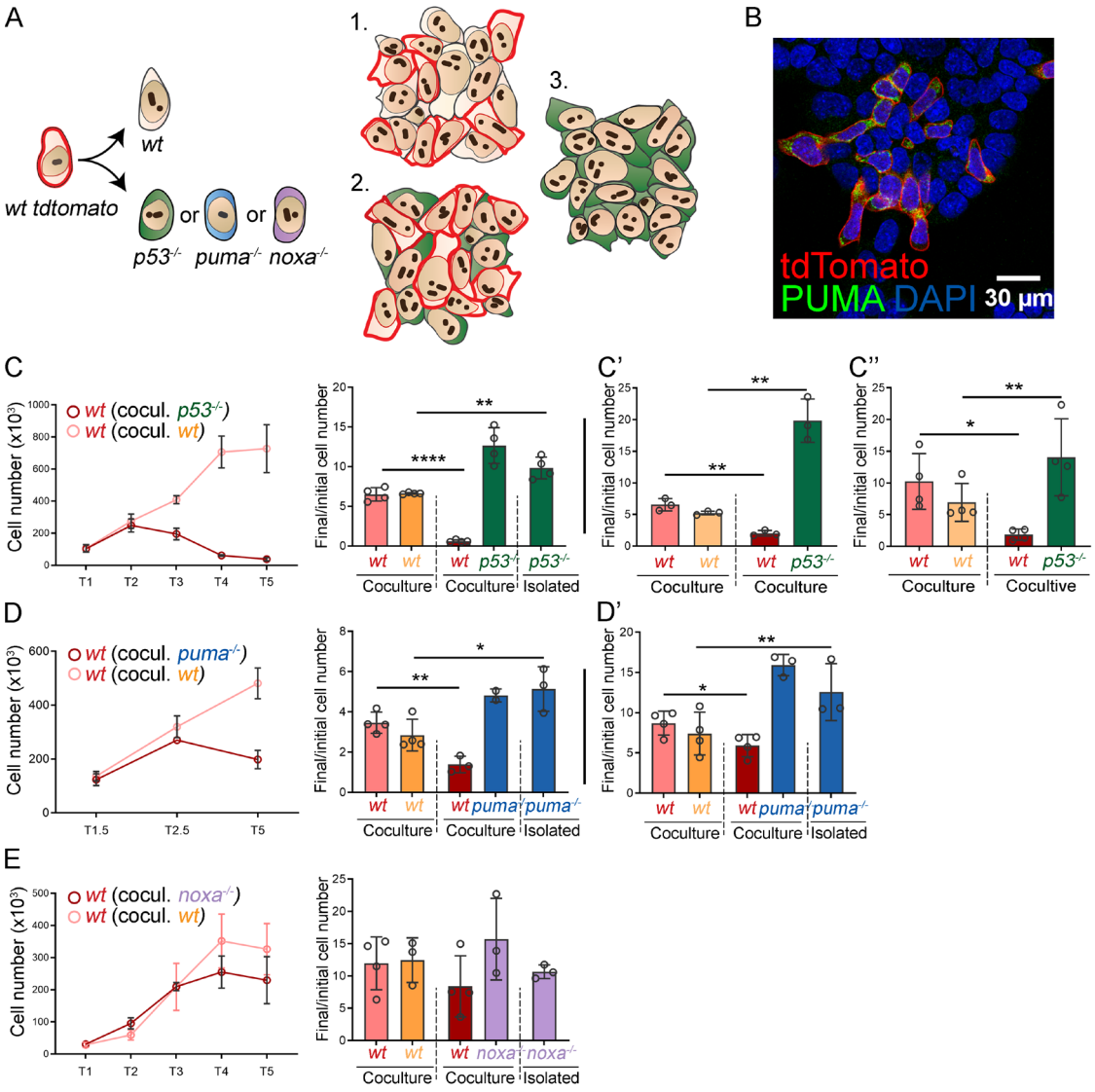

Figure 28. CC induced by *p53*$^{-/-}$, *puma*$^{-/-}$ and *noxa*$^{-/-}$.

A. (left) *tdTomato*-WT cells were confronted either with knockout cells or non-fluorescent WT cells as a control. Knockout lines are represented in different colours. **A. (right)** (1) We monitored the evolution of *tdTomato*-WT when confronted with non-fluorescent WT cells and (2) with each knockout cell lines. Here *p53*$^{-/-}$ cells (in green) are used as an example of KO cell line. (3) We also monitored the evolution of KO cells line in isolation. **B.** Confocal image showing *tdTomato*-WT and *puma* KO cells. **C, D, E.** Evolution of *tdTomato*-WT cell number in co-cultured with WT cells (light red line) or *p53*$^{-/-}$ cells **(C)**, *puma*$^{-/-}$ **(D)**, noxa **(E)** (dark red line) **(left)**. Bar graphs representing the ratio between the final and initial cell number in *wt* and *p53*$^{-/-}$, *puma*$^{-/-}$ or *noxa*$^{-/-}$ in isolated or co-culture condition **(right)**. Each dot represents a different *wt*, *p53*$^{-/-}$, *puma*$^{-/-}$ or *noxa*$^{-/-}$ clone. Four clones of *wt* and *p53*$^{-/-}$, *puma*$^{-/-}$ or *noxa*$^{-/-}$ were used in each experiment.

dium (Figure 29A, B). In 2i medium, *p53*$^{-/-}$ cells had a similar growth rate than WT cells, both in isolation (Figure 29B). When co-cultured, we observed a non-significant tendency to higher growth of the *p53*$^{-/-}$ ESCs at the expense of WT cells.

In 2i conditions, apoptosis in WT cells is reduced to similar levels than those observed in *p53*$^{-/-}$ cells (Figure 29C). Moreover, in similarity to what was observed in differentiating conditions, we did not find differences in the proportion of pH3^{+} cells between WT and *p53*$^{-/-}$ cells, although proliferation in 2i conditions was reduced in both populations in comparison to differentiating conditions (*pvalue*=0,02) (Figure 29D).

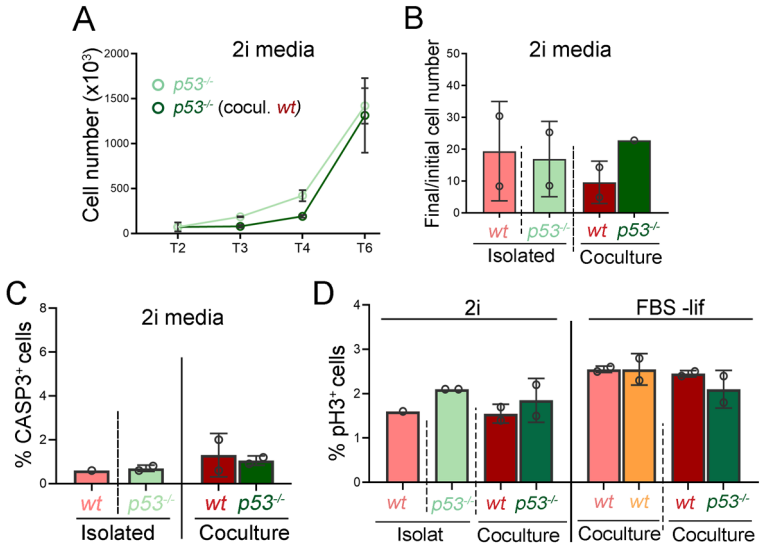

Figure 29. P53-induced CC in 2i conditions.

A. Evolution of *p53*$^{-/-}$ cells isolated or in co-culture with WT cells. **B.** Final/initial cell number ratio of *p53*$^{-/-}$ cells and WT cells isolated and in co-culture. **C.** Percentage of CASP3^{+} cells of *p53*$^{-/-}$ cells and WT cells. **D.** Percentage of pH3 positive cells in the indicated conditions.

Collectively, we have not observed the previously described acquisition of a loser status by *p53*$^{-/-}$ ESCs in 2i conditions, however, we observed a blunting of the winner phenotype of *p53*$^{-/-}$ ESCs in 2i conditions compared to the differentiating conditions. Additionally, in these conditions, some differential characteristics between WT and *p53*$^{-/-}$ when cultured in isolation equalize. Thus, apoptosis in WT cells decreased to similar levels to *p53*-KO cells and the higher growing rate in *p53*-KO cells is reduced to levels similar to WT cells.

3.3.2 CC and Mitochondrial Metabolism

Then, we wanted to explore how P53 and PUMA regulate fitness and induce CC. Regarding PUMA location in the mitochondria and its recently described role in glucose metabolism, we wanted to check mitochondrial status.

To do that, we decided to assess mitochondrial REDOX status as it can report differential mitochondrial function (Handy and Loscalzo, 2012). For that, we used the mitochondrial ratiometric reporter protein Grx1-roGFP$_2$, which we cloned within a lentiviral vec-

tor downstream the EF1 promoter and subsequently transfected in *wt, p53*-KO and *puma*-KO ESCs lines.

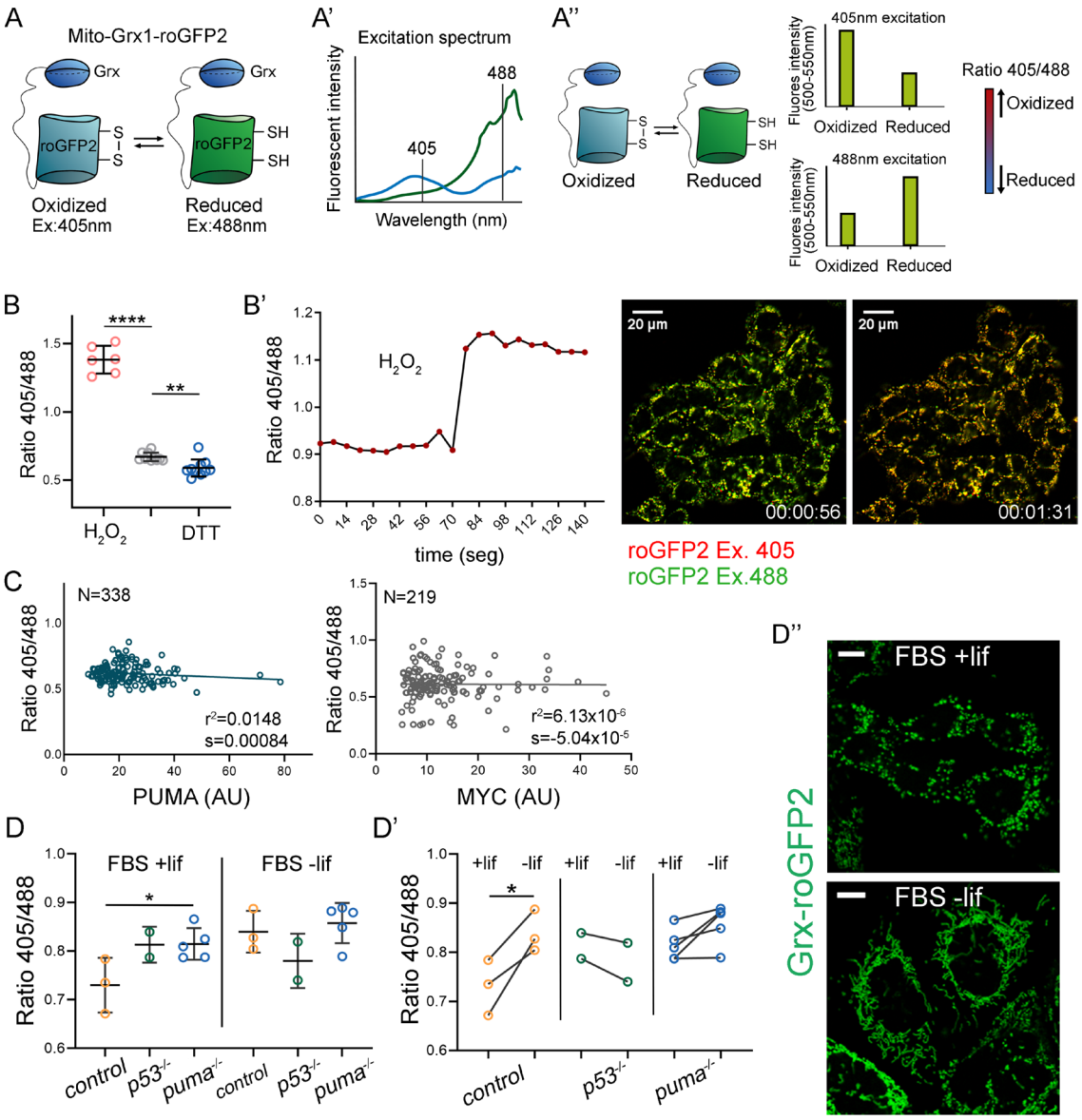

Figure 30. Mitochondrial REDOX status in *wt*, *p53-/-* and *puma-/-* cells.

A. Schematic representation of Grx1-roGFP$_2$ in an oxidized and reduced form, **(A')** excitation spectrum of roGFP$_2$ when it is oxidized or reduced, **(A'')** fluorescent emission of roGFP$_2$ detected at (500-550nm) when it is excited at 405 (upper) or 488 nm (lower). **B.** Ratio of emission intensity when Grx1-roGFP$_2$ is excited at 405nm versus 488nm upon treatment with H_2O_2 or DTT. **B'.** 405/488 ratio "in live"-increased upon H_2O_2 treatment and confocal capture at different time points. **C.** Quantification of 405/488 ratio and PUMA or MYC levels. **D, D'.** 405/488 ratio of *wt*, *p53*$^{-/-}$ and *puma*$^{-/-}$ cells in conventional and differentiating conditions and confocal captures of *wt* cells in these conditions **(D'')**.

roGFP can display an oxidized or reduced form. When it is reduced, its excitation spectrum has a maximum at λ=488nm. When it is oxidized, the excitation spectrum increases at λ=405nm. Thus, the emission intensity when roGFP is excited at 405 or 488nm varies along with REDOX status in the mitochondria, which can be monitored by the emission ratio after excitation at 405 and 488nm (Figure 30A-A''). As a control, we confirmed that inducing oxidation of roGFP-expressing cells with H_2O_2 increases emission intensity when roGFP is excited at 405nm and decreases emission when is excited at 488nm. Then, the ratio between this to emission intensities (405/488nm) increases. The opposite situation occurs inducing reduction with DTT (Figure 30A'', B). These controls demonstrated that the Grx1-roGFP$_2$ reporter was expressed and functional in ESCs (Figure 30B-B').

Next, we tested whether there is a correlation between mitochondrial REDOX status and MYC and PUMA expression in WT cells but we did not identify a significant correlation (Figure 30C). We then tested mitochondrial REDOX status in *wt, p53*$^{-/-}$ and *puma*$^{-/-}$ cells in conventional conditions and inducing differentiation. However, no major changes were detected, except that in conventional conditions WT cells seem to exhibit a more reduced mitochondrial status (Figure 30D). Differentiation induction promoted mitochondrial morphological changes. From non-fused spherical shape to more fused elongated morphology (Figure 30D'').

We found that in WT cells differentiation induced oxidation in mitochondria. In contrast, no significant change was found in *puma*$^{-/-}$ and *p53*$^{-/-}$ cells cells, which correlates with the fact that in undifferentiated conditions, they show higher mitochondrial oxidation than WT ESCs (Figure 30D').

Collectively, the fact that we did not find important differences between mitochondrial REDOX status among *wt, p53*$^{-/-}$ and *puma*$^{-/-}$ cells, together with the fact that no correlation was shown between mitochondrial REDOX status and MYC or PUMA expression, suggest that mitochondrial REDOX status does not play a principal role defining fitness. Therefore, other approaches will be necessary to evaluate the role of P53 and PUMA in the mitochondria and the metabolism and shed some light into the mechanisms by which BH3 and other factors downstream P53 regulate fitness and induced CC.

DISCUSSION

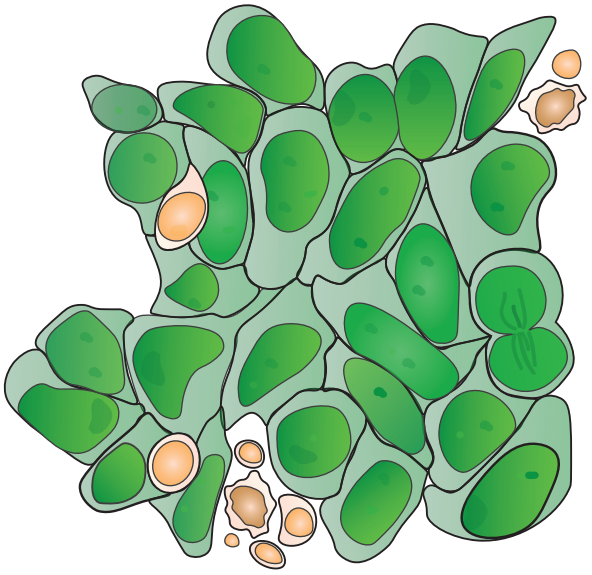

In this doctoral thesis, we have explored a number of candidate pathways and factors potentially involved in loser cell death. As a result, we have characterized different factors and mechanisms upregulated in low MYC cells contributing to the "loser status/signature". We then focused on the candidates P53 and the BCL-2 family members PUMA and NOXA and characterized their expression, regulation and their role defining competitive fitness in pluripotent stem cells.

1. CELL STRESS IN LOW-MYC CELLS

Live analysis in mESCs shows that low MYC cells are eliminated after persistent random contacts with high MYC cells (Díaz-Díaz et al., 2017). This observation suggested that these contacts could generate cell stress in "loser" cells, triggering its elimination. Additionally, we found activation of the stress kinase JNK upregulated in low MYC cells, which supports this notion.

JNK is a MAPK activated by different stress stimuli. JNK has been widely described in CC in *Drosophila* as a factor able to induce "loser" cell death (See Introduction). Additional roles described for JNK activation in loser cells are (1) inhibition of proliferation and (2) non-autonomously enhancement of proliferation in neighbouring winner cells (Chen et al., 2012; Kolahgar et al., 2015; Moreno et al., 2002). However, in mammals the role of JNK in CC is less explored. In fact, in *scrib*$^{-/-}$ induced CC in MDCK culture (Madin-Darby Canine Kidney) it has been reported that not JNK, but another stress MAPK; P38, is involved in loser cell elimination (Norman et al., 2012; Wagstaff et al., 2016).

In ESCs, JNK has been related to self-renewal, while its role in stress and apoptosis remained unknown (Semba et al., 2020). The fact that pJNK is higher in low MYC cells suggests that it is unlikely that JNK high activity levels correlate with pluripotency, given that low-MYC cells exhibit a more differentiated status than high MYC cells (Díaz-Díaz et al., 2017). Regarding its general function as a stress activated kinase, this result could support the idea that low-MYC cells are subjected to stress due to CC.

Therefore, we analysed two well-described and highly regulated stress stimuli in ESCs such as genotoxic and oxidative stress. We also checked mitochondrial status and two recent described factors involved in apoptosis, ARTS and HTRA1.

1.1 GENOTOXIC STRESS

Genome integrity maintenance is crucial for ESCs. Despite their fast proliferation, ESCs keep a low mutational level due to an efficient DNA Damage Repair response. In addition, when damage is unresolvable, ESCs undergo apoptosis or lose pluripotency. Indeed, ESCs have been described to be hypersensitive to DNA damage (Li and Huang, 2010; Vitale et al., 2017).

Here, we have analysed DSBs, the most harmful and frequent form of DNA damage during cell proliferation and did not find higher incidence of DNA lesion in low-MYC cells. On the contrary, we found a positive correlation between DSBs indicator γ-H2AX and MYC. The proposed role of γ-H2AX in ESCs pluripotency (Turinetto et al., 2012) and the fact that another DSBs marker; P53BP1, did not correlate with MYC levels, support that

this positive correlation is not related with DSBs and support a role for γ-H2AX in pluripotency, as high MYC cells exhibit a more "naïve" status.

Although the DSBs study did not indicate a higher DNA damage in low MYC cells, there is a vast variety of DNA lesions that we have not studied here and therefore we cannot discard a role of other types of DNA lesions in Cell Competition.

1.2 OXIDATIVE STRESS

Reactive Oxygen Species (ROS) are involved in cell signalling; however, excessive ROS production produces an oxidative stress that can damage macromolecules and induce apoptosis. In ESCs, ROS are maintained at very low levels (Bigarella et al., 2014). In our analysis, neither $O2^{\bullet-}/H_2O_2$ detection with DHE nor expression of the ROS-producing protein NOX4 indicated higher presence of ROS in low MYC cells.

Interestingly, an oxidative stress response has been related to Cell Competition in other models in *Drosophila.* Piddini and collaborators described that loser cells in two different models of CC, induced by either *Minute* or *Mahjong* mutations (See Introduction), both trigger an oxidative stress response in loser cells. In fact, the activation of the oxidative stress response in loser cells determines the loser fate in these models. However, as in our case, they did not find increased ROS in loser cells by DHE or CM-H2DCFDA staining but they did show less reduced glutathione in loser cells. In addition, they demonstrated that Nrf2 mosaic activation –but not homogeneous activation– was enough to turn WT cells into losers (Kucinski et al., 2017). These results suggested that, rather than the oxidative stress itself, it is the activation of the oxidative stress protection pathway in cells surrounded by non-stressed cells what triggers the loser cell phenotype.

Although we have neither explored reduced glutathione levels nor Nrf2 role in ESCs, data obtained in the lab showed that the antioxidant N-acetylcysteine (NAC) was unable to inhibit Cell Competition. Additionally, the mitochondrial REDOX reporter Grx1-roGFP$_2$ showed no correlation between MYC levels and mitochondrial REDOX status. Collectively, these results did not suggest a role of oxidative stress in ESCs CC.

On the other hand, we have reported an interesting NOX4 expression pattern in nucleoli, where we also found ROS (detected by DHE) in ESCs. The role of ROS in nucleoli has recently related to signalling and autophagy but remains unknown in ESCs (Pfister, 2019). Additionally, we have also shown a correlation between MYC and the area occupied by NOX4 and we have identified cells with a very high cytosolic NOX4 signal not related to MYC levels. These findings, although not related to low-MYC cell elimination, open new questions relating ROS regulation and ESCs biology.

1.3 MITOCHONDRIAL STATUS

Regarding mitochondrial status, we identified no changes in mitochondrial mass between the MYC-low and MYC-high populations, but we found a lower mitochondrial membrane potential in MYC-low cells.

Recently, T. Rodríguez and collaborators have reported that loser cells in the epiblast are associated with mitochondrial defects and lower mitochondrial membrane potential.

Indeed, they demonstrated that *bmpr1*$^{-/-}$ cells, which are loser in the presence of WT cells, are more glycolytic and exhibit less mitochondrial membrane potential. Interestingly, these features only appeared under differentiating conditions but affect loser cells both isolated and in co-culture with WT cells (CC conditions). Eventually, they showed that mutations in mitochondrial DNA or altering mitochondria by forcing mitochondrial fusion or fission is enough to induce CC (Lima et al., 2020).

As both *bmpr1* mutant cells and MYC-Low cells exhibit lower mitochondrial membrane potential, we hypothesized that both BMP-induced CC and natural MYC-driven CC can share a common mechanism through metabolism. In fact, T. Rodríguez and collaborators demonstrated a regulatory pathway between BMP, P53 and mTOR (Bowling et al., 2018), while we have reported a correlation between P53, mTOR and MYC.

A possible scenario could be that P53 is regulated by multiple stimuli as signalling translation ability, BMP signalling and others. In loser cells, P53 is activated and regulates metabolism through different targets, including mTOR and PUMA. These targets then modulate metabolism through different mechanisms such as autophagy or metabolites uptake. Eventually, the metabolic status can be reported by MYC expression.

In summary, mitochondrial status and metabolism is probably playing a role in defining fitness in different competitive scenarios, including MYC-driven CC, as it has been previously shown in *bmpr1*$^{-/-}$ induced-CC and in the epiblast (Lima et al., 2020). However, regarding metabolic stress as an inducer of loser cell death, the fact that *bmpr1*$^{-/-}$ loser cells display a lower MtMP both when they are separated or in co-culture with WT cells, makes it less probable that metabolic stress is operating as a mechanism triggering apoptosis.

Collectively, several evidences point out that loser cells suffer stress. Cell stress in low-fitness cells could be due to their autonomously reduced fitness. Additionally, it could result from a non-autonomous interaction with fitter cells. However, our data did not suggest an important role of the stresses and factors analysed in loser cell elimination.

2. LOSER CELL STATUS AND DEATH

If stress induction due to CC does not account for loser elimination, another scenario could be that CC promotes the activation of specific apoptotic factors triggering low-MYC cell death. To identify specific pathways related to “loser” death and loser cell status in an unbiased manner, we took advantage of transcriptomic data (Díaz-Díaz et al., 2017). Transcriptome analysis of MYC-low and MYC-high cells allowed us to identify P53 as an important pathway upregulated in MYC low cells (Díaz-Díaz et al., 2017).

2.1 P53

P53 is considered a general stress sensor protein involved in multiples functions. In CC, P53 has been involved both in defining fitness and in the execution of loser elimination.

Fitness. Regarding fitness, P53 activation has been associated to a loser status. For example, P53 is upregulated in loser cells endogenous CC in mouse epiblast and ESCs

(Bowling et al., 2018; Díaz-Díaz et al., 2017; Lima et al., 2020). Moreover, in other induced-CC models such as CC induced by *scrib* mosaic deficiency, P53 is upregulated in *scrib*$^{-/-}$ loser cells in mammalian epithelial cells (Wagstaff et al., 2016). Indeed, we found that genetic or chemical alteration of P53 modifies cell fitness inducing Cell Competition. In that way, P53 activation reduces fitness while P53 inhibition increases cell fitness. CC induced by P53 modulation will be discussed in greater depth in the following sections.

Loser cell elimination. Low MYC cells, which already express higher P53 levels than MYC-high cells, further upregulate P53 as they undergo apoptosis in ESCs. Similarly, *scrib*$^{-/-}$ cells express high P53 levels in monoculture. When in co-culture with WT cells, they further upregulate P53 (due to a WT-induced mechanical compaction). Knockout of P53 in *scrib*$^{-/-}$ cells blocks their outcompetition (Wagstaff et al., 2013).

Interestingly, different functions of P53 in CC have been described in a MYC-Supercompetition model in *Drosophila*. In this model, MYC-overexpressing cells (winner cells) undergo a set of metabolic changes upon interaction with WT cells. P53 is required in MYC-overexpressing cells to bear this metabolic switch. On the other hand, P53 is essential in this model to produce diffusible killing signals that induce WT cell death (De La Cova et al., 2014). This mode of action of P53, reported in *Drosophila* epithelial tissues, does not seem to apply to mammalian pluripotent stem cell competition.

In this thesis, we have confirmed that apoptotic cells upregulate P53 but also that non-apoptotic low-MYC cells express higher P53 levels than high-MYC cells. This confirms that P53 has a function defining fitness, but also in the execution of apoptosis in ESCs. Due to its relevance in CC, we focused on the identification of potential candidates involved in apoptosis and loser "status" downstream P53.

2.2 BCL-2-FAMILY PROTEIN

The BCL-2 family consists of a set of proteins involved in apoptosis by regulating MOMP. They have also been related to other non-apoptotic functions such as metabolism or Ca^{2+} homeostasis (see Introduction).

Here, we found different BH3 –only proteins upregulated in MYC-low cells such as *puma, noxa, bik* and *bnip3.* Others, as *bim* or *beclin1,* however, were not differentially expressed between low- and high-MYC populations. Other important members of this family, as *bid* or *bad*, are mainly regulated post-transcriptionally, so we cannot discard a potential role of these factors in CC from this analysis.

2.3 *Ddit4* AND BECLIN1

Other candidates upregulated in low MYC cells were *ddit4* and *tp53inp1*. These candidates suggest a role of mTOR inhibition and autophagy in CC. We confirmed an inhibition of mTOR in low MYC cells. mTOR has been described to regulate competitive fitness. Thus, mTOR upregulation increased fitness while its inhibition induced apoptosis (Bowling et al., 2018). Our results suggest that mTOR regulation in MYC-induced CC could be mediated, at least in part, by DDIT4.

We also reported the upregulation of *Beclin1* in a few cells with low levels of MYC. BECLIN1 is a central element in the initial formation of autophagosomes. Curiously, we identified a nuclear localization for BECLIN1 in ESCs. This had been previously described in other cell types, but not in ESCs, although BECLIN1 function in the nucleus is not clear (Xu et al., 2017). Therefore, due to this localization, we cannot discard that BECLIN1 is performing a role different from autophagy induction in ESCs. BECLIN1 showed a positive correlation with MYC; however, it was highly upregulated in cells with very low MYC levels. This could indicate that, in general, its expression correlates with competitive fitness, which is supported by the fact that autophagy deficient cells have a loser behaviour (Sancho et al., 2013). However, its strong upregulation could be related to the execution of loser cell death in ESCs.

2.4 MODEL PROPOSAL

By transcriptomics, P53 response is identified as the principal pathway upregulated in low-MYC cells during CC. Although, *P53* is not upregulated at the transcriptional level (Díaz-Díaz et al., 2017), higher nuclear P53 is detected in low-MYC cells. The identified candidates downstream P53 can play a role both in the execution of apoptosis and altering metabolism, which can contribute to a loser status (see Results 2.4). Thus, loser cells could exhibit a specific metabolic profile characterized by a reduced mitochondrial oxidative function and increased glycolysis, which is supported by the fact that MYC-low cells exhibit reduced MtMP and increased Glut1 expression. This metabolic status is compatible with the metabolic switch ESCs suffer during differentiation (Mathieu and Ruohola-Baker, 2017) and the fact that differentiating ESCs are outcompeted by naïve ESCs (Díaz-Díaz et al 2017). Consistent with this notion, a reduced OXPHOS and increased glycolysis has been reported in loser *bmpr1*$^{-/-}$ loser cells (Lima et al., 2020).

Additionally, we have shown an inverse correlation between MYC and P53, and MYC and their respective downstream targets mTOR and PUMA, which suggests that MYC act as a general loser status reporter.

Due to its ubiquitous expression, inversely correlating with MYC in ESCs and its recent described roles in metabolism, we decided to focus on the study of PUMA and P53 regulating fitness and CC.

3. P53 AND PUMA IN PLURIPOTENT CELL COMPETITION

puma (bbc3) has been described as one of the strongest apoptotic inducers of the BH3-only protein family. Indeed, it accounts for the majority, if not all, of the apoptotic activity of P53 upon genotoxic stress (Hikisz and Kiliańska, 2012; Yu and Zhang, 2008). In ESCs, we found that PUMA is widely expressed, showing cell-to-cell heterogeneous levels that inversely correlate with MYC levels.

Although apoptotic cells present higher PUMA levels than the general population, this difference is not quantitatively large; only 10% increase over non-apoptotic cells, while

more than a 100% increase was found for P53 expression in the same cells. Therefore, many non-apoptotic cells express similar PUMA levels to apoptotic cells. This suggests functions for PUMA different from apoptosis execution; in fact, it suggests that PUMA is not involved in the execution phase of apoptosis during CC. Rather, PUMA could be just making the cells more prone to suffer apoptosis or less competitive in a way inverse to MYC expression. Recently described roles of PUMA in mitochondria and metabolism suggest that PUMA could play a function regulating fitness and CC, downstream of P53 through metabolic regulation (Kim et al., 2019; Siddiqui et al., 2015). Thus, we wanted to explore these hypotheses.

3.1 P53 AND PUMA EXPRESSION IN ESCs AND EARLY MOUSE EMBRYO

First, we wanted to further describe P53 and PUMA expression and regulation in ESCs and in the mouse embryo. We found that in the absence of P53, there is no obvious PUMA signal in ESCs or in the embryo, indicating that P53 is essential for PUMA expression in pluripotent cells. Regarding the literature, *puma* can be transcriptionally activated by different factors aside from P53 such as E2f1, Myc, C-Jun, Sp1 (Yu and Zhang, 2008). In fact, different factors and apoptotic stimuli induce *puma* in the absence of *p53* e.g. P73, FoxO3a, CHOP, glucocorticoids and ischemia-reperfusion (Futami et al., 2005; Ming et al., 2008; Wu et al., 2007; You et al., 2006; Yu and Zhang, 2008). As many of these works are performed upon stress inductions, it would be interesting to explore whether P53 is also necessary for PUMA induction upon different apoptotic stimuli. This would allow to distinguish whether P53 is just essential for PUMA expression and function in ESCs in steady-state conditions or whether it is required for PUMA expression in different contexts. It would be also interesting to explore whether other BH3-ONLY protein exhibit expression patterns and P53-dependent regulation similar to PUMA in pluripotent cells.

In the epiblast, PUMA is expressed in every cell in a heterogeneous manner similar to ESCs. In fact, we also showed that high PUMA-expressing cells exhibited low MYC levels in the epiblast. On the other hand, P53 signal was not detected at E6.5. However, the fact that P53 is essential for PUMA expression in ESCs and in the epiblast indicates that P53 function is widespread in pluripotent cells, and the inability to detect P53 with antibodies is due to technical problems.

At E3.5, however, P53 signal was detected and we found a positive correlation between P53 and PUMA. However, we did not observe correlation between P53 and MYC, indicating that MYC depends on additional factors in the blastocyst, in contrast to ESCs. Curiously, Bowling et al., described that P53 activation with Nutlin3 is required to show a correlation between P53 and mTOR signalling.

Collectively, these data suggest that P53-PUMA and MYC are subjected to similar regulation in ESCs and *in vivo*, with the exception that we could not find a correlation between P53 and MYC in E3.5 embryos.

3.2 REGULATORY INTERACTIONS BETWEEN P53-PUMA AND MYC

We have described an inverse correlation between P53-PUMA and MYC. Quantification of P53, PUMA and MYC levels indicated that high P53-PUMA cells have low MYC levels,

although not all MYC-low cells express high P53-PUMA levels and can express low P53-PUMA levels (Figure 14 and 15). To understand whether Myc could be inhibiting P53-PUMA or on the contrary, P53 and PUMA can inhibit Myc expression, we used different knockout cell lines.

myc-KO cells did not modify the levels and heterogeneity of P53-PUMA. However, *p53*$^{-/-}$ cells upregulate MYC expression. These results suggest that P53 act upstream MYC defining fitness and have a function inhibiting MYC. Thus, P53 may impact competitive fitness at least to some extend by regulating MYC. Further exploration will be needed to address whether P53 can directly inhibit MYC expression or it is mediated by P53-downstream targets.

On the other hand, neither *puma* nor *noxa elimination* upregulated *myc* expression, indicating that these BH3-only proteins does not inhibit MYC expression. Curiously, some but not all *puma*$^{-/-}$ clones overexpressed MYC. This indicates that *puma*$^{-/-}$ cells competitive fitness is not dependent on MYC regulation. As PUMA is not expressed in *p53*$^{-/-}$ cells, these results indicate that P53-PUMA can regulate competitive fitness by mechanisms independent of MYC regulation.

We can hypothesize that P53 can impact on competitive fitness through different downstream elements including PUMA (and other BH3-only proteins), MYC as well as different factors previously identified by RNAseq (e.g.d*ddit4, tp53inp1, perp*). In the case of DDIT4, it is supported by the fact that it is a potent inhibitor of mTOR, which correlates with MYC expression and induces CC downstream P53 (Bowling et al., 2018).

Preliminary results *in vivo* indicated that MYC is not upregulated in *p53*$^{-/-}$ mouse embryos. Although the number of embryos analysed should be increased in order to obtain stronger conclusions, this suggests that in embryos, MYC regulation could depend on additional factors. This would be supported by the fact that no correlation was found between MYC and P53 in E3.5 mouse embryos. Moreover, this suggests that in the model of *p53*$^{-/-}$-induced CC, differences in fitness due to the absence of P53 would not be dependent on MYC.

3.3 P53-PUMA AND MYC ARE REGULATED BY PLURIPOTENCY

Pluripotency is the capacity of cells to produce all three embryonic germ layers. Pluripotency, however, is not a single status, and during development, cells transit through diverse sequential pluripotent states. We showed that naïve cells (promoted in “2i” medium) maintained low levels of P53 and PUMA and, as medium conditions are modified to allow the transit to a less naïve pluripotent status and the emergence of primed cells (“SR/FBS” medium), P53 and PUMA levels increase progressively. Such medium conditions actually produce a heterogeneous state in which naïve and primed cells coexist in vicinity.

While naïve pluripotent cells cultured in 2i also maintain low levels of MYC, the heterogeneity established in the SR/FBS medium promote higher MYC levels in the naïve cells and lower MYC levels in their primed neighbours. It would be interesting to explore what regulates MYC upregulation in more naïve cells when cultured in FBS or SR media in contrast to 2i media. One possibility is that this happens in response to contact with primed

cells, as part of a mechanism to detect and eliminate primed cells from naïve cell pools. During this process, our results suggest that P53 and other factors upregulated in more primed cells inhibit MYC expression. In agreement with this view, when we allowed differentiation by removing LIF, PUMA levels increased, while MYC levels were downregulated. This could indicate that PUMA, along with other factors, is upregulated in more primed cells and inhibits MYC levels. This upregulation could mediate a hypersensitivity in ESCs when they transit to a more primed status which is supported by the fact that ESCs become more sensitive to passaging after differentiation, while *puma*$^{-/-}$ and specially *p53*$^{-/-}$ are more resistant (data not shown).

Another interesting aspect of MYC regulation by P53 is that although P53 is inhibiting MYC expression in ESCs, in the absence of P53, MYC keeps its heterogeneous expression pattern. This shows that other factors in addition to P53 are regulating MYC and cell fitness, being pluripotency an important factor able to regulate both MYC and P53.

Regarding *in vivo* data, at E3.5 PUMA is just expressed at high levels in only some blastocyst. From E.5 to E6.5, it is heterogeneously expressed in all epiblast cells. However, when gastrulation begins, PUMA expression is decreased along the primitive streak. While in ESCs we found a good inverse correlation between P53/PUMA and Myc levels, in the embryo, this correlation seems to break at the primitive streak, where low levels of both PUMA and MYC are detected. It is possible, however, that the stages of differentiation recreated *in vitro* upon LIF withdrawal do not reach the primitive streak cell status.

We can hypothesize that epiblast cells and ESCs can heterogeneously acquire a more primed status and upregulate P53-PUMA (along with other factors) allowing competitive interactions among neighbouring cells. In contrast, gastrulation constitutes a programmed, coordinated and localized (primitive streak) differentiation process. During this process, both PUMA and MYC are downregulated and CC is blocked (Clavería et al., 2013; Díaz-Díaz et al., 2017). In particular, downregulation of PUMA could be required at gastrulation to avoid that the somatic cells derived from gastrulation enter apoptosis. In fact, PUMA is not normally expressed in non-pluripotent cells unless an apoptosis pathway is triggered. Therefore, PUMA downregulation at the primitive streak may correlate with the transition from a pluripotent stem cell-mode of action of PUMA to its inducible activation in non-pluripotent cells.

3.4 FUNCTIONAL CHARACTERIZATION OF P53, PUMA AND NOXA IN ESCs.

Most studied functions of P53 are induction of cell cycle arrest, senescence and apoptosis in response to DNA damage and other stresses. However, P53 is involved in many other functions as modulation of autophagy, control of ROS, alteration of metabolism or repression of pluripotency and cellular plasticity (Kastenhuber and Lowe, 2017). BCL-2 proteins such as PUMA and NOXA account for the apoptotic function downstream P53. In addition, BCL-2 proteins have been related to other functions in metabolism (Siddiqui et al., 2015).

In ESCs, previous efforts to study P53 function have produced contradictory results. Recent studies suggest that P53 functions in ESCs change depending on the pluripotent status (Fu et al., 2020; Hao et al., 2020; Jaiswal et al., 2020). Regarding BH3-only proteins,

there is little information about PUMA and NOXA function in ESCs.

Apoptosis. We have observed that *p53,* and to a lesser extent, *puma* and *noxa* KO ESCs have a reduced apoptosis rate in conventional conditions (FBS +LIF), which are known to allow spontaneous cell competition (Díaz-Díaz et al 2017). Jaiswal et al., have described that in ESCs cultured in similar conditions, apoptosis induced by doxorubicin, staurosporine or WX8 is independent of P53 and PUMA. However, in differentiating conditions (by LIF deprivation), cell death becomes P53 and PUMA dependent (Jaiswal et al., 2020). Nevertheless, we have found a role in apoptosis for P53, PUMA and NOXA cultured with "FBS" medium at least in steady-state conditions. A possible explanation could be that cell death dependent on P53 and BH3-only proteins in pluripotent cells (FBS +LIF) is due to CC, and therefore unrelated to cell damage.

Proliferation and cell cycle. We did not observe a significant function of P53, PUMA or NOXA in proliferation or cell cycle in FBS+LIF. This is consistent with a recent work in which showing that in standard ESC culture conditions, cell cycle regulation is independent of P53. However, when ESCs present a naïve pluripotent status, using "2i" media, P53 mediates the elongation of G1 cell cycle phase (Ter Huurne et al., 2020).

Differentiation. Regarding differentiation, P53 has been related to differentiation in ESCs. Indeed, this has been proposed as a mechanism to maintain genome stability in ESCs (Fu et al., 2020; Jain and Barton, 2018). Lin et al., showed that upon DNA damage induction, P53 is phosphorylated at Ser315 and inhibits NANOG (critical pluripotent factor), inducing differentiation of mESCs (Lin et al., 2005). Additionally, exogenous P53 expression induces differentiation as well as G1 phase elongation (Jain et al., 2012). On the other hand, differentiation induction by retinoic acid mediates P53 activation by Lys373 acetylation in hESCs (Jain et al., 2012). Regarding P53 and differentiation in unstressed conditions, Zhang et al., have shown that P53 induces differentiation, which is prevented by SIRT1 acting downstream OCT4 (Zhang et al., 2014).

Here, we described that p-ERK is higher in *p53*$^{-/-}$ cells in "FBS" medium. However, this correlation was not observed in *puma*$^{-/-}$ or *noxa*$^{-/-}$ cells. It is possible that, apart from its functions in differentiation, in unstressed conditions P53 plays a role in regulating pluripotency in mESCs. This has already being proposed by others, showing that *p53* knockdown cells inhibit *nanog* in unstressed conditions (Abdelalim and Tooyama, 2014). On the other hand, in a late primed pluripotent status, p-ERK could be mediating other functions apart from differentiation.

Regarding the regulation of the P53 pathway and MYC, we found that pluripotency status modifies P53, PUMA and MYC expression, so that, the range of expression levels increases in FBS+LIF (which allows the emergence of some primed cells) in comparison to 2i medium (which maintains more naïve status). Moreover, when differentiation is initiated in ESCs, MYC levels are reduced while PUMA levels increase. On the other hand, modulating MYC levels does not change the pluripotent status (Diaz Diaz et al., 2017; C. Clavería, unpublished). Therefore, although P53 may have a function in differentiation in unstressed conditions, it seems that progression in the pluripotency status towards differentiation priming is an essential factor to allow the emergence of cells with the "loser signature".

3.5 CELL COMPETITION

CC assays showed that fluorescent WT cells undergo a reduced growth when they are co-cultured with *p53* and *puma* KO cells, in comparison to other WT cells. This indicates that *p53* and *puma* have a function in competitive fitness regulation in ESCs, because not only they reduce apoptosis in winner cells but they also promote the elimination of neighbouring wild type cells. The function of P53 as a fitness regulator is consistent with previous data in which P53 overexpression can turn cells into losers, while P53 inhibition transforms them into winners (Bondar and Medzhitov, 2010; Wagstaff et al., 2013).

In ESCs, Dejosez et al., showed that in similarity with the early mouse embryo, $p53^{-/-}$ cells displace WT cells when they are cultured in differentiating conditions. However, it is not clear whether this effect is due to autonomous or non-autonomous effects. Interestingly, these authors showed that when ESCs are cultured in undifferentiated conditions, $p53^{-/-}$ cells become loser and are outcompeted by WT cells (Dejosez et al., 2013). We will discuss the relation of P53-induced CC and pluripotency in the following sections. Interestingly, Bowling et al., demonstrated that P53 regulates mTOR and that knocking-down *p53* in $bmpr1^{-/-}$ and 4N loser cells rescues them from CC. This suggests that P53 has a role defining fitness and inducing CC in ESCs, although this has not been directly demonstrated until our work here.

3.6 CELL COMPETITION AND PLURIPOTENCY

T. Rodríguez and collaborators have demonstrated that BMP-induced CC in ESCs occurs in differentiating conditions but it is inhibited when a more pluripotent status is maintained (Lima et al., 2020; Sancho et al., 2013). MYC-driven CC does not require inducing differentiation but it needs culture conditions that allow the emergence of primed cells coexisting with naïve cells. Dejosez et al., described that maintaining a pluripotent status turned $p53^{-/-}$ cells from winner to loser. They also described a similar behaviour for *topoisomerase I* gene (Dejosez et al., 2013), which has been less described in the CC field and how it regulates fitness or its relation with other pathways inducing CC is unknown.

Here we found that although *p53*-KO cells are not outcompeted by WT cells in 2i medium, the outcompetition of WT by $p53^{-/-}$ cells that we described in differentiating conditions is inhibited in 2i. In agreement with this, in 2i media, apoptosis of WT cells is reduced to similar levels than in *p53*-KO cells. These results indicate that as ESCs exit the naïve pluripotent status, they increase P53 levels and also P53-dependent apoptosis. This P53-dependent apoptosis that occurs only when naïve and primed cells coexist in the culture could be due to (1) cell autonomous P53-dependent apoptosis in unstressed ESCs in FBS+LIF medium or it could be due to CC. Then, in the absence of *p53,* CC would be blocked indicating that (2) P53 is required to define fitness. In other words, $p53^{-/-}$ cells do not have competitive interactions or (3) *p53* is required for the execution of loser cell death.

Moreover, in contrast to differentiating conditions, in which *p53*-KO cells exhibit an increased growth rate in comparison to WT cells, this growth rate is reduced to similar levels to WT cells rate in 2i conditions. This observation fits with reported data in undifferentiated conditions in which $p53^{-/-}$ and WT cells display similar growth rate (Dejosez et

al., 2013). We found that in differentiating conditions, ESCs increased their growth rate, however, P53 limited this growth rate. Given that no changes in pH3 were detected between *p53*$^{-/-}$ and WT cells in differentiating conditions, we assume that P53-dependent inhibition of growing rate could be due to the increased apoptosis.

In summary, in 2i conditions CC between *p53*$^{-/-}$ and WT cells is inhibited. When, cells exit the naïve status, competitive interactions increase. This is accompanied with an increase in P53 and PUMA levels and a decrease in MYC levels in differentiation-primed cells, which thereby acquire low competitive fitness. In contrast to *p53*$^{-/-}$ cells, WT cells have a lower growing rate, probably due to a higher apoptotic rate. Both effects are P53-dependent and inhibited by naïve pluripotency.

3.7 CELL COMPETITION AND MITOCHONDRIAL REDOX STATUS

We tested mitochondrial REDOX status by using the ratiometric reporter Grx1-roGFP$_2$. We found that ESCs show a REDOX status close to a "maximum reduction status" induced by DTT and is far from the "maximum oxidation status" induced by H_2O_2. This is in agreement with the notion that ROS is maintained at minimum levels in ESCs (Bigarella et al., 2014).

It has been described that different stem cells types exhibit distinct mitochondrial morphology, which is linked to mitochondrial function (Seo et al., 2018). Mitochondrial fusion produces tubular/branched mitochondria that are thought to produce energy more efficiently than the immature, globular mitochondria. Therefore, non-fused spherical mitochondria are associated to a more glycolytic metabolism, while more fused elongated are related to higher OXPHOS. However, this depends on complex factors as cell type. While ESCs show non-fused mitochondria, they present a bivalent energy production switching from more glycolysis to more mitochondrial respiration (Seo et al., 2018). Epiblast stem cells (EpiSCs), which are differentiation-primed cells, show more tubular and developed mitochondrial content; however they are more glycolytic and have low mitochondrial respiratory capacity due to low cytochrome c oxidase and HIF1α expression (Zhou et al., 2012).

Our results suggest that mitochondrial REDOX status is not involved in defining cell fitness. Therefore, other approaches will be necessary to evaluate the role of P53 and PUMA in the mitochondria and metabolism and identify the mechanism by which P53 and PUMA regulate fitness and Cell Competition.

PROPOSED MODEL

As mouse embryonic stem cells heterogeneously progress to a less naïve pluripotent status, competitive interactions are promoted between "low fitness" and "high fitness" cells.

We consider "low competitive fitness" cells those that are non-autonomously eliminated by "high competitive fitness" cells. According to this definition and regarding that MYC is a well reporter of fitness in ESCs, MYC-low cells are cells with decreased competitive fitness. Based on MYC expression, we identified P53 and several downstream targets

upregulated in MYC-low cells, as important candidates involved in “loser” cell death. These factors and pathways include BH3-only proteins, mTOR pathway and mitophagy induction. In addition to their function in apoptosis, the analysis of these factors suggests an important role in metabolic regulation.

Characterization of the loser cell signature is of great interest and is being sought in various models of Cell Competition (Kucinski et al., 2017; Lima et al., 2020; Nagata et al., 2019). Here, we describe a pattern of expression levels for various factors that corresponds to low competitive fitness and, therefore, represents a “loser signature”. From the factors studied, we propose that P53 and to a lesser extent, the BH3-only protein PUMA regulate competitive fitness and induce CC (Figure 31).

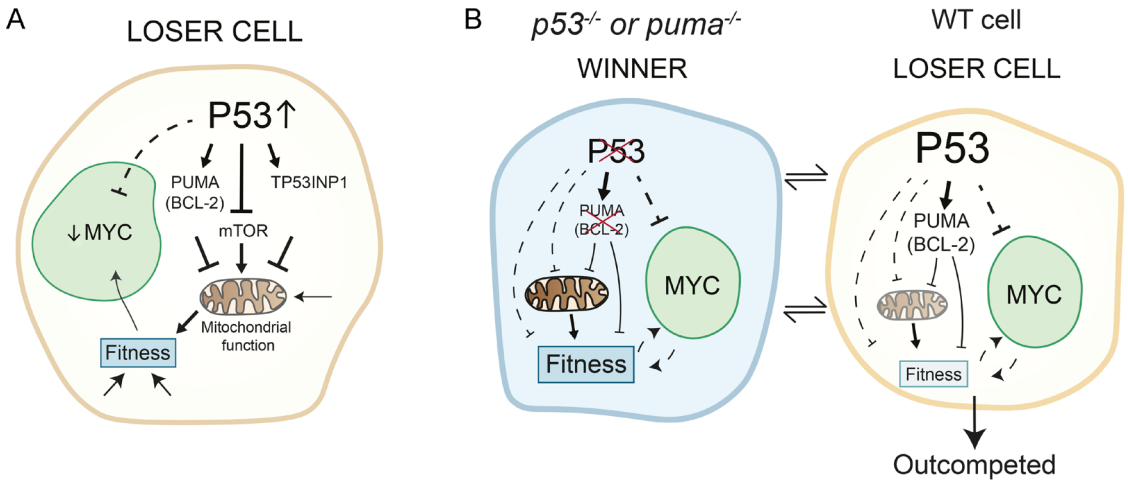

Figure 31. Proposed model.

A. Low-fitness cells are defined by a set of cell-autonomous features that constitute a “loser signature” and promote the “loser status”. P53 and several downstream targets contribute to that loser status. As these factors have been described to alter metabolism and reduce mitochondrial function, we propose that these factors could decreased fitness at least in part by regulating metabolism. Altered metabolism would have an impact on competitive fitness, along with other factors and eventually, would be reported by MYC expression levels. Competitive interactions between cells with the loser signature ($P53^{hi}$, $PUMA^{hi}$, MYC^{lo}) and cells with a winner profile ($P53^{lo}$, $PUMA^{lo}$, MYC^{hi}) leads to apoptosis of loser cells. Further upregulation of P53 and some of its downstream targets can contribute to MOMP and elicit apoptosis of loser cells. **B.** P53 and PUMA exert a function in competitive fitness. This function could be mediated by their metabolic regulatory functions, along with other roles. *$P53^{-/-}$* and *$puma^{-/-}$* cells adquire a “winner status” and mediate the outcompetition of WT cells.

CONCLUSIONS

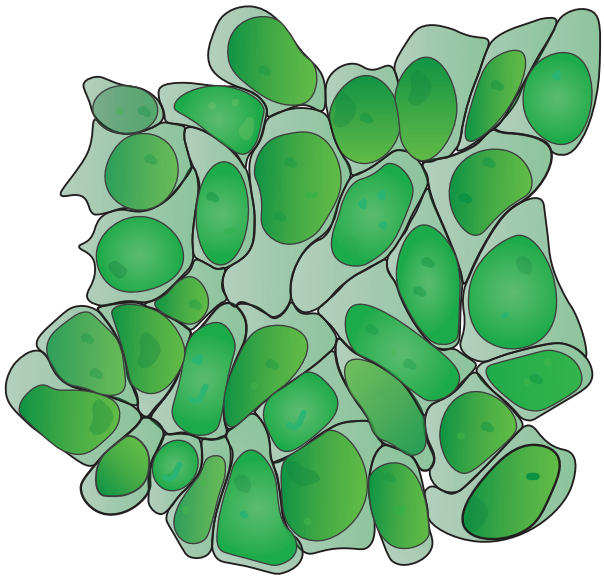

1. MYC-low cells do not present more Double Strand Breaks (DSBs), H_2O_2 and $O^{\bullet -}$ ROS or differential mitochondrial REDOX status, which suggests that genotoxic or oxidative stress do not determine loser cell low competitive fitness in ESCs.

2. MYC-low cells possess a "loser signature" characterized by activation of the P53 pathway. P53 targets upregulated include *puma, noxa, ddit4, tp53inp1* or *perp*, which are involved in cell death induction, autophagy and mitophagy and alteration of the mitochondrial function.

3. PUMA is not restricted to apoptotic cells but widely expressed in ESCs and in the early mouse embryo in a cell-to-cell graded heterogeneous pattern. P53 is essential for PUMA expression in pluripotent cells indicating that activity of P53-PUMA is not restricted to apoptotic cells in this context.

4. P53, but not PUMA or NOXA, acts upstream of MYC and inhibits its expression.

5. In conventional unstressed ESC culture conditions (FBS +LIF), P53, PUMA and NOXA have a function in apoptosis, but not in proliferation or cell cycle.

6. P53, PUMA and MYC are regulated by the ESC pluripotent status, with MYC levels decreasing and P53-PUMA increasing as cells progress towards differentiation.

7. P53 or PUMA elimination confers ESCs a winner status, allowing them to eliminate WT cells in co-culture, which indicates that P53 and PUMA activity negatively regulate competitive fitness in pluripotent stem cells.

8. Cell Competition induced by P53 loss is inhibited by maintaining cells in a naïve pluripotent status.

9. *p53*$^{-/-}$ and *puma*$^{-/-}$ cells do not present major differences in the mitochondrial REDOX status in comparison with *wt* cells, indicating that P53 and PUMA function on cell fitness is not mediated by differences in mitochondrial REDOX status.

1. Las células con bajos niveles de MYC no presentan más roturas de doble cadena, especies reactivas de oxígeno H_2O_2 o $O^{\bullet-}$ o diferencias en el estado REDOX mitocondrial, sugiriendo que ni estrés genotóxico ni el estrés oxidativo determinan el bajo *fitness* de las celulas *loser* en ESCs.

2. Las células con niveles bajos de MYC poseen una "*loser signature*" caracterizada por la activación de P53. Algunos genes dianas de P53 sobreexpresados incluyen *puma, noxa, ddit4, tp53inp1 o perp,* factores implicados en la inducción de la apoptosis, la autofagia y mitofagia y la alteración de la actividad mitocondrial.

3. PUMA no se expresa únicamente en células apoptóticas, sino que está ampliamente expresado en células ES y en el epiblasto, generando un patrón heterogéneo célula-a-célula. P53 es esencial para la expresión de PUMA en células pluripotentes.

4. P53, pero no PUMA o NOXA, se encuentra aguas arriba de MYC e inhibe su expresión.

5. En células ES, cultivadas en condiciones normales y empleado medio convencional (FBS + LIF), P53, PUMA y NOXA desempeñan una función en apoptosis, pero no en proliferación ni ciclo celular.

6. P53, PUMA y MYC son regulados por el estado de pluripotencia de las ES. A medida que las células adquieren un estado de mayor diferenciación, los niveles de MYC bajan, mientras que los de P53-PUMA se incrementan.

7. La eliminación de *p53* y *puma* confiere a las células ES un "*status winner*", capaces de eliminar células WT en co-cultivo. Por tanto, P53 y PUMA regulan negativamente el *fitness* en células madre Pluripotentes.

8. La Competición Celular generada por la eliminación de *p53* se inhibe al mantener un estado de pluripotencia *naïve*.

9. Las células $p53^{-/-}$ y $puma^{-/-}$ no presentan diferencias importantes en el estado REDOX mitocondrial, indicando que la función de P53 y PUMA regulando el *fitness* no es producida por el estado REDOX mitocondrial.

BIBLIOGRAPHY

"If I have seen further it is by standing on the shoulders of Giants"

Isaac Newton

Abdelalim, E. M. and Tooyama, I. (2014). Knockdown of p53 suppresses Nanog expression in embryonic stem cells. *Biochem. Biophys. Res. Commun.* **443**, 652–657.

Adachi-Yamada, T., Fujimura-Kamada, K., Nishida, Y. and Matsumoto, K. (1999). Distortion of proximodistal information causes JNK-dependent apoptosis in Drosophila wing. *Nature* **400**, 166–169.

Akieda, Y., Ogamino, S., Furuie, H., Ishitani, S., Akiyoshi, R., Nogami, J., Masuda, T., Shimizu, N., Ohkawa, Y. and Ishitani, T. (2019). Cell competition corrects noisy Wnt morphogen gradients to achieve robust patterning in the zebrafish embryo. *Nat. Commun.* **10**, 1–17.

Albrecht, S. C., Barata, A. G., Großhans, J., Teleman, A. A. and Dick, T. P. (2011). In Vivo Mapping of Hydrogen Peroxide and Oxidized Glutathione Reveals Chemical and Regional Specificity of Redox Homeostasis. *Cell Metab.* **14**, 819–829.

Alcolea, M. P., Greulich, P., Wabik, A., Frede, J., Simons, B. D. and Jones, P. H. (2014). *Differentiation imbalance in single oesophageal progenitor cells causes clonal immortalization and field change*.

Alpar, L., Bergantiños, C. and Johnston, L. A. (2018). Spatially Restricted Regulation of Spätzle/Toll Signaling during Cell Competition. *Dev. Cell* **46**, 706-719.e5.

Amoyel, M. and Bach, E. a (2014). Cell competition: how to eliminate your neighbours. *Development* **141**, 988–1000.

Baker, N. E. (2020). Emerging mechanisms of cell competition. *Nat. Rev. Genet.* **21**, 683–697.

Baker, S. J., Markowitz, S., Fearon, E. R., Willson, J. K. and Vogelstein, B. (1990). Suppression of human colorectal carcinoma cell growth by wild-type p53. *Science* **249**, 912–915.

Ballesteros-Arias, L., Saavedra, V. and Morata, G. (2013). Cell competition may function either as tumour-suppressing or as tumour-stimulating factor in Drosophila. *Oncogene* **33**, 1–8.

Baumgartner, M.E., Dinan, M.P., Langton, P.F., Kucinski, I., and Piddini, E. (2021). Proteotoxic stress is a driver of the loser status and cell competition. Nat. Cell Biol. 23, 136–146.

Bigarella, C. L., Liang, R. and Ghaffari, S. (2014). Stem cells and the impact of ROS signaling. *Dev.* **141**, 4206–4218.

Bilder, D. (2004). Epithelial polarity and proliferation control: links from the. *Genes Dev.* 1909–1925.

Böhni, R., Riesgo-Escovar, J., Oldham, S., Brogiolo, W., Stocker, H., Andruss, B. F., Beckingham, K. and Hafen, E. (1999). Autonomous control of cell and organ size by CHICO, a Drosophila homolog of vertebrate IRS1-4. *Cell* **97**, 865–875.

Bondar, T. and Medzhitov, R. (2010). p53-Mediated Hematopoietic Stem and Progenitor Cell Competition. *Cell Stem Cell* **6**, 309–322.

Boroviak, T., Loos, R., Bertone, P., Smith, A. and Nichols, J. (2014). The ability of inner-cell-mass cells to self-renew as embryonic stem cells is acquired following epiblast specification. *Nat. Cell Biol.* **16**, 516–528.

Bowling, S., Gregorio, A. Di, Sancho, M., Pozzi, S., Aarts, M., Signore, M., Schneider, M. D., Pedro, J., Barbera, M., Gil, J., et al. (2018). P53 and mTOR signalling determin-efitnessselection through cell competition during earlymouse embryonic development. *Nat. Commun.*

Bowling, S., Lawlor, K. and Rodr, T. A. (2019). Cell competition : the winners and losers of fitness selection.

Bradley, C. K., Peura, T., Dumevska, B., Jovasevic, A., Chami, O., Schmidt, U., Jansen, R. P. S. and Stojanov, T. (2014). Cell lines from morphologically abnormal discarded IVF embryos are typically euploid and unaccompanied by intrachromosomal aberrations. *Reprod. Biomed. Online* **28**, 780–788.

Brehme, K. S. (1939). A Study of the Effect on Development of "Minute" Mutations in Drosophila Melanogaster. *Genetics* **24**, 131–13161.

Bridges, C. B. and Morgan, T. H. (2011). *The third-chromosome group of mutant characters of Drosophila melanogaster,*.

Brons, I. G. M., Smithers, L. E., Trotter, M. W. B., Rugg-Gunn, P., Sun, B., Chuva de Sousa Lopes, S. M., Howlett, S. K., Clarkson, A., Ahrlund-Richter, L., Pedersen, R. A., et al. (2007). Derivation of pluripotent epiblast stem cells from mammalian embryos. *Nature* **448**, 191–195.

Brook, F. A. and Gardner, R. L. (1997). The origin and efficient derivation of embryonic stem cells in the mouse. *Proc. Natl. Acad. Sci. U. S. A.* **94**, 5709–5712.

Brumby, A. M. and Richardson, H. E. (2003). scribble mutants cooperate with oncogenic Ras or Notch to cause neoplastic overgrowth in Drosophila. *EMBO J.* **22**, 5769–5779.

Burke, R. and Basler, K. (1996). Dpp receptors are autonomously required for cell proliferation in the entire developing Drosophila wing. *Development* **122**, 2261–2269.

Certo, M., Del Gaizo Moore, V., Nishino, M., Wei, G., Korsmeyer, S., Armstrong, S. A. and Letai, A. (2006). Mitochondria primed by death signals determine cellular addiction to antiapoptotic BCL-2 family members. *Cancer Cell* **9**, 351–365.

Chen, C. L., Gajewski, K. M., Hamaratoglu, F., Bossuyt, W., Sansores-Garcia, L., Tao, C. and Halder, G. (2010). The apical-basal cell polarity determinant Crumbs regulates Hippo signaling in Drosophila. *Proc. Natl. Acad. Sci. U. S. A.* **107**, 15810–15815.

Chen, C.-L., Schroeder, M. C., Kango-Singh, M., Tao, C. and Halder, G. (2012). Tumor suppression by cell competition through regulation of the Hippo pathway. *Proc. Natl. Acad. Sci.* **109**, 484–489.

Cheng, J., Dutra, A., Takesono, A., Garrett-Beal, L. and Schwartzberg, P. L. (2004). Improved generation of C57BL/6J mouse embryonic stem cells in a defined serum-free media. *Genesis* **39**, 100–104.

Chien, J., Ota, T., Aletti, G., Shridhar, R., Boccellino, M., Quagliuolo, L., Baldi, A. and Shridhar, V. (2009). Serine Protease HtrA1 Associates with Microtubules and Inhibits Cell Migration. *Mol. Cell. Biol.* **29**, 4177 LP – 4187.

Clavería, C. and Torres, M. (2015). Cell Competition: Mechanisms and Physiological Roles.

Clavería, C., Giovinazzo, G., Sierra, R. and Torres, M. (2013). Myc-driven endogenous cell competition in the early mammalian embryo. *Nature* **500**, 39–44.

Coelho, D. S., Schwartz, S., Merino, M. M., Hauert, B., Topfel, B., Tieche, C., Rhiner, C. and Moreno, E. (2018). Culling Less Fit Neurons Protects against Amyloid-β-Induced Brain Damage and Cognitive and Motor Decline. *Cell Rep.* **25**, 3661-3673.e3.

Creed, S. and McKenzie, M. (2019). Measurement of Mitochondrial Membrane Potential with the Fluorescent Dye Tetramethylrhodamine Methyl Ester (TMRM). *Methods Mol. Biol.* **1928**, 69–76.

Crespo, F. L., Sobrado, V. R., Gomez, L., Cervera, A. M. and McCreath, K. J. (2010). Mitochondrial reactive oxygen species mediate cardiomyocyte formation from embryonic stem cells in high glucose. *Stem Cells* **28**, 1132–1142.

Danial, N. N., Gramm, C. F., Scorrano, L., Zhang, C.-Y., Krauss, S., Ranger, A. M., Datta, S. R., Greenberg, M. E., Licklider, L. J., Lowell, B. B., et al. (2003). BAD and glucokinase reside in a mitochondrial complex that integrates glycolysis and apoptosis. *Nature* **424**, 952–956.

Danilova, N., Sakamoto, K. M. and Lin, S. (2008). p53 family in development. *Mech. Dev.* **125**, 919–931.

De La Cova, C., Abril, M., Bellosta, P., Gallant, P. and Johnston, L. A. (2004). Drosophila myc regulates organ size by inducing cell competition. *Cell* **117**, 107–116.

De La Cova, C., Senoo-Matsuda, N., Ziosi, M., Wu, D. C., Bellosta, P., Quinzii, C. M. and Johnston, L. A. (2014). Supercompetitor status of drosophila Myc cells requires p53 as a Fitness sensor to reprogram metabolism and promote viability. *Cell Metab.* **19**, 470–483.

Deathridge, J., Antolović, V., Parsons, M. and Chubb, J. R. (2019). Live imaging of erk signalling dynamics in differentiating mouse embryonic stem cells. *Dev.* **146**,.

Dejosez, M. (2013). Safeguards for Cell Cooperation in. *Science (80-.).* **341**, 1511–4.

Dejosez, M., Ura, H., Brandt, V. L. and Zwaka, T. P. (2013). Safeguards for Cell Cooperation in Mouse Embryogenesis Shown by Genome-Wide Cheater Screen. *Science (80-.).* **341**, 1511 LP – 1514.

Díaz-Díaz, C., Manuel, L. F. De, Jimenez-carretero, D., Torres, M. and Claverıa, C. (2017). Pluripotency Surveillance by Myc-Driven Competitive Elimination of Differentiating Cells Article Pluripotency Surveillance by Myc-Driven Competitive Elimination of Differentiating Cells. 585–599.

Dickey, J. S., Redon, C. E., Nakamura, A. J., Baird, B. J., Sedelnikova, O. A. and Bonner, W. M. (2009). H2AX: Functional roles and potential applications. *Chromosoma* **118**, 683–692.

Doggett, K., Grusche, F. A., Richardson, H. E. and Brumby, A. M. (2011). Loss of the Drosophila cell polarity regulator Scribbled promotes epithelial tissue overgrowth and cooperation with oncogenic Ras-Raf through impaired Hippo pathway signaling. *BMC Dev. Biol.* **11**,.

Donehower, L. A., Harvey, M., Slagle, B. L., McArthur, M. J., Montgomery, C. A., Butel, J. S. and Bradley, A. (1992). Mice deficient for p53 are developmentally normal but susceptible to spontaneous tumours. *Nature* **356**, 215–221.

Dossou, A. S. and Basu, A. (2019). The Emerging Roles of mTORC1 in Macromanaging Autophagy. *Cancers (Basel).* **11**,.

Duarte, F., Amorim, J., Palmeira, C. and Rolo, A. (2015). Regulation of Mitochondrial Function and its Impact in Metabolic Stress. *Curr. Med. Chem.* **22**, 2468–2479.

Eaton, S. and Martin-Belmonte, F. (2014). Cargo sorting in the endocytic pathway: A key regulator of cell polarity and tissue dynamics. *Cold Spring Harb. Perspect. Biol.* **6**, 1–18.

Edison, N., Zuri, D., Maniv, I., Bornstein, B., Lev, T., Gottfried, Y., Kemeny, S., Kagan, J. and Larisch, S. (2011). The IAP-antagonist ARTS initiates caspase activation upstream of cytochrome C and SMAC / Diablo. *Cell Death Differ.* **19**, 356–368.

Edison, N., Curtz, Y., Paland, N., Mamriev, D., Chorubczyk, N., Haviv-Reingewertz, T., Kfir, N., Morgenstern, D., Kupervaser, M., Kagan, J., et al. (2017). Degradation of Bcl-2 by XIAP and ARTS Promotes Apoptosis. *Cell Rep.* **21**, 442–454.

Eichenlaub, T., Cohen, S. M. and Herranz, H. (2016). Cell competition drives the formation of metastatic tumors in a drosophila model of epithelial tumor formation. *Curr. Biol.* **26**, 419–427.

Eisenman, R. N. (2001). Deconstructing Myc. *Genes Dev.* **15**, 2023–2030.

Enomoto, M. and Igaki, T. (2013). Src controls tumorigenesis via JNK-dependent regulation of the Hippo pathway in Drosophila. *EMBO Rep.* **14**, 65–72.

Evans, M. J. and Kaufman, M. H. (1981). Establishment in culture of pluripotential cells from mouse embryos. *Nature* **292**, 154–156.

Fernandez-Antoran, D., Piedrafita, G., Murai, K., Ong, S. H., Herms, A., Frezza, C. and Jones, P. H. (2019). Outcompeting p53-Mutant Cells in the Normal Esophagus by Redox Manipulation. *Cell Stem Cell* **25**, 329-341.e6.

Froldi, F., Ziosi, M., Garoia, F., Pession, A., Grzeschik, N. A., Bellosta, P., Strand, D., Richardson, H. E., Pession, A. and Grifoni, D. (2010). The lethal giant larvae tumour suppressor mutation requires dMyc oncoprotein to promote clonal malignancy. *BMC Biol.* **8**,.

Fu, X., Cui, K., Yi, Q., Yu, L. and Xu, Y. (2017). DNA repair mechanisms in embryonic stem cells. *Cell. Mol. Life Sci.* **74**, 487–493.

Fu, X., Wu, S., Li, B., Xu, Y. and Liu, J. (2020). Functions of p53 in pluripotent stem cells. *Protein Cell* **11**, 71–78.

Fuchs, Y., Brown, S., Gorenc, T., Rodriguez, J., Fuchs, E. and Steller, H. (2013). Sept4/ARTS Regulates Stem Cell Apoptosis and Skin Regeneration. *Science (80-.).* **341**, 286 LP – 289.

Futami, T., Miyagishi, M. and Taira, K. (2005). Identification of a network involved in thapsigargin-induced apoptosis using a library of small interfering RNA expression vectors. *J. Biol. Chem.* **280**, 826–831.

Germani, F., Hain, D., Sternlicht, D., Moreno, E. and Basler, K. (2018). The Toll pathway inhibits tissue growth and regulates cell fitness in an infection-dependent manner. *bioRxiv* 1–10.

Green, D. R. and Kroemer, G. (2009). Cytoplasmic functions of the tumour suppressor p53. *Nature* **458**, 1127–1130.

Gregorio, A. Di, Bowling, S. and Rodriguez, T. A. (2016). Review Cell Competition and Its Role in the Regulation of Cell Fitness from Development to Cancer. *Dev. Cell* **38**, 621–634.

Grzeschik, N. A., Parsons, L. M., Allott, M. L., Harvey, K. F. and Richardson, H. E. (2010). Lgl, aPKC, and Crumbs Regulate the Salvador/Warts/Hippo Pathway through Two Distinct Mechanisms. *Curr. Biol.* **20**, 573–581.

Gutscher, M., Pauleau, A., Marty, L., Brach, T., Wabnitz, G. H., Samstag, Y., Meyer, A. J. and Dick, T. P. (2008). Real-time imaging of the intracellular glutathione redox potential. **5**, 553–559.

Hackett, J. A. and Surani, M. A. (2014). Regulatory principles of pluripotency: from the ground state up. *Cell Stem Cell* **15**, 416–430.

Hafezi, Y., Bosch, J. A. and Hariharan, I. K. (2012). Differences in levels of the transmembrane protein Crumbs can influence cell survival at clonal boundaries. *Dev. Biol.* **368**, 358–369.

Handy, D. E. and Loscalzo, J. (2012). Redox regulation of mitochondrial function. *Antioxid. Redox Signal.* **16**, 1323–1367.

Hao, Q., Chen, J., Liao, J., Huang, Y., Larisch, S., Zeng, S. X., Lu, H. and Zhou, X. (2020). p53 induces ARTS to promote mitochondrial apoptosis. *bioRxiv* 2020.05.14.096982.

Hara, K., Shiga, A., Fukutake, T., Nozaki, H., Miyashita, A., Yokoseki, A., Kawata, H., Koyama, A., Arima, K., Takahashi, T., et al. (2009). Association of HTRA1 Mutations and Familial Ischemic Cerebral Small-Vessel Disease. *N. Engl. J. Med.* **360**, 1729–1739.

Hashimoto, M. and Sasaki, H. (2019). Epiblast Formation by TEAD-YAP-Dependent Expression of Pluripotency Factors and Competitive Elimination of Unspecified Cells. *Dev. Cell* **50**, 139-154.e5.

Haupt, Y., Maya, R., Kazaz, A. and Oren, M. (1997). Mdm2 promotes the rapid degradation of p53. *Nature* **387**, 296–299.

He, X., Khurana, A., Maguire, J. L., Chien, J. and Shridhar, V. (2012). HtrA1 sensitizes ovarian cancer cells to cisplatin-induced cytotoxicity by targeting XIAP for degradation. *Int. J. cancer* **130**, 1029–1035.

Heilig, C., Brosius, F., Siu, B., Concepcion, L., Mortensen, R., Heilig, K., Zhu, M., Weldon, R., Wu, G. and Conner, D. (2003). Implications of Glucose Transporter Protein Type 1 (GLUT1)-Haplodeficiency in Embryonic Stem Cells for Their Survival in Response to Hypoxic Stress. *Am. J. Pathol.* **163**, 1873–1885.

Herz, H. M., Chen, Z., Scherr, H., Lackey, M., Bolduc, C. and Bergmann, A. (2006). Vps25 mosaics display non-autonomous cell survival and overgrowth, and autonomous apoptosis. *Development* **133**, 1871–1880.

Heyer, B. S., Macauley, A., Behrendtsen, O. and Werb, Z. (2000). Hypersensitivity to DNA damage leads to increased apoptosis during early mouse development. *Genes Dev.* **14**, 2072–2084.

Hikisz, P. and Kiliańska, Z. M. (2012). Puma, a critical mediator of cell death - one decade on from its discovery. *Cell. Mol. Biol. Lett.* **17**, 646–669.

Hogan, C., Dupré-crochet, S., Norman, M., Kajita, M., Zimmermann, C., Pelling, E., Piddini, E., Baena-lópez, L. A., Vincent, J., Itoh, Y., et al. (2009). Characterization of the interface between normal and transformed epithelial cells. **11**,.

Huang, C. Y., Bredemeyer, A. L., Walker, L. M., Bassing, C. H. and Sleckman, B. P. (2008). Dynamic regulation of c-Myc proto-oncogene expression during lymphocyte development revealed by a GFP-c-Myc knock-in mouse. *Eur. J. Immunol.* **38**, 342–349.

Huang, Y., Osorno, R., Tsakiridis, A. and Wilson, V. (2012). In Vivo differentiation potential of epiblast stem cells revealed by chimeric embryo formation. *Cell Rep.* **2**, 1571–1578.

Igaki, T., Pastor-Pareja, J. C., Aonuma, H., Miura, M. and Xu, T. (2009). Intrinsic Tumor Suppression and Epithelial Maintenance by Endocytic Activation of Eiger/TNF Signaling in Drosophila. *Dev. Cell* **16**, 458–465.

Irvine, K. D. and Rauskolb, C. (2001). B OUNDARIES IN D EVELOPMENT : Formation and Function. 189–214.

Jacks, T., Remington, L., Williams, B.O., Schmitt, E.M., Halachmi, S., Bronson, R.T., and Weinberg, R.A. (1994). Tumor spectrum analysis in p53-mutant mice. Curr. Biol. 4, 1–7.

Jain, A. K. and Barton, M. C. (2018). p53: emerging roles in stem cells, development and beyond. *Development* **145**,.

Jain, A. K., Allton, K., Iacovino, M., Mahen, E., Milczarek, R. J., Zwaka, T. P., Kyba, M. and Barton, M. C. (2012). p53 regulates cell cycle and microRNAs to promote differentiation of human embryonic stem cells. *PLoS Biol.* **10**, e1001268.

Jaiswal, S. K., Oh, J. J. and DePamphilis, M. L. (2020). Cell cycle arrest and apoptosis are not dependent on p53 prior to p53-dependent embryonic stem cell differentiation. *Stem Cells* **38**, 1091–1106.

Jin, Z., Kirilly, D., Weng, C., Kawase, E., Song, X., Smith, S., Schwartz, J. and Xie, T. (2008). Differentiation-Defective Stem Cells Outcompete Normal Stem Cells for Niche Occupancy in the Drosophila Ovary. *Cell Stem Cell* **2**, 39–49.

Johnston, L. A., Prober, D. A., Edgar, B. A., Eisenman, R. N. and Gallant, P. (1999). Drosophila myc regulates cellular growth during development. *Cell* **98**, 779–790.

Kajita, M. and Fujita, Y. (2015). EDAC: Epithelial defence against cancer--cell competition between normal and transformed epithelial cells in mammals. *J. Biochem.* **158**, 15–23.

Kajita, M., Hogan, C., Harris, A. R., Dupre-Crochet, S., Itasaki, N., Kawakami, K., Charras, G., Tada, M. and Fujita, Y. (2010). Interaction with surrounding normal epithelial cells influences signalling pathways and behaviour of Src-transformed cells. *J. Cell Sci.* **123**, 171–180.

Kale, a, Li, W., Lee, C.-H. and Baker, N. E. (2015). Apoptotic mechanisms during competition of ribosomal protein mutant cells: roles of the initiator caspases Dronc and Dream/Strica. *Cell Death Differ.* 1–13.

Kang, R., Zeh, H. J., Lotze, M. T. and Tang, D. (2011). The Beclin 1 network regulates autophagy and apoptosis. *Cell Death Differ.* **18**, 571–580.

Karim, F. D. and Rubin, G. M. (1998). Ectopic expression of activated Ras1 induces hyperplastic growth and increased cell death in Drosophila imaginal tissues. *Development* **125**, 1–9.

Kastenhuber, E. R. and Lowe, S. W. (2017). Putting p53 in Context. *Cell* **170**, 1062–1078.

Katsukawa, M., Ohsawa, S., Zhang, L., Yan, Y. and Igaki, T. (2018). Serpin Facilitates Tumor-Suppressive Cell Competition by Blocking Toll-Mediated Yki Activation in Drosophila. *Curr. Biol.* **28**, 1756-1767.e6.

Kim, Y. C., Guan, K., Kim, Y. C. and Guan, K. (2015). mTOR : a pharmacologic target for autophagy regulation. **125**, 25–32.

Kim, J., Yu, L., Chen, W., Xu, Y., Wu, M., Todorova, D., Tang, Q., Feng, B., Jiang, L., He, J., et al. (2019). Wild-Type p53 Promotes Cancer Metabolic Switch by Inducing PUMA-Dependent Suppression of Oxidative Phosphorylation. *Cancer Cell* **35**, 191-203. e8.

Klose, R., Prinz, A., Tetzlaff, F., Weis, E.-M., Moll, I., Rodriguez-Vita, J., Oka, C., Korff, T. and Fischer, A. (2019). Loss of the serine protease HTRA1 impairs smooth muscle cells maturation. *Sci. Rep.* **9**, 18224.

Kolahgar, G., Suijkerbuijk, S. J. E., Kucinski, I., Poirier, E. Z., Mansour, S., Simons, B. D. and Piddini, E. (2015). Cell Competition Modifies Adult Stem Cell and Tissue Population Dynamics in a JAK-STAT-Dependent Manner. *Dev. Cell* 1–13.

Kon, S., Ishibashi, K., Katoh, H., Kitamoto, S., Shirai, T., Tanaka, S., Kajita, M., Ishikawa, S., Yamauchi, H., Yako, Y., et al. (2017). Cell competition with normal epithelial cells promotes apical extrusion of transformed cells through metabolic changes. *Nat. Cell Biol.* **19**, 530–541.

Kroemer, G., Galluzzi, L., Vandenabeele, P., Abrams, J., Alnemri, E. S., Baehrecke, E. H., Blagosklonny, M. V, El-Deiry, W. S., Golstein, P., Green, D. R., et al. (2009). Classification of cell death: recommendations of the Nomenclature Committee on Cell Death 2009. *Cell Death Differ.* **16**, 3–11.

Kucinski, I., Dinan, M., Kolahgar, G. and Piddini, E. (2017). Chronic activation of JNK JAK/STAT and oxidative stress signalling causes the loser cell status. *Nat. Commun.* **8**,.

Kumari, R., Kohli, S. and Das, S. (2014). p53 regulation upon genotoxic stress: intricacies and complexities. *Mol. Cell. Oncol.* **1**, e969653.

Lane, D. P. and Crawford, L. V (1979). T antigen is bound to a host protein in SY40-transformed cells. *Nature* **278**, 261–263.

Lawrence, P. A. (1982). Cell lineage of the thoracic muscles of drosophila. *Cell* **29**, 493–503.

Lee, C. H., Kiparaki, M., Blanco, J., Folgado, V., Ji, Z., Kumar, A., Rimesso, G. and Baker, N. E. (2018). A Regulatory Response to Ribosomal Protein Mutations Controls Translation, Growth, and Cell Competition. *Dev. Cell* **46**, 456-469.e4.

Levayer, R., Hauert, B. and Moreno, E. (2015). Cell mixing induced by myc is required for competitive tissue invasion and destruction. *Nature* **524**, 476–480.

Levayer, R., Dupont, C. and Moreno, E. (2016). Tissue Crowding Induces Caspase-Dependent Competition for Space. *Curr. Biol.* **26**, 670–677.

Li, W. and Baker, N. E. (2007). Engulfment Is Required for Cell Competition. *Cell* **129**, 1215–1225.

Li, M. and Huang, J. (2010). A new puzzling role of p53 in mouse embryonic stem cells. *Cell Cycle* **9**, 1669–1670.

Li, M., He, Y., Dubois, W., Wu, X., Shi, J. and Huang, J. (2012). Distinct regulatory mechanisms and functions for p53-activated and p53-repressed DNA damage response genes in embryonic stem cells. *Mol. Cell* **46**, 30–42.

Lima, A., Lubatti, G., Burgstaller, J., Hu, D., Green, A., Gregorio, A. Di, Zawadzki, T., Pernaute, B., Mahammadov, E., Dore, M., et al. (2020). Differences in mitochondrial activity trigger cell competition during early mouse development. *bioRxiv* 2020.01.15.900613.

Lin, T., Chao, C., Saito, S., Mazur, S. J., Murphy, M. E., Appella, E. and Xu, Y. (2005). p53 induces differentiation of mouse embryonic stem cells by suppressing Nanog expression. *Nat. Cell Biol.* **7**, 165–171.

Linzer, D. I. and Levine, A. J. (1979). Characterization of a 54K dalton cellular SV40 tumor antigen present in SV40-transformed cells and uninfected embryonal carcinoma cells. *Cell* **17**, 43–52.

Liu, D. and Xu, Y. (2011). p53, oxidative stress, and aging. *Antioxid. Redox Signal.* **15**, 1669–1678.

Liu, J. C., Guan, X., Ryan, J. A., Rivera, A. G., Mock, C., Agarwal, V., Letai, A., Lerou, P. H. and Lahav, G. (2013). High mitochondrial priming sensitizes hESCs to DNA-damage-induced apoptosis. *Cell Stem Cell* **13**, 483–491.

Lolo, F. N., Casas-Tintó, S. and Moreno, E. (2012). Cell Competition Time Line: Winners Kill Losers, which Are Extruded and Engulfed by Hemocytes. *Cell Rep.* **2**, 526–539.

Lu, H. and Bilder, D. (2005). Endocytic control of epithelial polarity and proliferation in Drosophila. *Nat. Cell Biol.* **7**, 1132–1139.

Madan, E., Pelham, C. J., Nagane, M., Parker, T. M., Canas-Marques, R., Fazio, K., Shaik, K., Yuan, Y., Henriques, V., Galzerano, A., et al. (2019). Flower isoforms promote competitive growth in cancer. *Nature* **572**, 260–264.

Maraldi, T., Guida, M., Zavatti, M., Resca, E., Bertoni, L., La Sala, G. B. and De Pol, A. (2015). Nuclear Nox4 role in stemness power of human amniotic fluid stem cells. *Oxid. Med. Cell. Longev.* **2015**,.

Martins, V. C., Busch, K., Juraeva, D., Blum, C., Ludwig, C., Rasche, V., Lasitschka, F., Mastitsky, S. E., Brors, B., Hielscher, T., et al. (2014). Cell competition is a tumour suppressor mechanism in the thymus. *Nature* **509**, 465–70.

Marusyk, A., Porter, C. C., Zaberezhnyy, V. and DeGregori, J. (2010). Irradiation Selects for p53-Deficient Hematopoietic Progenitors. *PLoS Biol.* **8**, e1000324.

Mathieu, J. and Ruohola-Baker, H. (2017). Metabolic remodeling during the loss and acquisition of pluripotency. *Development* **144**, 541 LP – 551.

McDonnell, S. J., Spiller, D. G., White, M. R. H., Prior, I. A. and Paraoan, L. (2019). ER stress-linked autophagy stabilizes apoptosis effector PERP and triggers its co-localization with SERCA2b at ER–plasma membrane junctions. *Cell Death Discov.* **5**,.

Menéndez, J., Pérez-Garijo, A., Calleja, M. and Morata, G. (2010). A tumor-suppressing mechanism in Drosophila involving cell competition and the Hippo pathway. *Proc. Natl. Acad. Sci. U. S. A.* **107**, 14651–14656.

Menthena, A., Koehler, C. I., Sandhu, J. S., Yovchev, M. I., Hurston, E., Shafritz, D. A. and Oertel, M. (2011). Activin A, p15INK4b signaling, and cell competition promote stem/progenitor cell repopulation of livers in aging rats. *Gastroenterology* **140**, 1009-1020.e8.

Menut, L., Vaccari, T., Dionne, H., Hill, J., Wu, G. and Bilder, D. (2007). A mosaic genetic screen for Drosophila neoplastic tumor suppressor genes based on defective pupation. *Genetics* **177**, 1667–1677.

Merino, M. M., Rhiner, C., Lopez-gay, J. M., Buechel, D., Hauert, B. and Moreno, E. (2015). Article Elimination of Unfit Cells Maintains Tissue Health and Prolongs Lifespan. *Cell* **160**, 461–476.

Meyer, S. N., Amoyel, M., Bergantinos, C., de la Cova, C., Schertel, C., Basler, K. and Johnston, L. a. (2014). An ancient defense system eliminates unfit cells from developing tissues during cell competition. *Science (80-.).* **346**, 1258236–1258236.

Milán, M. (2002). Survival of the fittest. Cell competition in the Drosophila wing. *EMBO Rep.* **3**, 724–725.

Ming, L., Sakaida, T., Yue, W., Jha, A., Zhang, L. and Yu, J. (2008). Sp1 and p73 activate PUMA following serum starvation. *Carcinogenesis* **29**, 1878–1884.

Moberg, K. H., Schelble, S., Burdick, S. K. and Hariharan, I. K. (2005). Mutations in erupted , the Drosophila Ortholog of Mammalian Tumor Susceptibility Gene 101 , Elicit Non-Cell-Autonomous Overgrowth. **9**, 699–710.

Morata, G. and Ripoll, P. (1975). Minutes: mutants of drosophila autonomously affecting cell division rate. *Dev. Biol.* **42**, 211–221.

Moreno, E. and Basler, K. (2004). dMyc transforms cells into super-competitors. *Cell* **117**, 117–129.

Moreno, E., Basler, K. and Morata, G. (2002). Cells compete for decapentaplegic survival factor to prevent apoptosis in Drosophila wing development. *Nature* **416**, 755–759.

Moreno, E., Meyer, P., Moreno, E., Fernandez-marrero, Y., Meyer, P. and Rhiner, C. (2015). Brain Regeneration in Drosophila Involves Comparison of Neuronal Fitness Report Brain Regeneration in Drosophila Involves Comparison of Neuronal Fitness. *Curr. Biol.* **25**, 955–963.

Nagata, R., Nakamura, M., Sanaki, Y. and Igaki, T. (2019). Cell Competition Is Driven by Autophagy. *Dev. Cell* **51**, 99-112.e4.

Neto-Silva, R. M., de Beco, S. and Johnston, L. A. (2010). Evidence for a growth-stabilizing regulatory feedback mechanism between Myc and Yorkie, the drosophila homolog of Yap. *Dev. Cell* **19**, 507–520.

Nichols, J. and Smith, A. (2009a). Perspective Naive and Primed Pluripotent States. *Stem Cell* **4**, 487–492.

Nichols, J. and Smith, A. (2009b). Naive and primed pluripotent states. *Cell Stem Cell* **4**, 487–492.

Norman, M., Wisniewska, K. a, Lawrenson, K., Garcia-Miranda, P., Tada, M., Kajita, M., Mano, H., Ishikawa, S., Ikegawa, M., Shimada, T., et al. (2012). Loss of Scribble causes cell competition in mammalian cells. *J. Cell Sci.* **125**, 59–66.

Oertel, M., Menthena, A., Dabeva, M. D. and Shafritz, D. a. (2006). Cell competition leads to a high level of normal liver reconstitution by transplanted fetal liver stem/progenitor cells. *Gastroenterology* **130**, 507–520.

Ohsawa, S., Sugimura, K., Takino, K., Xu, T., Miyawaki, A. and Igaki, T. (2011). Elimination of Oncogenic Neighbors by JNK-Mediated Engulfment in Drosophila. *Dev. Cell* **20**, 315–328.

Oliver, E. R., Saunders, T. L., Tarlé, S. A. and Glaser, T. (2004). Ribosomal protein L24 defect in belly spot and tail (Bst), a mouse Minute. *Development* **131**, 3907–3920.

Panier, S. and Boulton, S. J. (2014). Double-strand break repair: 53BP1 comes into focus. *Nat. Rev. Mol. Cell Biol.* **15**, 7–18.

Penzo-Méndez, A. I., Chen, Y., Li, J., Witze, E. S. and Stanger, B. Z. (2015). Spontaneous Cell Competition in Immortalized Mammalian Cell Lines. 1–18.

Perciavalle, R. M., Stewart, D. P., Koss, B., Lynch, J., Milasta, S., Bathina, M., Temirov, J., Cleland, M. M., Pelletier, S., Schuetz, J. D., et al. (2012). Anti-apoptotic MCL-1 localizes to the mitochondrial matrix and couples mitochondrial fusion to respiration. *Nat. Cell Biol.* **14**, 575–583.

Pérez-Garijo, A., Martín, F. A. and Morata, G. (2004). Caspase inhibition during apoptosis causes abnormal signalling and developmental aberrations in Drosophila *Development* **131**, 5591 LP – 5598.

Pernaute, B., Spruce, T., Smith, K. M., Sánchez-Nieto, J. M., Manzanares, M., Cobb, B. and Rodríguez, T. A. (2014). MicroRNAs control the apoptotic threshold in primed pluripotent stem cells through regulation of BIM. *Genes Dev.* **28**, 1873–1878.

Petrova, E., López-Gay, J. M., Rhiner, C. and Moreno, E. (2012). Flower-deficient mice have reduced susceptibility to skin papilloma formation. *DMM Dis. Model. Mech.* **5**, 553–561.

Pfister, A. S. (2019). Emerging role of the nucleolar stress response in autophagy. *Front. Cell. Neurosci.* **13**, 1–18.

Portela, M., Casas-Tinto, S., Rhiner, C., López-Gay, J. M., Domínguez, O., Soldini, D. and Moreno, E. (2010). Drosophila SPARC is a self-protective signal expressed by loser cells during cell competition. *Dev. Cell* **19**, 562–573.

Posfai, E., Tam, O. H. and Rossant, J. (2014). Chapter One - Mechanisms of Pluripotency In Vivo and In Vitro. In *Stem Cells in Development and Disease* (ed. Rendl, M. B. T.-C. T. in D. B.), pp. 1–37. Academic Press.

Prober, D. A. and Edgar, B. A. (2000). Ras1 promotes cellular growth in the Drosophila wing. *Cell* **100**, 435–446.

Rhiner, C. and Moreno, E. (2009). Super competition as a possible mechanism to pioneer precancerous fields. *Carcinogenesis* **30**, 723–728.

Rhiner, C., Diaz, B., Portela, M., Poyatos, J. F., Fernandez-Ruiz, I., Lopez-Gay, J. M., Gerlitz, O. and Moreno, E. (2009). Persistent competition among stem cells and their daughters in the Drosophila ovary germline niche. *Development* **136**, 995–1006.

Rhiner, C., López-Gay, J. M., Soldini, D., Casas-Tinto, S., Martín, F. A., Lombardía, L. and Moreno, E. (2010). Flower forms an extracellular code that reveals the fitness of a cell to its neighbors in Drosophila. *Dev. Cell* **18**, 985–998.

Roberts, O. and Paraoan, L. (2020). PERP-ing into diverse mechanisms of cancer pathogenesis: Regulation and role of the p53/p63 effector PERP. *Biochim. Biophys. Acta - Rev. Cancer* **1874**, 188393.

Rodrigues, A. B., Zoranovic, T., Ayala-Camargo, A., Grewal, S., Reyes-Robles, T., Krasny, M., Christine Wu, D., Johnston, L. A. and Bach, E. A. (2012). Activated STAT regulates growth and induces competitive interactions independently of Myc, Yorkie, Wingless and ribosome biogenesis. *Dev.* **139**, 4051–4061.

Roseland, C. R. and Schneiderman, H. A. (1979). Regulation and metamorphosis of the abdominal histoblasts ofDrosophila melanogaster. *Wilhelm Roux's Arch. Dev. Biol.* **186**, 235–265.

Ryoo, H. D., Gorenc, T. and Steller, H. (2004). Apoptotic cells can induce compensatory cell proliferation through the JNK and the Wingless signaling pathways. *Dev. Cell* **7**, 491–501.

Saadi, H., Seillier, M. and Carrier, A. (2015). The stress protein TP53INP1 plays a tumor suppressive role by regulating metabolic homeostasis. *Biochimie* **118**, 44–50.

Sancho, M. and Rodríguez, T. a. (2014). Selecting for fitness in mammalian development. *Cell Cycle* **13**, 9–10.

Sancho, M., Di-Gregorio, A., George, N., Pozzi, S., Sánchez, J. M., Pernaute, B. and Rodríguez, T. A. (2013). Competitive interactions eliminate unfit embryonic stem cells at the onset of differentiation. *Dev. Cell* **26**, 19–30.

Sasaki, A., Nagatake, T., Egami, R., Gu, G., Takigawa, I., Ikeda, W., Nakatani, T., Kunisawa, J. and Fujita, Y. (2018). Obesity Suppresses Cell-Competition-Mediated Apical Elimination of RasV12-Transformed Cells from Epithelial Tissues. *Cell Rep.* **23**, 974–982.

Sato, N., Meijer, L., Skaltsounis, L., Greengard, P. and Brivanlou, A. H. (2004). Mainte-

nance of pluripotency in human and mouse embryonic stem cells through activation of Wnt signaling by a pharmacological GSK-3-specific inhibitor. *Nat. Med.* **10**, 55–63.

Schmeisser, K. and Parker, J. A. (2019). Pleiotropic Effects of mTOR and Autophagy During Development and Aging . *Front. Cell Dev. Biol.* **7**, 192.

Semba, T., Sammons, R., Wang, X., Xie, X., Dalby, K. N. and Ueno, N. T. (2020). JNK Signaling in Stem Cell Self-Renewal and Differentiation. *Int. J. Mol. Sci.* **21**,.

Senoo-Matsuda, N. and Johnston, L. a (2007). Soluble factors mediate competitive and cooperative interactions between cells expressing different levels of Drosophila Myc. *Proc. Natl. Acad. Sci. U. S. A.* **104**, 18543–18548.

Seo, B. J., Yoon, S. H. and Do, J. T. (2018). Mitochondrial Dynamics in Stem Cells and Differentiation. *Int. J. Mol. Sci.* **19**,.

Sheng, G. (2015). Epiblast morphogenesis before gastrulation. *Dev. Biol.* **401**, 17–24.

Siddiqui, W. A., Ahad, A. and Ahsan, H. (2015). The mystery of BCL2 family: Bcl-2 proteins and apoptosis: an update. *Arch. Toxicol.* **89**, 289–317.

Simpson, P. (1979). Parameters of cell competition in the compartments of the wing disc of Drosophila. *Dev. Biol.* **69**, 182–193.

Simpson, P. and Morata, G. (1981). Differential mitotic rates and patterns of growth in compartments in the Drosophila wing. *Dev. Biol.* **85**, 299—308.

Smith, A. G., Heath, J. K., Donaldson, D. D., Wong, G. G., Moreau, J., Stahl, M. and Rogers, D. (1988). Inhibition of pluripotential embryonic stem cell differentiation by purified polypeptides. *Nature* **336**, 688–690.

Snippert, H. J., Schepers, A. G., Es, J. H. Van, Simons, B. D. and Clevers, H. (2014). Biased competition between Lgr 5 intestinal stem cells driven by oncogenic mutation induces clonal expansion. **15**, 62–69.

Song, H., Chung, S.-K. and Xu, Y. (2010). Modeling disease in human ESCs using an efficient BAC-based homologous recombination system. *Cell Stem Cell* **6**, 80–89.

Sperber, H., Mathieu, J., Wang, Y., Ferreccio, A., Hesson, J., Xu, Z., Fischer, K. A., Devi, A., Detraux, D., Gu, H., et al. (2015). The metabolome regulates the epigenetic landscape during naive-to-primed human embryonic stem cell transition. *Nat. Cell Biol.* **17**, 1523–1535.

Suijkerbuijk, S. J. E., Kolahgar, G., Kucinski, I. and Piddini, E. (2016). Cell competition drives the growth of intestinal adenomas in Drosophila. *Curr. Biol.* **26**, 428–438.

Takino, K., Ohsawa, S. and Igaki, T. (2014). Loss of Rab5 drives non-autonomous cell proliferation through TNF and Ras signaling in Drosophila. *Dev. Biol.* **395**, 19–28.

Tamori, Y. and Deng, W. M. (2013). Tissue Repair through Cell Competition and Compen-

satory Cellular Hypertrophy in Postmitotic Epithelia. *Dev. Cell* **25**, 350–363.

Tamori, Y., Bialucha, C. U., Tian, A. G., Kajita, M., Huang, Y. C., Norman, M., Harrison, N., Poulton, J., Ivanovitch, K., Disch, L., et al. (2010). Involvement of Lgl and mahjong/VprBP in cell competition. *PLoS Biol.* **8**,.

Tasdemir, E., Maiuri, M. C., Galluzzi, L., Vitale, I., Djavaheri-Mergny, M., D'Amelio, M., Criollo, A., Morselli, E., Zhu, C., Harper, F., et al. (2008). Regulation of autophagy by cytoplasmic p53. *Nat. Cell Biol.* **10**, 676–687.

Ter Huurne, M., Peng, T., Yi, G., van Mierlo, G., Marks, H. and Stunnenberg, H. G. (2020). Critical Role for P53 in Regulating the Cell Cycle of Ground State Embryonic Stem Cells. *Stem cell reports* **14**, 175–183.

Tesar, P. J., Chenoweth, J. G., Brook, F. A., Davies, T. J., Evans, E. P., Mack, D. L., Gardner, R. L. and McKay, R. D. G. (2007). New cell lines from mouse epiblast share defining features with human embryonic stem cells. *Nature* **448**, 196–199.

Tiaden, A. N. and Richards, P. J. (2013). The emerging roles of HTRA1 in musculoskeletal disease. *Am. J. Pathol.* **182**, 1482–1488.

Tirado-Hurtado, I., Fajardo, W. and Pinto, J. A. (2018). DNA damage inducible transcript 4 gene: The switch of the metabolism as potential target in cancer. *Front. Oncol.* **8**,.

Tosolini, M. and Jouneau, A. (2016). In Vitro Differention of Pluripotent Stem Cells into Functional B Islets Under 2D and 3D Culture Conditions and In Vivo Preclinical Validation of 3D Islets. *Methods Mol. Biol.* 257–284.

Tsogtbaatar, E., Landin, C., Minter-Dykhouse, K. and Folmes, C. D. L. (2020). Energy Metabolism Regulates Stem Cell Pluripotency. *Front. Cell Dev. Biol.* **8**, 1–16.

Turinetto, V., Orlando, L., Sanchez-Ripoll, Y., Kumpfmueller, B., Storm, M. P., Porcedda, P., Minieri, V., Saviozzi, S., Accomasso, L., Rocchietti, E. C., et al. (2012). High basal γH2AX levels sustain self-renewal of mouse embryonic and induced pluripotent stem cells. *Stem Cells* **30**, 1414–1423.

Tyler, D. M., Li, W., Zhuo, N., Pellock, B. and Baker, N. E. (2007). Genes Affecting Cell Competition in Drosophila. *Genetics* **175**, 643–657.

Vander Heiden, M. G. and DeBerardinis, R. J. (2017). Understanding the Intersections between Metabolism and Cancer Biology. *Cell* **168**, 657–669.

Varum, S., Rodrigues, A. S., Moura, M. B., Momcilovic, O., Easley, C. A. 4th, Ramalho-Santos, J., Van Houten, B. and Schatten, G. (2011). Energy metabolism in human pluripotent stem cells and their differentiated counterparts. *PLoS One* **6**, e20914.

Vaughen, J. and Igaki, T. (2016). Slit-Robo Repulsive Signaling Extrudes Tumorigenic Cells from Epithelia. *Dev. Cell* **39**, 683–695.

Vervliet, T., Parys, J. B. and Bultynck, G. (2016). Bcl-2 proteins and calcium signaling: complexity beneath the surface. *Oncogene* **35**, 5079–5092.

Vidal, M., Larson, D. E. and Cagan, R. L. (2006). Csk-deficient boundary cells are eliminated from normal drosophila epithelia by exclusion, migration, and apoptosis. *Dev. Cell* **10**, 33–44.

Villa del Campo, C., Clavería, C., Sierra, R. and Torres, M. (2014). Cell Competition Promotes Phenotypically Silent Cardiomyocyte Replacement in the Mammalian Heart. *Cell Rep.* **8**, 1741–1751.

Vincent, J., Kolahgar, G., Gagliardi, M. and Piddini, E. (2011). Steep Differences in Wingless Signaling Trigger Myc-Independent Competitive Cell Interactions. *Dev. Cell* **21**, 366–374.

Vitale, I., Manic, G., De Maria, R., Kroemer, G. and Galluzzi, L. (2017). DNA Damage in Stem Cells. *Mol. Cell* **66**, 306–319.

Wagstaff, L., Kolahgar, G. and Piddini, E. (2013). Competitive cell interactions in cancer : a cellular tug of war. *Trends Cell Biol.* **23**, 160–167.

Wagstaff, L., Goschorska, M., Kozyrska, K., Duclos, G., Kucinski, I., Chessel, A., Neil, L. H., Bradshaw, C. R., Allen, G. E., Rawlins, E. L., et al. (2016). Mechanical cell competition kills cells via induction of lethal p53 levels.

Wang, Q. and Zou, M. H. (2018). Measurement of reactive oxygen species (ROS) and mitochondrial ROS in AMPK knockout mice blood vessels. *Methods Mol. Biol.* **1732**, 507–517.

Watanabe, H., Ishibashi, K., Mano, H., Kitamoto, S., Sato, N., Hoshiba, K., Kato, M., Matsuzawa, F., Takeuchi, Y., Shirai, T., et al. (2018). Mutant p53-Expressing Cells Undergo Necroptosis via Cell Competition with the Neighboring Normal Epithelial Cells. *Cell Rep.* **23**, 3721–3729.

Williams, R. L., Hilton, D. J., Pease, S., Willson, T. A., Stewart, C. L., Gearing, D. P., Wagner, E. F., Metcalf, D., Nicola, N. A. and Gough, N. M. (1988). Myeloid leukaemia inhibitory factor maintains the developmental potential of embryonic stem cells. *Nature* **336**, 684–687.

Woods, D. F. and Bryant, P. J. (1991). The discs-large tumor suppressor gene of Drosophila encodes a guanylate kinase homolog localized at septate junctions. *Cell* **66**, 451–464.

Wu, B., Qiu, W., Wang, P., Yu, H., Cheng, T., Zambetti, G. P., Zhang, L. and Yu, J. (2007). p53 independent induction of PUMA mediates intestinal apoptosis in response to ischaemia-reperfusion. *Gut* **56**, 645–654.

Xu, F., Fang, Y., Yan, L., Xu, L., Zhang, S., Cao, Y., Xu, L., Zhang, X., Xie, J., Jiang, G., et al. (2017). Nuclear localization of Beclin 1 promotes radiation-induced DNA damage repair independent of autophagy. *Sci. Rep.* **7**, 45385.

Yacoubian, T. A. and Standaert, D. G. (2009). Targets for neuroprotection in Parkinson's disease. *Biochim. Biophys. Acta* **1792**, 676–687.

Yamamoto, H., Itoh, N., Kawano, S., Yatsukawa, Y., Momose, T., Makio, T., Matsunaga, M., Yokota, M., Esaki, M., Shodai, T., et al. (2011). Dual role of the receptor Tom20 in specificity and efficiency of protein import into mitochondria. *Proc. Natl. Acad. Sci. U. S. A.* **108**, 91–96.

Yamamoto, M., Ohsawa, S., Kunimasa, K., Igaki, T. and N-terminal, J. (2017). The ligand Sas and its receptor PTP10D drive tumour-suppressive cell competition.

Ying, Q.-L., Wray, J., Nichols, J., Batlle-Morera, L., Doble, B., Woodgett, J., Cohen, P. and Smith, A. (2008). The ground state of embryonic stem cell self-renewal. *Nature* **453**, 519–523.

You, H., Pellegrini, M., Tsuchihara, K., Yamamoto, K., Hacker, G., Erlacher, M., Villunger, A. and Mak, T. W. (2006). FOXO3a-dependent regulation of Puma in response to cytokine/growth factor withdrawal. *J. Exp. Med.* **203**, 1657–1663.

Yu, J. and Zhang, L. (2008). PUMA, a potent killer with or without p53. *Oncogene* **27**, 71–83.

Zhang, Z.-N., Chung, S.-K., Xu, Z. and Xu, Y. (2014). Oct4 maintains the pluripotency of human embryonic stem cells by inactivating p53 through Sirt1-mediated deacetylation. *Stem Cells* **32**, 157–165.

Zhang, G., Xiea, Y., Zhou, Y., Xiang, C., Chen, L., Zhang, C., Hou, X., Chen, J., Zong, H. and Liu, G. (2017). P53 pathway is involved in cell competition during mouse embryogenesis. *Proc. Natl. Acad. Sci. U. S. A.* **114**, 498–503.

Zhou, W., Choi, M., Margineantu, D., Margaretha, L., Hesson, J., Cavanaugh, C., Blau, C. A., Horwitz, M. S., Hockenbery, D., Ware, C., et al. (2012). HIF1α induced switch from bivalent to exclusively glycolytic metabolism during ESC-to-EpiSC/hESC transition. *EMBO J.* **31**, 2103–2116.

Ziosi, M., Baena-López, L. A., Grifoni, D., Froldi, F., Pession, A., Garoia, F., Trotta, V., Bellosta, P., Cavicchi, S. and Pession, A. (2010). dMyc functions downstream of yorkie to promote the supercompetitive behavior of hippo pathway mutant Cells. *PLoS Genet.* **6**,.

Ziv, O., Suissa, Y., Neuman, H., Dinur, T., Geuking, P., Rhiner, C., Portela, M., Lolo, F., Moreno, E. and Gerlitz, O. (2009). The co-regulator dNAB interacts with Brinker to eliminate cells with reduced Dpp signaling. *Development* **136**, 1137–1145.

Zurawa-Janicka, D., Wenta, T., Jarzab, M., Skorko-Glonek, J., Glaza, P., Gieldon, A., Ciarkowski, J. and Lipinska, B. (2017). Structural insights into the activation mechanisms of human HtrA serine proteases. *Arch. Biochem. Biophys.* **621**, 6–23.

ANEXO I

1. CYTOPLASM MACRO

```
n = getNumber("How many nuclei", );
match = newArray(n);

for(i=0; i < n;i++){
        for(j=n; j< roiManager("count");j++){
                roiManager("Select", j);
                getSelectionBounds(x, y, width, height);
                xc = x + width/2;
                yc = y + height/2;
                roiManager("Select", i);
                roiManager("Set Line Width", 0);
                roiManager("Rename", "Cell_" + i+1);
                roiManager("Select", i);
                if(Roi.contains(xc, yc)){
                        match[i] = j;
                        roiManager("Select", j);
                        roiManager("Set Line Width", 0);
                        roiManager("Rename", "Nuclei_" + i+1);
                        j = roiManager("Count");              }          }
        roiManager("Select", newArray(i, match[i]));
        roiManager("XOR");
        roiManager("Add");
        roiManager("Select", roiManager("Count")-1);
        roiManager("Set Line Width", 0);
        roiManager("Rename", "cytosol_" + i+1);     }
```

2. FOCI NUMBER MACRO

```
run("Duplicate...", "duplicate channels=1");

    recuento=roiManager("Count");

    punctae=newArray(recuento);

    for(roi=0;roi<recuento;roi++){
        roiManager("Select",roi);
        roiManager("Rename","N"+roi+1);
        run("Find Maxima...", "noise=30 output=Count");
        punctae[roi]=getResult("Count",roi);          }

    //Crear tabla
    run("Clear Results");
    for(roi=0;roi<recuento;roi++){
        setResult("Puntae",roi, punctae[roi]);
        updateResults;    }
```

ACKNOWLEDGMENTS

Durante mi paso por el CNIC, he podido conocer a multitud de personas, las cuales han formado parte de esta etapa y me han aportado y enriquecido de una u otra manera. Sé que me llevo el cariño de mucha gente, al igual que ellos el mío.

Miguel, gracias por permitirme realizar esta tesis. Gracias por tu infinita paciencia y por todas las oportunidades que me has dado. Me has abierto las puertas al mundo de la investigación, has estado ahí siempre que he acudido a ti y has confiado en mí mucho más que yo mismo. Para nosotros eres un ejemplo de humidad, serenidad y disciplina. Nos valoras, nos enseñas a interpretar los resultados sin prejuicios y nos das libertad para crecer. Por todo ello, muchas gracias.

Gracias a todos los que formáis el grupo MT, a los que ya no están y a los que sí.

A Cristina Clavería y a Cova. Vuestras enormes aportaciones a la Competición hacen posible este humilde trabajo. A nuestras técnicos Vane, Susana y Rocío por vuestra ayuda y apoyo. A Cris Villa, Inés, Consuelo, Jorge, Óscar, Morena, Kenzo, Irene, Ghislaine y Lorena. Todos me habéis ayudado de una u otra forma y me habeis mostrado cualidades como la pasión por la ciencia, la creatividad y la constancia. Gracias por estar ahí, por vuestra ayuda y consejos.

A Ester y Noelia, gracias por vuestro cariño y por ser así, amables, sensatas y trabajadoras. Espero parecerme algo más a vosotras en mis próximas aventuras. A la "pequeña y dulce" Lin, gracias por todo. Por echarme una mano constantemente. Y es que no se me ocurre mejor compañera de lab. Ha sido un honor compartir esta etapa vosotras y crecer juntos.

A todos vosotros, lamento haberos dado el coñazo con mi desbordante negatividad/pesimismo en muchas ocasiones y espero haberos aportado al menos una parte de lo que vosotros a mí.

Agradecer la gran labor de las Unidades Técnicas. Al personal del Animalario, a las Unidades de Celómica (José Ligos, Mariano, Raquel, Elena) o Microscopía (Valeria, Moreno, Elvira, Verónica...). Porque lejos de haber sido un usuario ejemplar en determinados momentos, me habéis ofrecido vuestra ayuda, profesionalidad, consejos y simpatía durante todos estos años. Muchas gracias.

Quería destacar a la Unidad de Células Pluripotentes, gracias Giovanna y a tí y a tu equipo por enseñarme a manejar las ES, por ayudarme a generar las líneas *knockout*... Sin vosotros, este trabajo sería muy distinto. Y sobre todo, gracias Giovanna porque siempre has estado ahí para echarle un ojo a mis cultivos y ayudarme en mis momento s más difíciles.

Gracias también a otros grupos del CNIC, muchos compañeros que se ya fueron y otros

que han ido llegando, especialmente los compañeros de las 3N. Destacar también a Toño y su equpo (Andrea, Rocío, Raquel...) por toda su ayuda y consejo durante estos años. También al grupo de Nacho por cedernos su ratón *p53*$^{+/\Delta}$. Ha sido un placer trabajar en el CNIC, rodeado de gente tan inteligente, con metas y sueños comunes. Me habéis aportado ideas, una cantidad considerable de reactivos, y, además, habéis hecho mi día a día más ameno.

A Rebeca, Carlos, Isaac (Sir Jaisac), Javier e Irene, personas excepcionalmente capaces con los que me he compartido muy buenos momentos. Además de eso, a Rebeca, porque sin ti no habría llegado tan lejos. A Carlos, por tu apoyo bioinformático, lasañas y guía burocrático. A Sir Jaisac (el gris), por el cariño que sé que me has cogido. Ya tu sabeh, no hay ma ná.

A Fermín y a Míquel por aguantarme en el piso a diario. A Míquel, no me cabe duda de que con tu gran capacidad llegarás donde te propongas (en ciencia, finanzas o en el mundo de la escalada), gracias por las comidas, por tu ayuda y los buenos momentos y las risas.

Gracias Sandra, por todo lo que has hecho por mi desde que te conozco. Tu constancia, trabajo y bondad hacia todo lo que te rodea, te hacen una persona maravillosa y única, y por supuesto te llevarán a conseguir cualquier meta. Muchas gracias por tu enorme cariño.

Por supuesto, no puedo olvidarme de todas las personas que me han acompañado y guiado para llegar hasta aquí. He sido muy afortunado por disfrutar de muy buenos profesores, que han sabido desarrollar mi curiosidad y ganas de aprender. Hacer mención a los profesores de la Universidad de Murcia, en especial a Marisen y el grupo de Biomembranas. Gracias a ellos, descubrí el mundo de la Biotecnología, rodeado de compañeros y personas excepcionales que sacaron lo mejor de mí y llevo en el corazón.

A los amigos que me acompañan desde pequeño. Aunque esté lejos, siempre es un gran apoyo para mi saber que estáis ahí.

A mi familia. No puedo agradecer todo el amor y el apoyo incondicional que me dais. Todo lo bueno que haga (científico o no) os lo debo a vosotros. Espero que no me faltéis nunca.

Cover page. Confocal image of an ESC colony, showing DAPI (red), WGA (white) and pHH3 (green).

Universidad Autónoma
de Madrid